ESTIMATION OF HYDRAULIC PARAMETERS FROM AN UNCONFINED AQUIFER TEST CONDUCTED IN A GLACIAL OUTWASH DEPOSIT, CAPE COD, MASSACHUSETTS

By Allen F. Moench[1], Stephen P. Garabedian[2], and Denis R. LeBlanc[2]

U.S. GEOLOGICAL SURVEY Open-File Report 00-485

U.S. DEPARTMENT OF THE INTERIOR
BRUCE BABBITT, Secretary

U.S. GEOLOGICAL SURVEY
Charles G. Groat, Director

---

[1] USGS, Menlo Park, CA

[2] USGS, Northborough, MA

CONTENTS

CONVERSION FACTORS

Multiply	By	To obtain
inch (in)	2.540	centimeter (cm)
mile (mi)	1.609	kilometer (km)
foot (ft)	0.3048	meter (m)
square foot (ft^2)	0.09290	square meter (m^2)
cubic foot ft^3)	0.02832	cubic meter (m^3)
gallon (gal)	0.003785	cubic meter (m^3)

ABSTRACT

An aquifer test conducted in a sand and gravel, glacial outwash deposit on Cape Cod, Massachusetts was analyzed by means of a model for flow to a partially penetrating well in a homogeneous, anisotropic unconfined aquifer. The model is designed to account for all significant mechanisms expected to influence drawdown in observation piezometers and in the pumped well. In addition to the usual fluid-flow and storage processes, additional processes include effects of storage in the pumped well, storage in observation piezometers, effects of skin at the pumped-well screen, and effects of drainage from the zone above the water table. The aquifer was pumped at a rate of 320 gallons per minute for 72-hours and drawdown measurements were made in the pumped well and in 20 piezometers located at various distances from the pumped well and depths below the land surface. To facilitate the analysis, an automatic parameter estimation algorithm was used to obtain relevant unconfined aquifer parameters, including the saturated thickness and a set of empirical parameters that relate to gradual drainage from the unsaturated zone.

Drainage from the unsaturated zone is treated in this paper as a finite series of exponential terms, each of which contains one empirical parameter that is to be determined. It was necessary to account for effects of gradual drainage from the unsaturated zone to obtain satisfactory agreement between measured and simulated drawdown, particularly in piezometers located near the water table. The commonly used assumption of instantaneous drainage from the unsaturated zone gives rise to large discrepancies between measured and predicted drawdown in the intermediate-time range and can result in inaccurate estimates of aquifer parameters when automatic parameter estimation procedures are used.

The values of the estimated hydraulic parameters are consistent with estimates from prior studies and from what is known about the

aquifer at the site. Effects of heterogeneity at the site were small as measured drawdowns in all piezometers and wells were very close to the simulated values for a homogeneous porous medium. The estimated values are: specific yield, 0.26; saturated thickness, 170 feet; horizontal hydraulic conductivity, 0.23 feet per minute; vertical hydraulic conductivity, 0.14 feet per minute; and specific storage, 1.3×10^{-5} per foot.

It was found that drawdown in only a few piezometers strategically located at depth near the pumped well yielded parameter estimates close to the estimates obtained for the entire data set analyzed simultaneously. If the influence of gradual drainage from the unsaturated zone is not taken into account, specific yield is significantly underestimated even in these deep-seated piezometers. This helps to explain the low values of specific yield often reported for granular aquifers in the literature. If either the entire data set or only the drawdown in selected deep-seated piezometers was used, it was found unnecessary to conduct the test for the full 72-hours to obtain accurate estimates of the hydraulic parameters. For some piezometer groups, practically identical results would be obtained for an aquifer test conducted for only 8-hours. Drawdowns measured in the pumped well and piezometers at distant locations were diagnostic only of aquifer transmissivity.

INTRODUCTION

Proper management of ground-water resources requires an accurate evaluation of the parameters (hydraulic properties) that control the movement and storage of water. Aquifer tests, performed by pumping a well at a constant rate and observing the resulting changes in hydraulic head in the aquifer, are the most commonly used method for determination of aquifer hydraulic properties. Unconfined aquifers, also known as water-table aquifers, are of particular interest to hydrogeologists and to the general public not only because of their accessibility as a water supply but also because of their vulnerability to contamination from activities at the land surface. Unconfined aquifers have special features that set them apart from other aquifer types and make analyses of tests conducted in them more difficult. The primary added complication has to do with the existence of the free surface (or water table) and the overlying unsaturated zone.

Background

Hydraulic parameters that control an unconfined aquifer's capacity to transmit and store water are generally obtained by aquifer-test analysis using one of several classical analytical models, the most popular of which are those of Boulton (1954, 1963), Dagan (1967), and Neuman (1972, 1974). The model of Boulton (1954) was the first to provide a plausible explanation for changes in hydraulic head observed in unconfined aquifers in response to pumping from a well. The model takes into account gradual drainage of water from the zone above the water table, a feature that is now, belatedly, becoming recognized as being important for unconfined aquifers. The Boulton model has the drawback, however, that it does not account for vertical components of flow in the aquifer and, consequently, cannot be used to evaluate vertical hydraulic conductivity: the model is strictly valid only at large distances from the pumped well where the flow might be assumed to

be horizontal. Also, because of the horizontal flow assumption, the model cannot account for effects of partial penetration by the pumped well. (This limitation was subsequently eliminated in a paper by Boulton and Streltsova, 1975.)

The Dagan (1967) and Neuman (1972, 1974) models both account for vertical components of flow in the aquifer and, hence, for effects of partial penetration by the pumped well, but neither consider effects of gradual drainage from the zone above the water table to be an important consideration. Both models assume drainage from the unsaturated zone to occur instantaneously in response to lowering of the water table. The Dagan model, in contrast with both the Boulton and Neuman models, has the additional limitation that it does not account for compressive characteristics of the aquifer and therefore cannot be used to evaluate aquifer specific storage. The Neuman (1972, 1974) model has come to be accepted by many hydrogeologists as the preferred model ostensibly because it appears to make the fewest simplifying assumptions and because of the perception that neglecting the effects of gradual drainage from the zone above the water table is reasonable for purposes of aquifer parameter estimation.

While both the Boulton and Neuman models account for aquifer compressive characteristics, they make the mathematical simplifying assumption that the pumped well is a line-sink (that is, the pumped well is assumed to be infinitesimal in diameter). Thus, it is impossible to account for effects of wellbore storage. This limits the usefulness of the models for accurate evaluation of specific storage. The line-sink assumption in these models requires that observation piezometers be located at large distances from the pumped well to reduce the influence of wellbore storage. Unfortunately, this last requirement makes it difficult to make accurate early-time measurements because of small drawdowns at large distances.

Use of the Boulton and Neuman models for analysis of early-time data from piezometers located near the pumped well may result in values

of specific storage that are overestimated by as much as one or two orders of magnitude (Moench, 1997), depending on aquifer compressibility. Moench (1997) extended the range of validity of the Neuman (1974) model by accounting for the finite diameter of the pumped well. This greatly improves upon the accuracy of specific storage estimates made by using drawdown data from piezometers located near the pumped well. It also makes it theoretically possible to evaluate other unconfined-aquifer parameters from pumped-well data. Unfortunately, however, effects of well-bore skin, turbulence, and other non-ideal flow conditions make the use of pumped well data difficult and frequently impossible for parameter estimation.

As mentioned above, the Boulton (1963) model differs from the Neuman (1974) model in that the latter assumes instantaneous drainage of water from the unsaturated zone and the former assumes the drainage occurs gradually in response to a lowering of the water table. Boulton (1954, 1963) approximates drainage from the zone above the water table by using an exponential relation containing an empirical parameter or 'delay index'. Neuman (1975) found that the delay index as used by Boulton (1963) is not a characteristic property of the aquifer. (He found it to be a function of radial distance from the pumped well.) Also, based on numerical modeling, Neuman (1972) found that effects of gradual drainage from the unsaturated zone could be neglected in aquifer tests. It has since been found, however, that there may exist a significant difference between measured field data and theoretical drawdowns in observation piezometers, particularly those located near the water table (see Moench, 1995). These differences exist independently of whether the Boulton model, which does not account for vertical components of flow in the saturated zone, or the Neuman model, which does not account for gradual drainage, is used.

In order to reduce the magnitude of this discrepancy and still account for vertical flow in the aquifer's saturated zone, Moench (1995) substituted Boulton’s (1963) convolution integral for Neuman’s (1972,

1974) boundary condition for the free surface and solved the revised boundary-value problem. By so doing, the redefined delay index becomes, for the particular test, a property of the homogeneous aquifer and associated homogeneous unsaturated zone, albeit not a very accurate one. No physical basis was assigned to the revised delay index other than that it could be considered the inverse of a "characteristic drainage time" for the particular medium. Nevertheless, the discrepancy between measured and theoretical drawdowns was diminished (over a limited time range) as seen in piezometers located near the water table (Moench, 1995). One reason that the discrepancy is not completely eliminated is likely due to Boulton's convolution integral not accurately describing the drainage process (see, Narasimhan and Zhu, 1993). Boulton's approach is based on the incorrect but plausible assumption that drainage from the unsaturated zone follows an exponential decline in response to a step decline in the elevation of the water table. Boulton and Pontin (1971) recognized deficiencies in Boulton's (1954, 1963) original theory; that is, the exponential relation did not accurately reflect physical reality and that it was necessary to account for vertical components of flow in the aquifer. To improve upon the single-parameter exponential relation, they used two exponential terms containing four adjustable parameters (two delay indices and two delayed yield parameters that when summed and added to a third parameter called 'instantaneous' yield, form the total specific yield). To account for vertical components of flow, they adapted the model of Dagan (1967) to meet their needs. Unfortunately, their model (like Dagan's) does not account for aquifer compressibility. Also, the treatment of specific yield (as the sum of three components rather than as a characteristic constant) is rather cumbersome for purposes of analysis.

In 1990, the U.S. Geological Survey (USGS) conducted an aquifer test at its Cape Cod Toxic Substances Research Site in Falmouth, MA in order to evaluate the hydraulic parameters of the unconfined aquifer. Moench and others (1996) provide a preliminary analysis of this test

using hand-measured drawdown data, the Neuman (1974) model, and traditional type-curve matching methods. The traditional approach to evaluation of the hydraulic parameters is by visual trial-and-error matching of field data with dimensionless type curves (for recommended procedures see, for example, Prickett, 1965; Kruseman and de Ridder, 1990; Moench, 1994; and Batu, 1998). A single match point was found that yielded excellent late-time matches between theoretical and measured drawdowns in the 16 piezometers used for the analysis. Thus, a single set of hydraulic parameters (vertical hydraulic conductivity, horizontal hydraulic conductivity, and specific yield) was obtained. The agreement suggested a remarkable degree of homogeneity in hydraulic conductivity to ground water flow at the scale of the test. Early-time drawdowns, however, recorded with the help of transducers located in seven of the piezometers and in the pumped well, and intermediate-time drawdowns recorded in all piezometers, but especially those located near the water table, could not be interpreted satisfactorily with the Neuman model.

Purpose and Scope

It is the purpose of this report to provide a thorough interpretation of the aquifer test that was conducted in the summer of 1990 at the USGS Cape Cod Toxic Substances Research Site in Falmouth, Mass. It is intended to expand upon the preliminary analysis of Moench and others (1996) by using a modification of a model developed by Moench (1997) and a method of automatic parameter estimation. The model modification is designed to permit an accurate representation of the process of gradual drainage from the zone above the water table.

The Moench (1997) model in its unmodified form allowed for evaluation of specific storage, and the other unconfined aquifer parameters, but did not fully account for discrepancies observed between measured and theoretical drawdowns calculated by the Neuman (1974) model in the intermediate-time range. Discrepancies that exist between

theoretical and measured drawdowns in the intermediate-time range are found to be a consequence of neglecting gradual drainage from the unsaturated zone. These discrepancies are only partially eliminated with a model that assumes exponentially declining drainage of water from the unsaturated zone in response to a step decline in the elevation of the water table (Moench, 1995, 1997). This is corroborated indirectly by the results of laboratory (Vachaud, 1968), field (Nwankwor and others, 1992), and numerical experiments (Narasimhan and Zhu, 1993). In this report, a necessary additional modification is made in the water-table boundary condition by including a series of exponential terms to represent drainage from the unsaturated zone caused by a decline in the elevation of the water table. The drainage in this instance is controlled by a finite number of empirical parameters α_M. It is not intended in this report that the empirical parameters α_M be ascribed a physical basis. However, it is possible to set up and solve a simple boundary-value problem demonstrating that the parameters can be used in combination to approximate the rate of flow across the water table in response to a step change in its elevation (R.L. Cooley, USGS, written commun., 2000).

In addition to the improved interpretation of the aquifer test, resulting from the model used, apparent homogeneity of the aquifer, and extent and quality of the data set, a number of secondary analyses are performed so that some general recommendations about unconfined aquifer tests can be made concerning: 1. the number of piezometers needed, 2. the placement of piezometers, 3. the timing and frequency of data sampling, and 4. the minimum test duration required to obtain satisfactory results. Computer simulations are also conducted to examine the consequences of specific model assumptions.

The scope of this report is limited to analyses of the aquifer test by means of an analytical model assisted by automated parameter estimation using nonlinear least squares. Because of the apparent homogeneity of the aquifer, the lack of interference from recharge or

evapotranspiration, and the apparent validity of the model assumptions, this aquifer test might be deemed a benchmark test and a good candidate for illustration of a broad range of unconfined aquifer phenomena.

Response of an Idealized Unconfined Aquifer to Pumping

Figure 1a is a schematic diagram showing a typical well/aquifer configuration and depicting the response of an idealized granular, homogeneous and anisotropic unconfined aquifer to pumping. The vertical (K_z) and horizontal (K_r) hydraulic conductivity vectors, the relative magnitude of which is indicated by the length of the arrows in the inset, indicate the anisotropic character of the aquifer. Flow to the finite-diameter pumped well is axisymmetric and three-dimensional.

Drawdowns (changes in hydraulic head due to pumping) in the pumped well may be greater than that in the aquifer adjacent to the well because of resistance to flow (wellbore skin) at the well screen. Vertical components of flow in the aquifer near the pumped well are enhanced if the length of the pumped-well screen is less than the full saturated thickness of the aquifer (that is, the pumped well partially penetrates the aquifer). Because of vertical components of flow, drawdowns observed in piezometers located near the pumped well cannot be assumed to accurately indicate the position of the falling water table. In addition, the response of finite-diameter piezometers to rapid changes in hydraulic head in the aquifer may be delayed due to wellbore storage in the piezometer.

With regard to the unsaturated zone in the idealized unconfined aquifer: 1. Water held by adsorption and surface tension in the unsaturated zone is in direct hydraulic connection with the falling water table. 2. The equilibrium moisture distribution in the unsaturated zone decreases monotonically with an increase in elevation (z_u) as depicted in figure 1a, where $\theta(z)$ is the moisture content and θ_s is the moisture content at saturation. 3. The zone of near saturation

immediately above the water table is referred to as the capillary fringe and will vary in thickness depending on the soil texture.

Figure 1b depicts a typical plot of drawdowns versus time (using double-logarithmic coordinates) and defines what is described in this report as 'early time', 'intermediate time', and 'late time'. The time ranges are approximate and would vary depending upon the aquifer parameters.

Hydrogeology of the Aquifer-Test Site

The aquifer at the study site is composed of unconsolidated glacial outwash sediments that were deposited during the recession, 14,000 to 15,000 years before present, of the late Wisconsinan continental ice sheet that had previously covered New England. Although the unconsolidated sediments in the test area overlie crystalline bedrock at a depth of approximately 300 ft, detailed lithologic studies indicate that there exists a transition from clean, medium to coarse-grained, high-permeability glacial outwash deposits to fine-grained, relatively low-permeability material at a depth of about 160 ft below the water table (LeBlanc, 1984; LeBlanc, and others, 1986; Masterson, and others, 1997). The horizontal hydraulic conductivity of the upper material in western Cape Cod generally, ranges from 150 to 350 ft/d with a ratio of horizontal to vertical hydraulic conductivity of 3:1 to 10:1. The horizontal hydraulic conductivity of the material below the transition ranges from 10 to 70 ft/d with a ratio of horizontal to vertical hydraulic conductivity of 30:1 to 100:1. The estimate of the saturated thickness is corroborated hydraulically by the preliminary analysis of the aquifer test (Moench and others, 1996).

Acknowledgments

The USGS Toxic Substances Hydrology Program provided funding for the aquifer test. The logistical and field support from the

Massachusetts District office is gratefully acknowledged. In particular, thanks are given to Kathryn M. Hess and Richard D. Quadri for their assistance during the field experiment. It is because of the careful work of all participants that the test successfully yielded the high quality data needed for the analysis. The analysis could not have been accomplished otherwise. The detailed and insightful reviews of the manuscript by Paul M. Barlow and Richard L. Cooley greatly enhanced the content and presentation of the report.

MATHEMATICAL MODEL

In this section the mathematical model of Moench (1997) is presented in a slightly modified form. The modification is to allow for improved representation of drainage from the zone above the water table. The bulk of the material in this section derives from Moench (1997). It is presented here for the convenience of the reader and to incorporate the necessary modifications.

Assumptions

As with all mathematical models, several simplifying assumptions are required. Most of the assumptions are identical to those of Neuman (1974). Those that are identical are as follows. 1. The aquifer is homogeneous, infinite in lateral extent, horizontal, and of uniform thickness. 2. The aquifer can be anisotropic provided that the principal directions of the hydraulic conductivity tensor are parallel to the coordinate axes. 3. Vertical flow across the lower boundary of the aquifer is negligible. 4. A well discharges at a constant rate from a specified zone below an initially horizontal water table. 5. The change in saturated thickness of the aquifer due to pumping is small compared with the initial saturated thickness. 6. The porous medium and fluid are slightly compressible and have physical properties that do not

vary in space or time. 7. The initial hydraulic head is the same everywhere.

The Neuman (1972, 1974) model assumes that water in the unsaturated zone is released instantaneously as the water table declines. It is pointed out in the introduction that, under this assumption, there may exist a significant difference between measured and theoretical drawdowns in piezometers located near the water table. The introduction of Boulton's (1963) convolution integral by Moench (1995) into the boundary condition for the free surface reduces this discrepancy. Moench (1995) assumed, as did Boulton (1954, 1963), that the vertical flux of water into the aquifer occurs in a manner that varies exponentially with time in response to a step decline in the elevation of the water table. The rate of exponential decline is controlled by an empirical constant α_1 (see Moench, 1995). (The subscript on α is included to avoid confusion with Boulton's reciprocal of 'delay index' (Boulton, 1963), which has a meaning that is slightly different from the α_1 used by Moench (1995). The difference in meaning is due to the fact that Boulton worked with vertically averaged heads (no vertical components of flow) in the aquifer and included the term containing α in the governing partial differential equation rather than as a boundary condition for the water-table.)

It is known, however, that the assumption of an exponential decline provides only a crude approximation of the actual drainage process (see, Vachaud, 1968; Narasimhan and Zhu, 1993). In this report, the representation of the actual drainage process can be made as precise as desired by extending the single, empirical-parameter approximation to multiple empirical parameters. It should be pointed out that the same set of parameters should not be assumed to accurately represent the reverse process (i.e., absorption of water during recovery) due to effects of hysteresis or entrapped air. Nor should it be assumed to represent the drainage process at a different time or

location. This is because conditions in the unsaturated zone may differ from time to time and place to place. Although, in this report, the empirical parameters are given little physical meaning individually, as a group they can be used to quantify drainage from the unsaturated zone in response to a driving force such as the lowering of the water table.

The assumptions pertaining to the finite-diameter pumped well are identical to those of Dougherty and Babu (1984) and are listed here as follows. 1. The head within the well does not vary vertically. 2. The radial flux from the aquifer to the well does not vary along the length of the screened section. 3. Vertical flux from the aquifer through the base of the well is negligible. 4. A thin skin of homogeneous porous material having no significant storage capacity may be present at the interface between the well screen and the aquifer. The hydraulic conductivity of this material may be less than or greater than that of the aquifer, and is assumed to be constant during the course of the aquifer test. (Low hydraulic conductivity skin may be present for a number of reasons as, for example, flow constrictions due to the well screen itself, bridging by sand particles across screen openings, or damage to the aquifer caused by drilling. High hydraulic conductivity skin may be due to well development or to the presence of a gravel pack installed to increase well productivity.)

The influence of a delayed response of the observation piezometers is often overlooked in the analysis of aquifer tests. The effect is treated approximately in this report (following Black and Kipp, 1977) by assuming the hydraulic head in an observation piezometer changes with a rate that is proportional to the head difference between the piezometer and the adjacent aquifer material. Delayed piezometer response is most important at early time when the head changes are most rapid, and if not taken into account, the estimate of specific storage may be exaggerated.

Figure 2 is a diagrammatic cross-section through a part of an idealized unconfined aquifer with a finite-diameter partially penetrating pumped well, an observation piezometer, and an observation

well (or long-screened piezometer). The figure illustrates the parameters used to define the well radii, the location of the screens, the location of the observation piezometer, and the saturated thickness of the aquifer. Also shown is the location of the origin of the coordinate system. Symbols used in the mathematical development are defined in the Notation section.

Boundary-Value Problem

The governing equation in the domain $r_w \le r \le \infty$ and $0 \le z \le b$ for axisymmetric flow to a pumped well in a slightly compressible, anisotropic, unconfined aquifer may be written as

$$\frac{\partial^2 h}{\partial r^2} + \frac{1}{r}\frac{\partial h}{\partial r} + \frac{K_z}{K_r}\frac{\partial^2 h}{\partial z^2} = \frac{S_s}{K_r}\frac{\partial h}{\partial t} \qquad (1)$$

The initial condition in the domain of equation 1 is

$$h_i - h(r, z, 0) = 0 \qquad (2)$$

where h_i is the initial hydraulic head. The outer boundary condition at $r=\infty$ is

$$h_i - h(\infty, z, t) = 0 \qquad (3)$$

The inner boundary condition at $r=r_w$ requires a wellbore balance equation for a partially penetrating well. Following Dougherty and Babu (1984), this condition is

$$2\pi\, r_w(\ell - d)K_r \left.\frac{\partial h}{\partial r}\right|_{r=r_w} = Q + C\frac{\partial h_w}{\partial t} \qquad b - \ell \le z \le b - d \qquad (4a)$$

where $\ell - d$ is the length of the screen, Q is the pumping rate, C is the wellbore storage (assumed constant), and h_w is the average head in the

wellbore. Ramey and Agarwal (1972) point out that effects of wellbore storage can occur as a result of changing liquid level in the well or, for confined and leaky aquifers, by virtue of wellbore-fluid compressibility in a pressurized test. Effects of wellbore storage are greatest when due to changing water level. In this case, C is the cross-sectional area of the free surface in the well. In this report, for convenience, $C=\pi r_c^2$ where r_c is the effective radius of the well in the interval where water levels are changing. The term “effective radius” is used here to allow for the presence of a column pipe or other tubing that might reduce the cross-sectional area of the pumped well in the vicinity of changing water levels.

The radial flow through the screen from the aquifer to the well, expressed by the left-hand-side of equation 4a, is assumed to be independent of z and to vary only with time. Ruud and Kabala (1997) found that flow variations along the well screen can be significant, especially for wells with short screen lengths in thick aquifers; however, the effect upon drawdowns in the wellbore was found to be insignificant.

The vertical average of the head in the wellbore, h_w, is related to the average head in the aquifer adjacent to the pumped-well screen, h^*, by

$$K_s \frac{(h^* - h_w)}{d_s} = K_r \left. \frac{\partial h}{\partial r} \right|_{r=r_w} \qquad (4b)$$

where K_s is the hydraulic conductivity of the wellbore skin, d_s is the skin thickness, and h^* is defined by

$$h^* = \frac{1}{(\ell - d)} \int_{b-\ell}^{b-d} h(r_w, z, t)\, dz \qquad (4c)$$

Equation 4b derives from the heat-flow literature (Carslaw and Jaeger, 1959, p. 20). For simplicity, the storage capacity of the skin is assumed negligible. One additional equation is required for completion of the boundary condition at the interface between the pumped well and the aquifer. Namely,

$$\left.\frac{\partial h}{\partial r}\right|_{r=r_w} = 0 \qquad \begin{matrix} z < b-\ell \\ z > b-d \end{matrix} \qquad (4d)$$

This condition implies that a well casing of constant external radius r_w extends from the top of the screened section to the water table, and that no radial flow occurs across an imaginary cylinder that extends from the bottom of the screened section of the well to the base of the aquifer.

The condition along the base of the aquifer (z=0) for $r \geq r_w$ is that of a no-flow boundary and is written as

$$\frac{\partial h}{\partial z}(r,0,t) = 0 \qquad (5)$$

The condition used by Moench (1997) at the water table (z=b) for $r \geq r_w$, which approximates the rate of drainage per unit area from the unsaturated zone, is written as

$$K_z \frac{\partial h}{\partial z}(r,b,t) = -\alpha_1 S_y \int_0^t \frac{\partial h}{\partial t'}(r,b,t)\exp[-\alpha_1(t-t')]\,dt' \qquad (6)$$

Moench (1995) provides details pertaining to the theoretical justification for the use of equation 6, which derives from the work of Boulton (1954). As $\alpha_1 \rightarrow \infty$, equation 6 approaches the boundary condition used by Neuman (1972, 1974). Also, it can be seen by inspection that if $\alpha_1 = 0$, a no-flow condition is obtained for equation 6 and the boundary-

value problem reduces to that solved by Dougherty and Babu (1984) for a confined, single-porosity aquifer.

It was stated at the beginning of this section that a single-parameter exponential relation doesn't represent drainage from the unsaturated zone very well. In this report, drainage from the unsaturated zone is represented by a modification to equation 6 such that, instead of the single exponential relation suggested by Boulton (1954, 1963), a finite series of M exponential terms is used, each with a different empirical parameter α_m:

$$K_z \frac{\partial h}{\partial z}(r,b,t) = -S_y \int_0^t \frac{\partial h}{\partial t'}(r,b,t) \sum_{m=1}^{M} \frac{\alpha_m}{M} \exp[-\alpha_m (t-t')]\, dt' \qquad (7)$$

The summation term in equation 7, in systems terminology, is an input response function or kernel of the convolution integral. It represents an average of a series of exponential terms. If M=1, equation 7 reverts to equation 6.

The parameters used in equation 7 might be found to differ from one aquifer test to the next, even at the same location, but are assumed to be unique for a given test. Due to the assumption of homogeneity, the same set of α_M parameters should apply irrespective of the location of the individual piezometers. This set of empirical parameters will be subject to change, however, as antecedent conditions in the unsaturated zone change. This arrangement allows the hydrogeologist to obtain not only better agreement between measured and predicted drawdowns over the entire intermediate time range of a time-drawdown curve but also allows for improved parameter estimation, as will be shown. The representation of the drainage process suggested by Boulton and Pontin (1971) makes use of two empirical α parameters and a combination of instantaneous, short-term, and long-term "delayed-yield" parameters summed together to represent specific yield. In this report, a single value of specific

yield is used in order to be consistent with the hypothesis that specific yield is a characteristic property of the aquifer and does not vary with time.

Dimensionless Boundary-Value Problem

By substituting the dimensionless parameters listed in table 1 into the above equations, one obtains the following dimensionless boundary-value problem:

$$\frac{\partial^2 h_D}{\partial r_D^{\,2}} + \frac{1}{r_D}\frac{\partial h_D}{\partial r_D} + \beta_w \frac{\partial^2 h_D}{\partial z_D^{\,2}} = \frac{\partial h_D}{\partial t_D} \tag{8}$$

$$h_D(r_D, z_D, 0) = 0 \tag{9}$$

$$h_D(\infty, z_D, t_D) = 0 \tag{10}$$

$$-\frac{\partial h_D}{\partial r_D} = \frac{2}{(\ell_D - d_D)} - W_D \frac{\partial h_{wD}}{\partial t_D} \qquad \begin{matrix} 1-\ell_D \le z_D \le 1-d_D \\ r_D = 1 \end{matrix} \tag{11a}$$

$$\frac{\partial h_D}{\partial r_D} = 0 \qquad \begin{matrix} z_D < 1-\ell_D; z_D > 1-d_D \\ r_D = 1 \end{matrix} \tag{11b}$$

$$h_{wD} = h_D^* - S_w \frac{\partial h_D}{\partial r_D} \qquad 1-\ell_D \le z_D \le 1-d_D \tag{11c}$$

$$h_D^* = \frac{1}{(\ell_D - d_D)} \int_{1-\ell_D}^{1-d_D} h_D(1, z_D, t_D)\, dz_D \tag{11d}$$

$$\frac{\partial h_D}{\partial z_D}(r_D, 0, t_D) = 0 \tag{12}$$

$$\frac{\partial h_D}{\partial z_D}(r_D, 1, t_D) = -\int_0^{t_D} \frac{\partial h_D}{\partial \tau}(r_D, 1, t_D) \sum_{m=1}^{M} \frac{\gamma_m}{M} \exp[-\gamma_m \sigma \beta_w (t_D - \tau)]\, d\tau \tag{13}$$

Laplace Transform Solution

Use of Laplace transforms and Fourier cosine series leads to a Laplace transform solution to the above dimensionless boundary-value problem. The derivation is provided in Appendix I. The Laplace transform solution for dimensionless drawdown in the pumped well is

$$\bar{h}_{wD}(p) = \frac{2(A + S_w)}{p(\ell_D - d_D)[1 + W_D p(A + S_w)]} \tag{14}$$

And the solution for the dimensionless drawdown in the aquifer is

$$\bar{h}_D(r_D, z_D, p) = \frac{2E}{p(\ell_D - d_D)[1 + W_D p(A + S_w)]} \tag{15}$$

where

$$A = \frac{2}{(\ell_D - d_D)} \sum_{n=0}^{\infty} \frac{K_0(q_n)\{\sin[\varepsilon_n(1-d_D)] - \sin[\varepsilon_n(1-\ell_D)]\}^2}{\varepsilon_n q_n K_1(q_n)[\varepsilon_n + 0.5\sin(2\varepsilon_n)]} \tag{16}$$

$$E = 2\sum_{n=0}^{\infty} \frac{K_0(q_n r_D)\cos(\varepsilon_n z_D)\{\sin[\varepsilon_n(1-d_D)] - \sin[\varepsilon_n(1-\ell_D)]\}}{q_n K_1(q_n)[\varepsilon_n + 0.5\sin(2\varepsilon_n)]} \tag{17}$$

$$q_n = (\varepsilon_n^2 \beta_w + p)^{1/2} \tag{18}$$

$$q_n r_D = (\varepsilon_n^2 \beta + p r_D^2)^{1/2} \tag{19}$$

and ε_n, where n=0,1,2,…, are the roots of

$$\varepsilon_n \tan(\varepsilon_n) = \frac{p}{M} \sum_{m=1}^{M} \frac{1}{(\sigma\beta_w + p/\gamma_m)} \tag{20}$$

K_0 and K_1 are the modified Bessel functions of the second kind and of zero and first order, respectively.

For long screened piezometers (observation wells) it is assumed that the measured drawdown is the average drawdown over the screened interval z_{D2}-z_{D1} as determined by

$$\bar{h}_D(r_D, z_{D1}, z_{D2}, p) = \frac{1}{z_{D2} - z_{D1}} \int_{z_{D1}}^{z_{D2}} \bar{h}_D(r_D, z_D, p)\, dz_D \tag{21}$$

The Laplace transform solution for dimensionless drawdown in a long-screened piezometer in the aquifer then becomes

$$\bar{h}_D(r_D, z_{D1}, z_{D2}, p) = \frac{2E'}{p(\ell_D - d_D)[1 + W_D p(A + S_w)]} \tag{22}$$

where

$$E' = 2\sum_{n=0}^{\infty} \frac{K_0(q_n r_D)\{\sin[\varepsilon_n(1-d_D)] - \sin[\varepsilon_n(1-\ell_D)]\}}{\varepsilon_n q_n K_1(q_n)[\varepsilon_n + 0.5\sin(2\varepsilon_n)]} \cdot \frac{[\sin(\varepsilon_n z_{D2}) - \sin(\varepsilon_n z_{D1})]}{(z_{D2} - z_{D1})} \tag{23}$$

Equations 15 and 22 are solutions for head changes in the aquifer. Observation wells or piezometers used to measure hydraulic head variations in an aquifer are often open holes containing a significant quantity of stored water. With the start of pumping, rapid changes in head in the aquifer may not be accurately reflected by measurements in the piezometer because of the finite time it takes to dissipate stored water and come into equilibrium with the hydraulic head in the aquifer. This delayed piezometer response is important for accurate evaluation of specific storage and is treated analytically in the manner described in detail by Moench (1997). By choosing an appropriate shape factor F'=F/2π, where F is defined by Hvorslev (1951) for various geometrical configurations, and, assuming good hydraulic connection between the piezometer and the aquifer so that screen clogging is not a factor, it

is possible to account for delayed piezometer response by use of the following equation:

$$\bar{h}_{mD} = \frac{\bar{h}_D}{1 + W'_D\, p} \qquad (24)$$

where $\bar{h}_{mD}$ is the Laplace transform solution for the piezometer response and W'_D is the dimensionless piezometer storage parameter defined in table 1. In the event that screen clogging is a factor, it is possible to estimate F for use in (24) by slug testing the piezometer and following the procedure indicated by Black and Kipp (1977).

Dimensionless or dimensional drawdowns are obtained by numerical inversion of equations 14, 15, or 22. The Stehfest (1970) algorithm is particularly useful in this regard because of its computational efficiency. The FORTRAN code WTAQ3 (Moench, 1997) was modified to enhance speed of computation and to include the summation in equation 20. The modified computer code WTAQ3 used in this report can be sent to interested readers upon request from the first author. Available for downloading from the World Wide Web is a fully documented computer program WTAQ, described by Barlow and Moench (1999), that includes all the physical processes available in WTAQ3. It can be used for both type-curve analysis and automated parameter estimation for both confined and unconfined aquifers.

AQUIFER-TEST DESIGN AND OPERATION

As part of an effort to quantify the hydraulic properties of the unconfined, sand and gravel, glacial-outwash aquifer at the Cape Cod Toxic-Substances Hydrology Research site near Falmouth, Massachusetts, a three-day aquifer test was carried out from August 28-31, 1990. The test was conducted by pumping a well at a constant rate and by observing the resulting changes in hydraulic head at locations that differ in distance and azimuth from the pumped well and in depth below the water table.

Figure 3 shows the location of the study area and the locations in plan view, within an abandoned gravel pit, of the pumped well and points of observation. The reference piezometer (F343-036) is included in figure 3 as its position is the location of the origin of coordinates of a magnetic north-oriented grid that was overlaid on the site and used to locate the positions of points of observation for this study and others (LeBlanc, and others, 1991). Figure 4 illustrates the positions of the observation well screens in vertical section and is drawn roughly to scale. The pumped well was drilled in July 1990 by cable tool methods to a depth of 80 ft below land surface. An 8-inch, inside-diameter (i.d.) polyvinyl chloride (PVC) casing was installed with an 8-inch i.d. PVC screen along the bottom 47 ft of the well. Backfill consisted of natural collapse material and cuttings from the hole. The top and bottom of the screen were located 13.2 and 60 ft, respectively, below the initial water table, which was approximately 19 ft below land surface. Immediately prior to the test, the elevation of the water table at the pumped well was 46.80 ft above mean sea level. The regional temporal trend of the water table was determined by measuring the elevation of the water table, in areas unaffected by pumping, before, during, and after the aquifer test. The water table was found to have declined at a rate of 9.26×10^{-6} ft/min over this time period,

requiring a slight correction (diminution) in the late-time drawdown data. Observation piezometers and wells were constructed by auguring to prescribed depths and installing 2-inch i.d., PVC casings with 2-ft-, 9-ft-, or 39-ft-long PVC screens. Details with regard to the exact radial and vertical positions and lengths of the well screens are given in table 2. Henceforth, for convenience, the various observation piezometers and wells will be referred to as piezometers regardless of the length of the screen.

Well F507-080 was pumped at a rate of approximately 320 gal/min (42.8 ft^3/min) for 72 hours. Discharge water was diverted through a fire hose to a Massachusetts Military Reservation sewage-infiltration bed located about 500 to 600 ft up gradient (north) of the test area. The rate of well discharge was monitored (1) by a manometer and orifice at the discharge point in the infiltration bed and (2) by noting the time required to fill a 55-gal drum at the end of the fire hose. Adjustments to the wellhead valve were made as necessary to maintain a constant flow rate.

Water levels in all piezometers were measured manually using a steel tape. In addition, drawdown data were collected in the pumped well and in seven piezometers with pressure transducers connected to data loggers. An electric tape was used for manual collection of drawdown data in the pumped well. Recovery measurements also were made in selected piezometers and in the pumped well.

Appendix II (fig. A-K) shows plots of the drawdown data used for analysis, which have been corrected for the regional decline of the water table, mentioned above. Where transducer data are available, the plots show hand-measured values at late time (solid circles) continuing beyond the transducer values (dots). This is because, after about 300 min of pumping, the transducer values of drawdown are discarded since, with one exception (F377-037), they appear to drift apart from the hand-measured values. The latter are considered more accurate than the transducer values in the late-time range. Values of drawdown (open

diamonds, squares, and circles) selected for use in the automatic parameter estimation algorithm are also shown. Numerical values for parameter estimation are listed in Appendix II table A. Recovery data are not analyzed in this report, but were measured in three piezometers with transducers (F505-032, F504-032, and F377-037). All measured data (both drawdowns and recovery) are available from the USGS in electronic form.

ANALYSES

Preliminary Analysis

The preliminary analysis of Moench and others (1996) involved traditional type-curve matching procedures using Neuman's (1974) model and late-time drawdown data to obtain the aquifer parameters K_r, K_z, and S_y. Type curves were generated with WTAQ1 (Moench, 1993) for the particular well screen/aquifer configuration, taking partial penetration of the pumped well into consideration and assuming the saturated thickness to be a known quantity. This preliminary analysis involved use of the hand-measured data only, because the rapidly changing early-time data, required for evaluation of S_s, was not needed. The preliminary analysis involved the use of composite plots of drawdowns versus time divided by the square of the distance between the observation point and the pumped well (double logarithmic plots of h vs. t/r^2). The procedure is essential for accurate evaluation of the aquifer hydraulic properties by analytical methods (see Moench, 1994) as it allows the hydrogeologist to obtain a single match point and, hence, a single set of hydraulic parameters for data obtained from a number of observation points simultaneously.

Initially, based on limited local well-log information, a saturated thickness of 80 ft was assumed (see Hess and others, 1992). This resulted in three problems: (1) complete inability to match theoretical type curves with composite plots of drawdown data from piezometers located near the pumped well, (2) significant differences between the estimated parameters and estimates based on prior studies (for example, the value of K_r obtained by the Jacob method was twice the expected value), and (3) having to account for head variations in a

piezometer located 28 ft below the assumed base of the aquifer. A second analysis was then performed after doubling the saturated thickness to 160 ft. The justification for this change was not just based on the three problems listed but also on regional geological studies (see LeBlanc, 1984, fig. 5) that indicate the presence of a sharp transition from very coarse to very fine-grained sediments with increased depth at about 150 ft. Upon changing the saturated thickness to 160 ft, an estimate of K_r was obtained that was consistent with prior studies at the site, and excellent matches were obtained for composite plots of all late-time drawdowns leading to a single match point (see Moench and others, 1996). The values of vertical and horizontal hydraulic conductivity and specific yield calculated from the match point are given in table 3. Also shown in table 3 is the value of saturated thickness b that was derived, in part, from the preliminary analysis. The fact that a doubling of the saturated thickness could make such a difference in the theoretical responses was an indication that an aquifer test conducted in a homogeneous aquifer might be used to obtain an estimate of saturated thickness (in addition to the primary unconfined aquifer parameters). The agreement between the hand-measured drawdowns and the theoretical late-time responses, obtained with a single set of hydraulic parameters, provide support for the primary assumptions in the Neuman model that control late-time piezometer responses. The preliminary analysis also shows that the use of an incorrect estimate of the saturated thickness could lead one to conclude that the lack of agreement between measured and theoretical responses is due to aquifer heterogeneity.

Analysis by Nonlinear Least Squares

In this report, various analyses are performed by automatic nonlinear parameter estimation using the model WTAQ3 (Moench, 1997). In this approach, differences between simulated drawdowns based on

estimated hydraulic parameters and measured (observed) drawdowns are minimized using a weighted sum of squared errors objective function. The parameter-estimation code used in this report, PEST[#] (Doherty, 1994) and the upgraded version PEST2000, runs WTAQ3 repeatedly while automatically varying the hydraulic parameters in a systematic manner from one run to the next until the objective function is minimized. Statistics are provided showing the precision of the estimated parameters (for example, the 95 percent confidence limits, and correlation coefficients). The literature on automatic parameter estimation is extensive and is not reviewed in this report. Papers by Poeter and Hill (1997) and Hill (1998) provide excellent discussions of the methodology. The manual and code documentation that comes with PEST software provides additional helpful information regarding parameter estimation methodology.

Proper use of PEST, or any parameter estimation algorithm, often requires a certain amount of fine-tuning accomplished only by trial and error. Such adjustments involve, for example, the proper selection of initial parameter estimates, whether or not to use logarithmic parameter transformations, or other adjustments necessary to optimize PEST's performance. Probably because of the relatively high quality of the test data and the scale of the aquifer test relative to the correlation length of the heterogeneity (discussed at greater length later in the report), the necessary trial and error adjustments were minimal for the analysis of the Cape Cod data reported here.

In this report, a systematic (5 step) approach to data interpretation was taken in order to gradually gain confidence in the validity of the parameters obtained by the parameter estimator.

1. The parameters S_y, K_r, and K_z were estimated using very late-time data and the instantaneous drainage assumption. This allowed for

---

[#] The use of this product does not imply endorsement by the U.S. Government

comparison with estimates reported in the preliminary analysis (Moench and others, 1996).

2. The parameters S_y, b, K_r, and K_z were estimated using very late-time data and the instantaneous drainage assumption. This again allowed for comparison with parameter estimates reported in the preliminary analysis.

3. Based on the previously estimated aquifer parameters, the late-time pumped-well data were used alone to obtain the wellbore skin factor (S_w).

4. The parameter S_s was estimated with the exclusive use of very early-time transducer data, the previously obtained aquifer parameters, the wellbore skin factor, and by accounting for delayed piezometer response.

5. Finally, under the gradual drainage assumption, the complete data set with 461 drawdown values in 20 piezometers was analyzed with PEST to obtain all relevant aquifer parameters simultaneously (S_s, S_y, b, K_r, K_z, and three empirical α_m parameters). Table 2 provides the numbers used by the parameter estimator to identify the measured observations.

Evaluation of S_y, K_r, K_z Using Late-Time Data (Step 1)

An analysis was performed on drawdowns measured in all piezometers at times greater than one day (about three values for each piezometer at approximately 2,000, 3,000, and 4,300 minutes; see Appendix II figures B-K). The analysis assumes instantaneous drainage from the unsaturated zone. With the chosen saturated thickness of 160 ft, used in the preliminary analysis by Moench and others (1996), the parameter-estimation code produced the parameter values listed in table 4. Table 4 also shows the upper and lower values of the 95 percent confidence limits and initial values used in the simulation. The 60 observation

values used in the simulation were given equal weights. The parameter values in table 4 agree reasonably well with the values shown in table 3, although S_y in table 4 is about 25 percent greater than the value in table 3. This difference is apparently a consequence of the reduced time span of the selected data and the unbiased treatment performed by parameter-estimation code as compared with visual type-curve matching. An experiment conducted by using a reduction in the initial time span (2,000-4,300 min), to 3,000-4,300 min, gave rise to an increase in the value of S_y from 0.287 to 0.304, which is consistent with what one might expect as a consequence of gradual drainage from the unsaturated zone. In the reverse sense, if the time span is expanded to include values of time closer to the start of pumping, the estimated values of S_y decrease, evidently as a consequence of the assumption of instantaneous drainage. Such was the case in the analysis of the hand-measured data from this aquifer test performed by Heidari and Moench (1997, table 5) whereby only the first 10 minutes of data were excluded from the analysis and a value of S_y=0.183 was obtained. In general, attempts to incorporate as much data as possible from the intermediate-time range without placing emphasis on the late-time data can explain the relatively small values of specific yield often obtained by both visual type-curve matching and by methods of automatic parameter estimation.

Evaluation of S_y, b, K_r, K_z Using Late-Time Data (Step 2)

Results of a PEST simulation with the same data set but allowing the saturated thickness to be one of the estimated parameters is shown in table 5. Interestingly, the estimated saturated thickness is close to the value of 160 ft chosen for use in the preliminary analysis. The finding suggests that late-time drawdown measurements in piezometers properly located in the aquifer are sensitive to the effective base of the saturated zone. Unfortunately, other factors may be at play, such

as possible leakage from the fine-grained material underlying the aquifer and/or flow paths diverted by heterogeneous materials or lithologic structures located in the aquifer at depth. These factors might lead to an estimated saturated thickness (based on the hydraulic data) that is, by coincidence, close to the value obtained from the geologic cross section. Results from additional, carefully designed aquifer tests conducted in homogeneous unconfined aquifers are therefore needed before hydraulic tests can be considered an effective method to identify aquifer thickness.

Evaluation of S_w Using Late-Time Pumped-Well Data (Step 3)

In addition to the aquifer parameters evaluated from the late-time piezometer data, it was necessary to use late-time pumped-well data (Appendix II, fig. A) to evaluate the wellbore skin factor (S_w). The latter was needed for an improved estimate of specific storage (S_s), as shown in the next section. If the ability of a skin to transmit water is less than that of the aquifer, drawdowns in the pumped well are enhanced, and there is an apparent increase in wellbore storage, the consequence of which is to reduce drawdowns in the aquifer at early time over the value that would have been obtained with no skin (see, Moench, 1985, figure 7b). If the hydraulic conductivity of the skin is enhanced over that of the aquifer (as by gravel pack or well development), drawdowns in the pumped well are decreased and there is an apparent decrease in wellbore storage, which increase drawdowns in the aquifer at early time. The decrease in wellbore storage in this instance is due to an effective increase in wellbore radius r_w as a consequence of the gravel pack or well development (see table 1). Because an accurate evaluation of specific storage is dependent on proper analysis of early-time data, it is important to obtain an estimate of S_w (or an effective r_w). The factor S_w is easily evaluated by a trial and error comparison

of measured late-time pumped-well data with drawdowns predicted for the pumped well at late time using known values of the aquifer parameters and known pumped-well dimensions. This can be accomplished by visual data matching or by automated procedures.

Using the parameters listed in table 5, a negligibly small value of specific storage, and the drawdown data in Appendix II (table A) for the pumped well (F507-080), the PEST algorithm yields S_w=1.375 with a 95 percent confidence range of 1.301 to 1.454. Figure 5 shows a plot of measured and simulated drawdowns using the parameters in table 5 and S_w=1.4. The curves in figure 5 for S_w=1.2 and 1.6 demonstrate the sensitivity of drawdowns in the pumped well to variation in wellbore skin. Note that the larger value of S_w in figure 5 produces greater theoretical drawdowns in the pumped well. Additional discussion and analysis of the pumped well data can be found in the discussion section.

Evaluation of S_s Using Early-Time Data (Step 4)

With estimates of the aquifer parameters (S_y, K_r, and K_z) and the wellbore skin factor (S_w) obtained from late-time data, it was possible to estimate the specific storage (S_s) of the aquifer. The additional parameters needed for the computations are the wellbore radii for the pumped well (r_c and r_w), and the radii (r_p) and screen lengths (L) of the observation piezometers. Inclusion of delayed piezometer response can be accomplished either by slug testing each piezometer, which is the recommended approach if piezometers respond slowly to slug testing, or by use of a theoretical formula derived by Hvorslev (1951). The latter was used in this report and was obtained from the following formula (Moench, 1997):

$$F' = \frac{L}{\ln[x + (1 + x^2)^{1/2}]} \qquad (25)$$

where $x=kL/2r_p$, $k=(K_r/K_z)^{1/2}$, and $L=z_2-z_1$. The screen length L is given in table 2, r_p=1 inch for all piezometers, and K_r/K_z has been determined from the late-time data (table 5). From Appendix II (fig. B-E, which show drawdowns in the piezometers that have transducers), it is evident that early time data exist only for a few tens of seconds after the onset of pumping.

In this section, for estimation of S_s, the analysis was performed using only the first 6 values of drawdown selected for PEST (see fig. B-E, Appendix II) from piezometers F505-080 and F504-080, the first 5 values from piezometers F504-060, F505-032, F504-032, and F377-037, and the first 4 values from piezometer F505-059. The values of S_y, K_r, K_z and b used were those in table 5, and the value of S_w (1.4) was that determined in the previous section. From these early-time values of drawdown only the estimated value of S_s was determined to be 1.26×10^{-5} ft^{-1}.

It is of interest to note that if delayed piezometer response is not included in the analysis, the value of S_s is increased by 50 percent to 1.97×10^{-5} ft^{-1}, demonstrating that an accurate estimate of specific storage requires inclusion of this effect. It is also of interest to determine the value of S_s obtained if effects of wellbore skin are not included in the analysis. Ignoring the effects of both wellbore skin at the pumped well and delayed piezometer response results in a value of S_s equal to 2.33×10^{-5} ft^{-1}. If a line-source model is used a value of S_s equal to 3.6×10^{-5} ft^{-1} is obtained.

Having estimated the primary aquifer parameters from the late-time data, and the specific storage from the early-time data, it should be noted that the parameters can also be estimated simultaneously, using

PEST, by weighting the early-time data and late-time data equally and giving the intermediate-time data zero weight. The results of such an analysis are shown in table 6, with small differences in parameter values from those in table 5. Figures 6-12 show the comparison of measured and simulated drawdowns, using the parameters in table 6 and assuming instantaneous release of water from the unsaturated zone.

Evaluation of S_s, S_y, b, K_r, K_z, and α_m Using Data for Entire Time Range (Step 5)

Drawdowns in the shallow piezometers that have transducers clearly show the early-, intermediate-, and late-time ranges defined in the Introduction (see the responses for piezometers F505-032, F504-032, and F377-037 illustrated in fig. 8 and 9). It is evident upon close examination of figures 6-12 that the difference between measured and simulated drawdowns in the intermediate-time range is most apparent in piezometers closest to the water table and that the difference appears to increase with distance from the pumped well. Any attempt to estimate the aquifer parameters by visual or automated methods without accounting for this difference is likely to yield inaccurate results. Accuracy can be improved by avoiding the use of shallow piezometers as discussed by Moench (1994), or by restricting the analysis to very late-time data and early-time data as was done to obtain the parameter estimates in table 6.

As discussed previously, it is possible to account for effects of gradual drainage by insertion of a modified form of the Boulton (1963) integral, which includes more than one empirical parameter, into the boundary condition for the free surface (see equation 7). To demonstrate that three empirical parameters are necessary and apparently sufficient for the model to simulate actual drawdowns in the intermediate-time range, parameter-estimation runs were made by fixing the primary hydraulic parameters with the values given in table 6 and

allowing the algorithm to estimate the best-fit empirical parameters using data from piezometer F377-037 (figure E, Appendix II). Figure 13 compares measured data with the simulated responses for instantaneous drainage (fig. 13a), and gradual drainage using one (fig. 13b), two (fig. 13c), or three (fig. 13d) parameters. Experimentation led to the conclusion that three parameters are adequate for purposes of parameter estimation for this aquifer test. Because of local head variations caused by aquifer heterogeneity, the use of additional empirical drainage parameters did not appear justified.

Table 7 shows the values of the 5 characteristic aquifer parameters and 3 empirical parameters estimated simultaneously using the PEST algorithm. The complete set of evenly weighted drawdown data from all 20 piezometers was used (see Appendix II, figures B-K and table A). A unit weight was applied to each data point. Experiments with different weighting schemes resulted in little or no change in the estimated primary water-table parameters. For example, when weights were made proportional to the ratio of maximum drawdown in a given piezometer to the value at the time of interest, the estimated value of S_y decreased about 1 percent, K_r and K_z each increased about 2 percent, the value of b increased by about 4 percent, and the value of estimated S_s increased from 1.3×10^{-5} ft^{-1} to 2.3×10^{-5} ft^{-1}. The value of wellbore skin (S_w=1.4) required for the computations had been determined independently, as discussed previously.

The correlation coefficient matrix provided by PEST for the results presented in table 7 is shown in table 8. The table suggests that the various estimated parameters should be independent of one another; that is, the estimated value of one parameter does not significantly influence the estimated value of any other. However, because of the method used by PEST to calculate the correlation coefficients, the reader is cautioned against placing a great deal of reliance on values that differ significantly from unity (Hill, 1998). A

recommended approach to examine the uniqueness of the estimated parameters is to rerun PEST using different initial parameter estimates. The results of one rerun are shown in table 9, and are offered as evidence of the reproducibility of the results in table 7. Differences in the estimated values do not have a noticeable effect upon simulated drawdown responses. The reproducibility in tables 7 and 9 is due in large measure to the quality and quantity of the data set. It is shown in the discussion section of this report that the use of a limited number or arrangement of piezometers may not always provide consistent and unique results.

Comparisons of observed and simulated drawdowns based on the parameters in table 7 are shown in figures 14-20. The degree of agreement between observed and simulated drawdowns demonstrates that: (1) the relevant physical processes occurring in the course of the aquifer test appear to not only include the horizontal and vertical flow and storage of water in the aquifer, but also the time-dependent drainage of water from the unsaturated zone across the water table and (2) the scale of the aquifer test (that is, the pumping rate and the size of the drawdown cone) was large enough that the known aquifer heterogeneity at this site (Hess and others, 1992) had little influence on the properties estimated from the aquifer test analysis. (The inter-bedded nature of the sand and gravel, glaciofluvial deposits is revealed in a photograph published by LeBlanc and others (1991, fig. 3) and described by Hess and others (1992, p. 2012).) The estimated parameters (S_s, S_y, b, K_r, and K_z) are entirely reasonable for this type of aquifer and can be supported, in part, by independent investigations at the site (Hess and others, 1992; Springer, 1991).

DISCUSSION

Many hydrogeologists would likely agree that the aquifer test analyzed in this report is atypical. Not only is the scale of the test large enough to average the effects of smaller-scale heterogeneity in the aquifer, but also there appear to be few or no interfering effects (for example, effects of recharge or discharge due to precipitation or evapotranspiration, extraneous pumping, lateral boundaries, and so forth) over the duration of the test. In addition, the test was designed and executed with a minimum of problems: the pumping rate varied only slightly over the course of the test; the pumping rate was set at a rate that was sufficiently great to obtain accurate drawdown measurements, but not so great as to cause significant changes in saturated thickness near the pumped well; the well-discharge disposal site was sufficiently remote that infiltrating water had a negligible effect upon evaluation of aquifer parameters or prediction of aquifer response; and, the piezometers were positioned at such depths and distances that the aquifer parameters could be accurately diagnosed from the transducer and hand-measured drawdown data. Although the aquifer test described in this report is ideal in several respects, the approach used here should be applicable elsewhere given data of sufficient quality and quantity.

Parameter values in table 5 show that Neuman's model, which assumes instantaneous drainage from the unsaturated zone and a line source for the pumped well, yields reasonable estimates of the primary unconfined aquifer parameters S_y, K_r, and K_z when using late-time test data. It also appears that Neuman's model produces an estimate of the saturated thickness of the aquifer that is consistent with that which is known from the regional geology. As mentioned previously, leakage from the "impermeable" base of the aquifer and, perhaps, undetected heterogeneity at depth, casts some doubt on whether an aquifer test

analysis can be used in general for the estimation of aquifer thickness. To obtain accurate estimates of these four parameters with the Neuman (1974) model, the aquifer test should be run without interference from extraneous influences for an extended period of time (three days, in the test examined here), the analysis must be weighted heavily toward the late-time data (times greater than 2,000 minutes), the piezometers should be located near a partially penetrating pumped well at various depths and distances such as illustrated in figures 3 and 4, and the model assumptions must be reasonably met.

Results illustrated in figures 6-12 demonstrate that the assumption of instantaneous drainage from the unsaturated zone does not provide a satisfactory description of flow processes in the time range of about 1 to 1,000 minutes. All piezometers, with three exceptions, show significant differences between measured and theoretical responses in this time range. The three exceptions (F505-059, F505-080, and F504-080) are relatively deep piezometers located in close proximity to the pumped well where effects of drainage from the unsaturated zone, although present, do not manifest themselves to the same extent as in the other piezometers. The differences between measured and theoretical drawdowns in the logarithmic plots shown in figures 6-12 are greatest in piezometers located closest to the water table, and appear to increase with distance from the pumped well. It is of interest to note that the short-screened piezometers located closest to the water table are still at least 9 ft below the water table. Thus, one might expect to see even greater differences in piezometers located closer to the water table. In addition, the aquifer is coarse-grained and highly permeable, so one might expect to find still greater differences in aquifers that are less permeable.

The above findings, demonstrated in figures 6-12, contradict statements by Neuman (1972, 1974, 1975, 1979, 1987) that drawdowns in unconfined aquifers are not significantly affected by drainage from the unsaturated zone. It is only in the three deep-seated piezometers

located close to the pumped well (F505-059, F505-080, and F504-080), mentioned above, that Neuman's assumption of instantaneous drainage might appear to be satisfactory. This point is examined in greater detail toward the end of this discussion. In general, if automated methods are used for parameter estimation with models that assume instantaneous drainage from the unsaturated zone, without judicious weighting of the data to eliminate intermediate-time data (and early-time data if line-source models are used), then one should be skeptical of the validity of the estimated parameters. On the other hand, if type-curve methods are used for parameter estimation with models using the instantaneous drainage assumption, an experienced practitioner can accomplish the judicious weighting visually and the results should be satisfactory.

The results shown in figures 14-20 demonstrate that the differences (seen in fig. 6-12) between theoretical and measured drawdowns can be almost entirely eliminated by use of a single set of three empirical parameters, estimated by PEST, designed to account for the effects of gradual drainage of water from the unsaturated zone across the water table. The fact that the same set of empirical parameters essentially eliminates the intermediate-time discrepancies in all piezometers simultaneously shows that they can be considered constants for this particular aquifer test. As discussed in the section that follows, minor deviations between measured and simulated drawdowns as seen in one plot relative to another in figures 14-20 appear to be randomly distributed and can be attributed to local variations in aquifer properties (heterogeneity). Two possible exceptions to this statement can be seen in figure 19a and 19b for piezometers F385-032 and F376-037, which are located about 225 ft north of the pumped well (see fig. 3). Close examination of figure 19 reveals that the measured late-time drawdowns in these piezometers is less than the expected drawdowns based on the simulated responses. A likely explanation for these diminished drawdowns, which are in the range of 0.01-0.03 ft after about

1,000 minutes of pumping, is the influence of recharge from the disposal of the well discharge water in the infiltration pit some 300-400 feet further north.

Effect of Heterogeneity on Aquifer Test Results

Although the fit of the gradual drainage model to drawdown measurements is quite good, there are minor differences noted between simulated and measured drawdowns (see fig. 14-20). The analysis approach used in this report was to fit all of the observations of drawdown as a group, and in so doing, produce an estimate of the average aquifer properties. It was expected that there would be differences (errors) between the simulated and measured drawdowns caused by local variations in aquifer properties (that is, aquifer heterogeneity, primarily in hydraulic conductivity), and that these deviations would be small and random in distribution across the area of the aquifer test. In general, these differences can be characterized as minor fluctuations in an otherwise uniformly varying drawdown distribution around the pumped well. The output from the PEST algorithm for the results in table 7 indicate the sum of squared residuals between simulated and measured drawdowns to be 0.0848 ft^2, from which the variance and standard deviation are calculated to be 1.75×10^{-4} ft^2 and 0.013 ft, respectively. Deviations from the mean head distribution are expected at the test site because the aquifer is mildly heterogeneous (Hess and others, 1992), and the variations in aquifer properties (particularly hydraulic conductivity) produce perturbations in the head field relative to the mean distribution.

A comparison of aquifer characteristics developed as a result of this test to those reported by Hess and others (1992) for the same aquifer help put the effects of heterogeneity on the test results reported here in some context. The average values of horizontal and vertical hydraulic conductivity found by Hess and others (1992) were

0.123 cm/s (0.242 ft/min) and 0.099 cm/s (0.195 ft/min), respectively. These compare closely with the values reported for this test (K_r=0.233 ft/min and K_z=0.142 ft/min, see table 7) considering the comparatively large radial and vertical extent of the aquifer test. Measurements of horizontal hydraulic conductivity reported by Hess and others (1992) were made using flowmeter tests conducted in the upper 25 ft of the saturated zone. Estimates of vertical hydraulic conductivity were made using geostatistical analyses, as was the spatial correlation structure of the aquifer. The flowmeter tests are small-scale single-well tests conducted in wells located within the cone of depression of the aquifer test approximately 30-50 ft northeast of the pumped well. The flowmeter tests produced hundreds of small-scale measurements of hydraulic conductivity in the upper aquifer, and the above values are geometric means of those measurements. The close comparison between the results of these two independent sets of experiments indicates that not only are the results of the aquifer test good estimates of average conditions, but also that the average hydraulic conductivity values don’t vary much at the scale of the aquifer test. This latter conclusion supports the assumption of homogeneity made for the analysis reported here, if homogeneity is viewed in an average sense. That is, although the aquifer is known to be heterogeneous, the statistical variability of the aquifer properties is constant across the area of the test, and therefore, the average aquifer properties remain constant over the area of the test.

Hess and others (1992) also estimated a variance of 0.24, a horizontal correlation scale of 3.5-8 m (11.5-26.2 ft), and a vertical correlation scale of 0.19-0.38 m (0.62-1.25 ft) for log hydraulic conductivity (ln K_r) at the site. These estimates indicate that the sand and gravel sediments at the site are mildly heterogeneous and that the correlation scales are about the same size as the lenses and layers that compose the aquifer (see photograph in LeBlanc and others, 1991,

fig. 3; and description by Hess and others, 1992, p. 2012). A comparison of the correlation scales to the size of the cone of depression formed during the aquifer test, with measurable drawdowns over a radial distance of over 200 ft (60m) and depth below the water table of up to 110 ft, also indicate that the size of the aquifer test was many times larger than of the aquifer correlation scales. This is additional evidence that the aquifer test very likely integrated the effect of many different values of hydraulic conductivity, and that the analysis of the test measurements should result in a good estimate of the average values of the aquifer properties.

The value of the variance of ln K_r can be used to estimate the expected anisotropy of aquifer hydraulic conductivity (the ratio of horizontal to vertical hydraulic conductivity) by use of an equation modified from the results of Gelhar and Axness (1983, equation 59):

$$K_r/K_z = (1+\alpha_f^2/2)/(1-\alpha_f^2/2) \qquad (26)$$

where α_f^2 is the variance of ln K_r. Using the value of ln K_r variance given above (0.24), this equation produces an aquifer anisotropy ratio of 1.27, which is reasonably close to the value that can be calculated from K_r/K_z in table 7 (1.64). These values are also very similar to the value reported by Hess and others (1992) (1.24). This provides another indication that the aquifer test results are comparable to the earlier results of Hess and others, and are reasonable estimates of average aquifer conditions.

An estimate of the expected variance of head in the aquifer can be made using an equation developed by Naff and Vecchia (1986) for three-dimensional flow in a horizontally stratified aquifer:

$$\alpha_{3Dh}^2 = \pi \alpha_f^2 J^2 \lambda_1 \lambda_3 / 8 \qquad (27)$$

where α_{3Dh}^2 is the variance of head for three-dimensional flow, J is the horizontal hydraulic gradient, λ_1 is the ln K_r correlation scale in the

horizontal plane, and λ_3 is the ln K_z correlation scale in the vertical plane. A one-dimensional version of the equation can also be used (Gelhar, 1993, p. 143):

$$\alpha_{1Dh}^2 = 5.34\alpha_f^2 J^2 \lambda_1^2 \quad (28)$$

where α_{1Dh}^2 is the variance of head for one-dimensional flow. A uniform gradient was assumed in the derivation of equations 27 and 28.

In order to calculate the head variance using the above equations, an estimate of the hydraulic gradient is needed. This could be obtained using the gradual drainage equation, but a simpler approximation can also be applied by taking the spatial derivative of the Jacob (1950) straight-line equation:

$$h = (Q/4\pi T')\ln(2.25\ Tt/r^2S) \quad (29)$$

where T is the aquifer transmissivity and S is the storage coefficient, or storativity. The derivative of drawdowns with radial distance for the above equation is:

$$dh/dr = -Q/2\pi Tr \quad (30)$$

If the values for the aquifer test are used (Q = 42.8 ft^3/min and T = 39.1 ft^2/min), hydraulic gradients can be calculated; these vary from about 0.01 (ft/ft) at a distance of 17.4 ft to 0.001 (ft/ft) at a distance of 174 ft from the pumped well. (For purposes of comparison, the measured horizontal hydraulic gradient prior to the test was approximately 0.0015 ft/ft and just prior to the end of the test near the pumped well, between piezometers F505-059 and F504-060, was approximately 0.014 ft/ft).

Tables 10a and 10b provide values of the variance and standard deviation in metric and English units, respectively, for the indicated values of α_f^2, J, λ_1, and λ_3. The tables indicate that the standard deviation of the aquifer head variations (columns 6 and 8) are likely small, and if the normal range of these head variations are

approximately four (that is, ± 2) standard deviations, then this range is on the order of a few centimeters (0.1 ft) or less. This magnitude of head variation around the mean compares well with those differences seen between the simulated and measured drawdowns for the aquifer test (standard deviation 0.014 ft and a range of 0.06 ft).

There are limitations to the above analysis that should be noted. First, the analysis is strictly valid only for a stationary hydraulic gradient, that is, one that is constant in space. This is certainly not true for the case of radially convergent flow around a pumped well; however, it would be unlikely that the head variations would be larger than those for the one-dimensional case, as the standard deviations are about an order of magnitude larger than those for three-dimensional flow, and represent an extreme case where flow is forced to travel within each nonuniformity in the aquifer. The reader is referred to Gelhar (1993, chapter 4.1) for a discussion of this assumption and the effect of dimensionality on the head variance. In addition, equations 27 and 28 are based on an assumption of a small value of ln K_r variance, which appears to be satisfied here because the value of 0.24 is much lower than the often-observed value of approximately 1.0 for the ln K_r variance (see Gelhar, 1993, p.103). Finally, the assumption of steady flow conditions for these equations isn't strictly satisfied, but the small variation over time that would be necessary for the Jacob straight-line method could be applied. Here, the value of the dimensionless parameter u (= $r^2S/4Tt$) would need to be less than 0.05, and with this assumption the hydraulic gradient would be changing very slowly over time, satisfying the basic assumption of steady flow conditions.

One can conclude that given the assumptions and limitations noted above, the effects of heterogeneity on the results of the aquifer test site are small, and in general it was observed that the measured drawdowns at piezometers and wells were very close to the simulated

values for a homogeneous porous medium. In addition, the calculated aquifer property values from the aquifer test results are very similar to geometric mean values calculated from many small-scale measurements made in the same aquifer, supporting the contention that the aquifer test values are average results for the aquifer in the area of the test.

Parameter-Estimation Experiments with Measured Drawdown

Because of the quality and quantity of the measured drawdown data, the scale of the test relative to the aquifer heterogeneity, and the availability of the necessary information, some general recommendations can be made about the planning, execution, and analysis of unconfined aquifer tests. Addressed are the consequences of (1) having only pumped-well data to analyze, (2) having a limited number and distribution of piezometers and assuming (a) gradual drainage from the unsaturated zone, and (b) instantaneous drainage from the unsaturated zone, and (3) having an aquifer test of limited duration.

Experiments with Pumped-Well Data

Because observation piezometer data are often unavailable, hydrogeologists will commonly attempt to estimate aquifer parameters from pumped-well data alone. It is shown in this section that the pumped-well data obtained during this aquifer test, although of reasonably good quality, do not lend themselves to accurate evaluation of the aquifer parameters. In general, efforts to obtain reliable estimates of aquifer parameters other than transmissivity with pumped-well data are unlikely to be successful. To do so would require that the test be designed with that in mind and special precautions would have to be taken. Such precautions might involve the use of hydraulic packers to reduce effects of wellbore storage and/or involve the use of special devices to monitor and control the flow rate accurately. Although special drilling methods were used in this investigation to

avoid the introduction of foreign material, effects of wellbore skin were nonetheless apparent. This was likely because of turbulence in the well bore or flow constrictions caused by the well screen.

Figure 21 is a semi-logarithmic plot similar to figure 5 but with an expanded drawdown scale that amplifies the fluctuations in drawdown as recorded by a transducer. The fluctuations appear to be a consequence of minor variations in discharge. A plot of theoretical drawdowns, simulated by using the parameters listed in table 6 and with S_w=1.375 (as determined previously), is superimposed on the transducer data. With the exception of the first 0.3 min, and a portion of the intermediate-time data between 10 and 100 min, the simulated response fits the measured data reasonably well. The slope of the straight line in the late-time portion of the simulated drawdown curve is 0.21/log cycle and, by the method of Cooper and Jacob (1946), gives rise to the expected value of transmissivity (38 ft^2/min) corresponding to the product of K_r and b in table 6. Thus, by judicious placement of a straight edge on the measured late-time data, or by means of a least squares polynomial fit, it should be possible to obtain a reasonable estimate of the transmissivity. It is evident from the data, however, that the choice of slope is open to interpretation. Unfortunately, for several reasons, transmissivity is about the only parameter that can be estimated to any degree of reliability from pumped well data. This is due, in large part, to enhanced drawdowns in the pumped well because of wellbore skin, fluctuations in drawdowns due to discharge variations, and insensitivity of drawdowns in the pumped well to vertical components of flow in the aquifer.

An attempt (using PEST) to estimate the aquifer parameters S_y, K_r, and K_z, from the pumped well data (figure A, Appendix II) using the 'known' value of b (170 ft) and assuming, for lack of contrary information, that S_w equal zero, gave rise to the values S_y=0.094,

K_r=0.21 ft/min, and K_z=0.018 ft/min. Because of variations in measured drawdowns at early time, the first 0.5 min of data (see figure A, Appendix II) were eliminated from the analysis. The results were not significantly different when the analysis was restricted to drawdowns at late time (times greater than 400 min). These estimated aquifer property values are clearly at odds with the parameters obtained by using the 20 observation piezometers. Even with known wellbore skin parameters (which could conceivably be estimated by means of a step-drawdown test) analyses of the pumped-well data did not yield improved estimation results. Repetition of the above tests with S_w=1.375 gave rise to the values S_y=0.056, K_r=0.26 ft/min, and K_z=0.032 ft/min.

Based on these results, it is recommended that analysis of pumped-well data without supporting aquifer piezometer data be approached with extreme caution, if at all.

Experiments with Limited Piezometer Distribution

In this section, the results of a number of computer runs performed on selected piezometer groups, listed in table 12, are presented in an effort to determine the effectiveness of one location or distribution of piezometers compared with another. Because of the reduced data sets, it was not always possible to find the global optimum using the original initial values (shown in table 6) for the characteristic aquifer parameters (S_s, S_y, b, K_r, and K_z). These instances involved two groups of piezometers located near the water table. The alternative initial values were for the parameters S_y, K_r, and K_z and are 0.2, 0.1 ft/min, and 0.1 ft/min, respectively. In all instances, the initial values of the empirical parameters α_1, α_2, and α_3 are, respectively, 10^{-4}, 10^{-2}, and 10^{-1}. Letters A-H in table 11

correspond to columns of estimated parameters in tables 12-15. Columns A-D in tables 12-15 contain results of analyses conducted on groups of piezometers located at similar depths, column E on the group of long-screened wells, and columns F-H on groups of piezometers located at different distances (i.e., the three piezometer clusters).

Gradual drainage. Table 12 shows the results of PEST simulations using the selected piezometer groups with the assumption of gradual drainage from the unsaturated zone and adjustable saturated thickness. The values of the characteristic aquifer parameters (S_s, S_y, b, K_r, and K_z) should be compared with the values determined using all piezometers (table 7), which are shown in table 12 (and 13) for convenience. Results in table 12 (and 13), columns A, B, and E-H, were obtained using initial values for the characteristic aquifer parameters that are the same as those in table 6. Results in table 12 (and 13), columns C and D required the use of initial values for S_y, K_r, and K_z that were close to the expected values as indicated above.

The estimated characteristic aquifer parameters in table 12 columns A and B, for deep-seated and mid-depth piezometers, are reasonably close to the values given in table 7 and are reproducible using different initial values. The differences found in the empirical parameters between the values given in table 7 and the values in columns A and B are not surprising and are indicative of the sensitivity of these parameters to measurement error and aquifer heterogeneity. They do not noticeably change the match between theoretical and measured drawdown seen in figures 14, 15, and 18. The results in columns C and D for the shallow, close-in piezometers and shallow, distant piezometers do not appear to be unique. They appear to require the use of initial values for K_r, K_z, and S_y that are close to the expected values (namely, 0.2, 0.1, and 0.1, respectively, as indicated above). In the case of column C, however, through further experimentation, it was found that the need to revise the initial values of K_r, K_z, and S_y was a

consequence of the attempt to estimate specific storage. By fixing the value of specific storage at the value given in table 7 it was found unnecessary to change the initial values of any parameters. Also, the use of an additional empirical parameter α_4 improved the estimate of specific storage (1.6×10^{-5} ft^{-1}) but did not significantly change the other parameters. In the case of column D, the reason for the need to revise the initial values of K_r, K_z, and S_y may be partially explained by inaccurate hand measurements of small drawdowns early in the test (see figures E-I in Appendix II), and the fact that the flow regime at the larger distances is essentially horizontal and would likely not be sensitive to the aquifer saturated thickness or vertical hydraulic conductivity. The results in both columns C and D suggest that analyses performed using only shallow piezometers may not always be trusted, and that deep-seated piezometers may be required to obtain satisfactory parameter estimates.

The results presented in columns E-H of table 12 are, with one exception, reasonably consistent with the results in table 7. The exception is the simulation using the piezometer cluster F383 (column H), whose results depart significantly from the others. Note the near equality of K_r and K_z and the large values of S_y and b. (The choice of initial values close to the values in table 7 did not change the final results shown in column H.) Further experimentation with this piezometer cluster, wherein drawdowns at times less than 100 min were eliminated from the estimation process, yielded a totally unrealistic estimate of specific yield (S_y=0.739). These results suggest that the locations of the piezometers in the F383 cluster are such that the aquifer response there is insensitive to the exact value of the hydraulic parameters. This is apparently due to essentially horizontal flow at that location, which is at a distance of approximately 95 ft from the pumped well.

Because it is the usual procedure to specify the saturated thickness as a known quantity, the runs in table 12 were repeated by using a fixed value of saturated thickness (170 ft). The results of these runs are presented in table 13 and, with one or two exceptions, appear to be reasonably consistent with the values in table 7. The primary exception is the value of K_z in column D for the shallow distant piezometers. This result again suggests a lack of sensitivity of the data from the shallow, distant piezometers to aquifer thickness (b) and vertical hydraulic conductivity (K_z). Specification of the saturated thickness clearly results in an improvement in the estimated hydraulic conductivities in column H for the most distant piezometer cluster as compared with column H in table 12.

Instantaneous drainage. As mentioned repeatedly, many conventional analyses of aquifer test data make the assumption that drainage from the unsaturated zone occurs instantaneously in response to a decline in elevation of the water table. This assumption was made to obtain the results shown in table 5, but to do so with the PEST algorithm it was necessary to utilize only the very late-time data (times greater than 2,000 minutes) measured in each piezometer. Tables 14 and 15 show results obtained under the assumption of instantaneous drainage without and with, respectively, an assumed known saturated thickness (b). Because there are significant discrepancies between measured and simulated drawdowns during the intermediate time range for most piezometers (see fig. 6-12), it would be counterproductive to use PEST with the model assumption of instantaneous drainage over the entire time range without appropriate weighting considerations. For the results presented in tables 14 and 15, the analyses are limited to data occurring over the final log cycle of time (generally the last 7 values chosen for analysis by PEST, or time greater than 430 min; (see figures B-K in Appendix II). Over this time period, and for most piezometers the discrepancies mentioned above (see fig. 6-12) are not large and one might expect to get reasonable estimates of the aquifer parameters

either by type-curve analysis or by application of the PEST algorithm. That this may not always be the case is evident from tables 14 and 15.

Inspection of the estimated parameters in each of the selected piezometer groups of table 14 reveals that there is at least one parameter that is significantly different from the parameters listed in table 5. Table 15 shows that specification of the saturated thickness reduces some of the variability that is evident from one piezometer group to the next. In all columns of table 15 the specific yield is less than the values obtained under the model assumption of gradual drainage from the unsaturated zone (table 13). The low values of S_y are a consequence, in large part, of the extended time range used in these analyses compared with the significantly shorter time range used to obtain the parameters in table 5. The values of hydraulic conductivity in table 15 show greater variability than the values in table 13 even though early-time data, and most of the intermediate-time data, were eliminated from the analysis. The results suggest the significant influence of gradual drainage processes (even for times greater than 430 minutes) and the importance of using a model that takes account of this process.

Experiments with Reduced Length of Test

Tables 16a and 16b show the results of PEST simulations for different piezometer groups with the model assumption of gradual drainage from the unsaturated zone for aquifer tests of different duration. Some important findings emerge from examination of these tables: tables 16a and 16b demonstrate (1) that it may not have been necessary to run this aquifer test for as long as it was and (2) a few piezometers located in proximity to the pumped well at appropriate depths may be all that were needed to define the aquifer characteristics. By use of either the complete set of piezometers or just the deep-seated piezometers (see table 16a for both), it appears

that the results for an 8-hour test are as valid as the results for a 72-hour test. This finding indicates that the drawdown data obtained in the first 8 hours of this aquifer test are adequate to define the primary aquifer characteristics as well as the three empirical parameters that account for gradual drainage. Of course, without measurements made in distant piezometers it would not be possible to judge the aerial extent to which the evaluated aquifer characteristics apply.

Results obtained for the long-screened piezometers and the combination of three piezometer clusters shown in table 16b show that the shorter 16-hour and 8-hour tests do not agree as well with the results of the 72-hour test as do the results of the 24-hour test. The parameters with the greatest differences are the specific yield and the saturated thickness. The differences are not great, however, and may be perfectly satisfactory for most applications.

Examination of figures 6-12 reveals that the piezometers whose measured responses deviate the least from simulated responses (based on the assumption of instantaneous drainage) are the deep-seated, close-in piezometers (F505-059, F505-080, F504-080, and F383-129). This set of piezometers is the same as the set of deep-seated piezometers in table 16a except that F383-082 is replaced by F505-059. The results of analyses of the drawdown data from these piezometers based on the assumptions of gradual drainage on the one hand and instantaneous drainage on the other, are shown in table 17. The primary difference in the estimated parameters is in the estimate of specific yield. Under the assumption of instantaneous drainage, the specific yield is a little more than half of that obtained under the assumption of gradual drainage from the unsaturated zone. In each instance it does not matter whether the test was run for 8-hours or 72-hours.

Based on the parameters in table 17 for the 8-hour test, simulated and measured drawdown responses are compared for the case of instantaneous drainage in figure 22 and for the case of gradual drainage

in figure 23. The improvement seen in figure 23, although marginal, is evident in the intermediate time range. There are no noticeable differences, however, in the simulated responses at late time (last log cycle of time). The explanation for the significantly larger value of S_y obtained by including gradual drainage lies in the fact that a larger value of S_y is needed to compensate for the fact that water is retained in the unsaturated zone and gives rise to only small increased drawdowns in the deep-seated observation piezometers.

SUMMARY

A model for flow to a well in an unconfined aquifer was applied to the analysis of a 72-hour aquifer test conducted in a sand and gravel, glacial-outwash deposit in Cape Cod, Massachusetts. This model allows for gradual drainage from the unsaturated zone, wellbore storage and skin at the pumped well, and delayed piezometer response. An automated parameter estimation algorithm was used to obtain all relevant unconfined aquifer parameters, including the saturated thickness. The detailed analysis supports the results of a preliminary type-curve analysis, reported by Moench and others (1996), which made use of an analysis method of Neuman (1974) to evaluate horizontal and vertical hydraulic conductivity and specific yield. Although the preliminary analysis showed good agreement between simulated and measured drawdowns at late time, there were found to be significant discrepancies between simulated responses and the intermediate-time data. The analysis was extended using a modified version of the Moench (1997) model, with the result that simulated responses based on the estimated aquifer parameters compare well with measured drawdowns in all piezometers at all times. Due to the high quality and quantity of the data and the relative uniformity of the aquifer it was possible to provide some guidelines for the design and execution of unconfined aquifer tests of the type found at this site.

The model modification involves the substitution of multiple empirical parameters (as coefficients in exponential relations) for the single empirical parameter used previously to describe drainage from the zone above the water table. The single empirical parameter, which assumes that the vertical flux of water at the free surface varies exponentially in response to a step change in the elevation of the water table, was found to provide only moderate improvement over the assumption of instantaneous drainage. The introduction of a finite series of terms, each with an additional empirical parameter,

effectively eliminated discrepancies between measured and computed drawdowns. Three such terms appeared to provide an adequate representation of the drainage process that occurred during this test.

The values of the estimated hydraulic parameters are consistent with estimates from prior studies and from what is known about the aquifer at the site. The estimated values are: specific yield, 0.26; saturated thickness, 170 feet; horizontal hydraulic conductivity, 0.23 feet per minute; vertical hydraulic conductivity, 0.14 feet per minute; and specific storage, 1.3×10^{-5} per foot.

Apart from the aquifer parameters, the principal findings that result from the analysis and the additional parameter-estimation experiments are the following:

(1) Pumped-well data by themselves are not useful for estimating most unconfined aquifer parameters. The primary information obtained using these data is an approximate value of aquifer transmissivity from the late-time drawdown values. Pumped-well data are needed, however, in order to estimate the wellbore skin factor that is used to improve estimates of specific storage.

(2) An analysis of early-time data from piezometers with transducers can yield reasonable estimates of specific storage (S_s) provided wellbore skin, wellbore storage, and delayed piezometer responses are included in the analysis.

(3) Under the assumption of instantaneous drainage, estimates of specific yield (S_y), saturated thickness (b), horizontal hydraulic conductivity (K_r) and vertical hydraulic conductivity (K_z) can be obtained using late-time drawdown data, given a number of piezometers strategically located at depth in the vicinity of the pumped well and

given that the duration of the aquifer test is sufficient (72 hours in this instance).

(4) The assumption of instantaneous drainage from the unsaturated zone does not always lead to an adequate simulation of drawdowns in the intermediate time range, which in this test are times from approximately 1 to 1,000 min. Even in those situations where analysis using the assumption of instantaneous drainage might be deemed appropriate (for example, with deep-seated piezometers located relatively close to the pumped well), estimates of specific yield will likely be low relative to values obtained using an assumption of gradual drainage or relative to values obtained from late-time data alone.

(5) Drawdown data from the shallow piezometers located at large distances from the pumped well where flow is essentially horizontal appear to be diagnostic of only horizontal hydraulic conductivity and specific yield. Data from the shallow piezometers located near the pumped well, even though in a part of the aquifer that is strongly influenced by vertical components of flow, do not necessarily yield a unique set of aquifer parameters. It is possible that this is partly a consequence of the variably distributed drainage from the unsaturated zone due to heterogeneity in the material overlying the piezometers.

(6) Data from mid-depth and deep-seated piezometers located near the pumped well, treated independently, appear to provide parameter estimates that are consistent with results from the data set as a whole and would be the recommended locations given limited resources.

(7) Tests performed with the modified model on the complete set of piezometers and on selected piezometer groups, independent of one another, indicate that it is not necessary to run the aquifer test for as long as 72-hours. It appears that for some piezometer groups a test

as short as 8-hours may be adequate. For other piezometer groups, a 16-hour test may be adequate.

It may be concluded from the analysis provided here that accurate estimates of unconfined aquifer parameters using automatic parameter estimation techniques require a model that accounts for all the physical processes that influence the measured drawdowns, even then it is necessary that the test be well designed and executed. If the relevant processes are not taken into account, the parameter estimation algorithm treats differences between measured and simulated drawdowns as errors in measurement with a subsequent degradation in the validity of the estimated parameters.

It has been mentioned repeatedly that the Cape Cod aquifer test is exceptional: the data are of unusually good quality, there are a sufficient number of observation piezometers, the scale of heterogeneity is small in comparison with the scale of the aquifer test resulting in estimated parameters that are average values for the aquifer in the area of the test, the boundary conditions of the physical system appear to conform satisfactorily with the mathematical model, and interference from extraneous sources is minimal. Field conditions do not often reach this ideal: the aquifer may have large-scale heterogeneity in hydraulic conductivity or saturated thickness; the aquifer may be bounded laterally within the cone of depression; piezometers may be too few in number, improperly located, or not in good hydraulic connection with the aquifer; there may be interference from one or more extraneous sources; and relevant pumped-well and observation-piezometer characteristics may not be known. Because of the nearly ideal conditions and high data quality, it is recommended that this aquifer test be used as a standard against which other tests, conducted under less than ideal conditions, are compared.

NOTATION

b initial saturated thickness of aquifer, L

C wellbore storage, L^2

d vertical distance from initial water table to top of pumped well screen, L

d_s thickness of the wellbore skin, L

F' modified Hvorslev shape factor, L

F Hvorslev shape factor, L

h hydraulic head, L

h^* vertical average of hydraulic head in the aquifer adjacent to and over the length of the pumped-well screen, L

h_i initial hydraulic head, L

h_m measured hydraulic head in a piezometer, L

h_w average hydraulic head in the pumped well, L

J hydraulic gradient in the horizontal direction

k square root of ratio K_r/K_z

K_z hydraulic conductivity in the vertical direction, LT^{-1}

K_r hydraulic conductivity in the horizontal direction, LT^{-1}

K_s hydraulic conductivity of the wellbore skin, LT^{-1}

ℓ vertical distance from initial water table to bottom of pumped-well screen, L

L length of a piezometer screen, L

M number of empirical constants for gradual drainage from the unsaturated zone

Q pumping rate, L^3T^{-1}

p Laplace transform variable

r radial distance from axis of pumping well, L

r_c effective radius of the pumped well in the interval where water levels are changing, L

r_p radius of observation piezometer in the interval where water levels are changing, L

r_w outside radius of the pumped-well screen, L

S storativity

S_s specific storage, L^{-1}

S_w wellbore skin factor

S_y specific yield

T transmissivity, L^2T^{-1}

t time since start of pumping, T

t' variable of integration equation 6

u dimensionless parameter defined as $r^2S/4Tt$

z vertical distance above bottom of aquifer, L

z_p elevation of the midpoint of an observation-piezometer screen above the base of the aquifer, L

z_u vertical distance above the water table, L

z_1 elevation of the bottom of an observation-well screen above the base of the aquifer, L

z_2 elevation of the top of an observation-well screen above the base of the aquifer, L

α Boulton's (1963) reciprocal 'delay index', T^{-1}

α_m m empirical constants for gradual drainage from the unsaturated zone, T^{-1}

α_f^2 variance of ln K_r

α_{1Dh}^2 variance of head for one-dimensional flow, L^2

α_{3Dh}^2 variance of head for three-dimensional flow, L^2

λ_1 horizontal log hydraulic conductivity correlation scale, L

λ_3 vertical log hydraulic conductivity correlation scale, L

θ_s moisture content above the water table at saturation

$\theta(z)$ moisture content of unsaturated zone

τ variable of integration in equation 13

REFERENCES

Barlow, P.M., and Moench, A.F., 1999, WTAQ — A computer program for calculating drawdowns and estimating hydraulic properties for confined and water-table aquifers: U.S. Geological Survey, Water-Resources Investigations Report 99-4225, 74 p. (Program and documentation available on the World Wide Web, accessed May 22, 2000, at URL http://ma.water.usgs.gov/publications/WRIR_99-4225/index.htm)

Batu, Vedat, 1998, Aquifer Hydraulics — a comprehensive guide to hydrogeologic data analysis: New York, Wiley, 727 p.

Black, J.H., and Kipp, K.L., Jr., 1977, Observation well response time and its effect upon aquifer test results: Journal of Hydrology, v. 34, p. 297-306.

Boulton, N.S., 1954, Unsteady radial flow to a pumped well allowing for delayed yield from storage: International Association of Scientific Hydrology, Rome, Publication 37, p. 472-477.

_____1963, Analysis of data from non-equilibrium pumping tests allowing for delayed yield from storage: Proceedings of the Institution of Civil Engineers, v. 26, p. 469-482.

Boulton, N.S., and Pontin, J.M.A., 1971, An extended theory of delayed yield from storage applied to pumping tests in unconfined anisotropic aquifers: Journal of Hydrology, v. 14, p. 53-65.

Boulton, N.S., and Streltsova, T.D., 1975, New equations for determining the formation constants of an aquifer from pumping test data: Water Resources Research, v. 11, no. 1, p. 148-153.

Carslaw, H.S., and Jaeger, J.C., 1959, Conduction of heat in solids (2d ed.): London, Oxford University Press, 510 p.

Cooper, H.H., Jr., and Jacob, C.E., 1946, A generalized graphical method for evaluating formation constants and summarizing well-field

history: American Geophysical Union Transactions, v. 27, p. 526-534.

Dagan, Gedeon, 1967, A method of determining the permeability and effective porosity of unconfined anisotropic aquifers: Water Resources Research, v. 3, no. 4, p. 1059-1071.

Doherty, John, 1994, PEST — model-independent parameter estimation: Corinda, Australia, Watermark Computing, 122 p.

Dougherty, D.E., and Babu, D.K., 1984, Flow to a partially penetrating well in a double-porosity reservoir: Water Resources Research, v. 20, no. 8, p. 1116-1122.

Gelhar, L.W., 1993, Stochastic subsurface hydrology: Englewood Cliffs: N.J., Prentice Hall, 390 p.

Gelhar, L.W., and Axness, C.L., 1983, Three-dimensional stochastic analysis of macrodispersion in aquifers: Water Resources Research, v. 19, no. 1, p. 161-180.

Heidari, Manoutchehr, and Moench, Allen, 1997, Evaluation of unconfined-aquifer parameters from pumping test data by nonlinear least squares: Journal of Hydrology, v. 192, p. 300-313.

Hess, K.M., Wolf, S.H., and Celia, M.A., 1992, Large-scale natural gradient tracer test in sand and gravel, Cape Cod, Massachusetts, 3. Hydraulic conductivity variability and calculated macrodispersivities: Water Resources Research, v. 28, no. 8, p. 2011-2027.

Hill, M. C., 1998, Methods and guidelines for effective model calibration: U.S. Geological Survey, Water-Resources Investigations Report 98-4005, 90 p.

Hvorslev, M.J., 1951, Time lag and soil permeability in ground-water observations: U.S. Army Corps of Engineers, Waterways Experiment Station, Bulletin 36, Vicksburg, Mississippi, 50 p.

Jacob, C.E., 1950, Flow of ground water, chap. 5 *in* Rouse, Hunter, Engineering hydraulics: New York, John Wiley & Sons.

Kruseman, G.P., and de Ridder, N.A., 1990, Analysis and evaluation of pumping test data (2d ed.): Publication 47, International Institute for Land Reclamation and Improvement, Wageningen, The Netherlands, 377 p.

LeBlanc, D.R., 1984, Sewage plume in a sand and gravel aquifer, Cape Cod, Massachusetts: U.S. Geological Survey, Water-Supply Paper 2218, 28 p.

LeBlanc, D.R., Guswa, J.H., Frimpter, M.H., and Londquist, C.J., 1986, Ground-water resources of Cape Cod, Massachusetts: U.S. Geological Survey Hydrologic-Investigations Atlas HA-692, 4 pls.

LeBlanc, D.R., Garabedian, S.P., Hess, K.M., Gelhar, L.W., Quadri, R.D., Stollenwerk, K.G., and Wood, W.W., 1991, Large-scale natural gradient tracer test in sand and gravel, Cape Cod, Massachusetts, 1. Experimental design and observed tracer movement: Water Resources Research, v. 27, no. 5, p. 895-910.

Masterson, J.P., Stone, B.D., Walters, D.A., and Savoie, Jennifer, 1997, Hydrogeologic framework of western Cape Cod, Massachusetts: U.S. Geological Survey Hydrologic-Investigations Atlas HA-741.

Moench, A.F., 1985, Transient flow to a large-diameter well in an aquifer with storative semiconfining layers: Water Resourcecs Research, v. 21, no. 8, p. 1121-1131.

_____1993, Computation of type curves for flow to partially penetrating wells in water-table aquifers: Ground Water, v. 31, no. 6, p. 966-971.

_____1994, Specific yield as determined by type-curve analysis of aquifer-test data: Ground Water, v. 32, no. 6, p. 949-957.

_____1995, Combining the Neuman and Boulton models for flow to a well in an unconfined aquifer: Ground Water, v. 33, no. 3, p. 378-384.

_____1997, Flow to a well of finite diameter in a homogeneous, anisotropic water table aquifer: Water Resources Research, v. 33, no. 6, p. 1397-1407.

_____1998, Correction to "Flow to a well of finite diameter in a homogeneous, anisotropic water table aquifer": Water Resources Research, v. 34, no. 9, p. 2431-2432.

Moench, A.F., LeBlanc, D.R., and Garabedian, S.P., 1996, Preliminary type-curve analysis of an aquifer test in an unconfined sand and gravel aquifer, Cape Cod, Massachusetts, *in* Morganwalp, D.W., and Aronson D.A., eds., 1995, U.S. Geological Survey Toxic Substances Hydrology Program — Proceedings of the Technical Meeting, Colorado Springs, Colorado, September 20-24, 1993: U.S. Geological Survey Water-Resources Investigations Report 94-4015.

Naff, R.L., and Vecchia, A.V., 1986, Stochastic analysis of three-dimensional flow in a bounded domain: Water Resources Research, v. 22, no. 5, p. 695-704.

Narasimhan, T.N., and Zhu, Ming, 1993, Transient flow of water to a well in an unconfined aquifer — applicability of some conceptual models: Water Resources Research, v. 29, no. 1, p. 179-191.

Neuman, S.P., 1972, Theory of flow in unconfined aquifers considering delayed response of the water table: Water Resources Research, v. 8, no. 4, p. 1031-1044.

_____1974, Effects of partial penetration on flow in unconfined aquifers considering delayed aquifer response: Water Resources Research, v. 10, no. 2, p. 303-312.

_____1975, Analysis of pumping test data from anisotropic unconfined aquifers considering delayed gravity response: Water Resources Research, v. 11, no. 2, p. 329-342.

_____1979, Perspective on 'delayed yield': Water Resources Research, v. 15, no. 4, p. 899-908.

_____1987, On methods of determining specific yield: Ground Water, v. 25, no. 6, p. 679-684.

Nwankwor, G.I., Gillam, R.W., van der Kamp, Garth, and Akindunni, F.F., 1992, Unsaturated and saturated flow in response to pumping of an unconfined aquifer — field evidence of delayed drainage: Ground Water, v. 30, no. 5, p. 690-700.

Poeter, E.P., and Hill, M.C., 1997, Inverse models — A necessary next step in ground-water modeling: Ground Water, v. 35, no. 2, p. 250-260.

Prickett, T.A., 1965, Type-curve solution to aquifer tests under water-table conditions: Ground Water, v. 3, no. 3, p. 5-14.

Ramey, H.J., Jr., and Agarwal, R.G., 1972, Annulus unloading rates as influenced by wellbore storage and skin effect: Transactions of the Society of Petroleum Engineers, AIME, v. 253, p. 453-462.

Ruud, N.C., and Kabala, Z.J., 1997, Response of a partially penetrating well in a heterogeneous aquifer — integrated well-face flux versus uniform well-face flux boundary conditions: Journal of Hydrology, v. 194, p. 76-94.

Springer, R.K., 1991, Application of an improved slug test analysis to the large-scale characterization of heterogeneity in a Cape Cod Aquifer: Cambridge, Massachusetts, Massachusetts Institute of Technology, M.S Thesis, 162 p.

Stehfest, Harald, 1970, Numerical inversion of Laplace transforms: Communications of the Association for Computing Machinery (ACM), v. 13, no. 1, p. 47-49.

Vachaud, Georges, 1968, Contribution à l'étude des problèmes d'écoulement en milieux poreux non saturés: Grenoble, France, University of Grenoble, Ph.D. thesis, 159 p.

APPENDIX I

Derivation of the Laplace transform solution

In this section, a derivation of the Laplace transform solution is provided. Application of the method of Laplace transformation to equations 8-13 leads to the following subsidiary boundary-value problem:

$$\frac{\partial^2 \overline{h}_D}{\partial r_D^{\,2}} + \frac{1}{r_D}\frac{\partial \overline{h}_D}{\partial r_D} + b_w \frac{\partial^2 \overline{h}_D}{\partial z_D^{\,2}} = p\overline{h}_D \qquad \text{(A1)}$$

$$\overline{h}_D(\infty, z_D, p) = 0 \qquad \text{(A2)}$$

$$\frac{\partial \overline{h}_D}{\partial r_D} = -\frac{2}{p(\ell_D - d_D)} + W_D p\overline{h}_{wD} \qquad 1-\ell_D \le z_D \le 1-d_D,\ r_D = 1 \qquad \text{(A3a)}$$

$$\frac{\partial \overline{h}_D}{\partial r_D} = 0 \qquad z_D < 1-\ell_D\ ;\ z_D > 1-d_D,\ r_D = 1 \qquad \text{(A3b)}$$

$$\overline{h}_{wD} = \overline{h}_D^{*} - S_w \frac{\partial \overline{h}_D}{\partial r_D} \qquad 1-\ell_D \le z_D \le 1-d_D \qquad \text{(A3c)}$$

$$\overline{h}_D^{*} = \frac{1}{(\ell_D - d_D)} \int_{1-\ell_D}^{1-d_D} \overline{h}_D(1, z_D, p)\, dz_D \qquad \text{(A3d)}$$

$$\frac{\partial \overline{h}_D}{\partial z_D}(r_D, 0, p) = 0 \qquad \text{(A4)}$$

$$\frac{\partial \overline{h}_D}{\partial z_D}(r_D, 1, p) = -\overline{h}_D(r_D, 1, p)\frac{p}{M}\sum_{m=1}^{M}\frac{1}{(\sigma\beta_\omega + p/\gamma_m)} \qquad \text{(5A)}$$

The solution to the above problem is obtained with the help of Fourier cosine series in the manner followed by Dougherty and Babu (1984) for well tests in confined double-porosity aquifers and by Moench (1997, 1998).

A solution to equation A1 that satisfies equations A4 and A5 is

$$\bar{h}_D = \sum_{n=0}^{\infty} \bar{f}_n(r_D, p)\cos(\varepsilon_n z_D) \qquad \text{(A6)}$$

where n = 0, 1, 2,... ,and ε_n are the roots of

$$\varepsilon_n \tan(\varepsilon_n) = \frac{p}{M}\sum_{m=1}^{M}\frac{1}{(\sigma\beta_\omega + p/\gamma_m)} \qquad \text{(A7)}$$

Substitution of equation A6 into A1 yields

$$\sum_{n=0}^{M}[\bar{f}''_n + \frac{1}{r_D}\bar{f}'_n - (\varepsilon_n^2\beta_w + p)\bar{f}_n]\cos(\varepsilon_n z_D) = 0 \qquad \text{(A8)}$$

Hence, $\bar{f}_n$ must satisfy

$$\bar{f}''_n + \frac{1}{r_D}\bar{f}'_n - (\varepsilon_n^2\beta_w + p)\bar{f}_n = 0 \qquad \text{(A9)}$$

the general solution of which can be written as

$$\bar{f}_n = u_n(p)K_0(q_n r_D) + v_n(p)I_0(q_n r_D) \qquad \text{(A10)}$$

where $q_n = (\varepsilon_n^2\beta_w + p)^{1/2}$. K_0 and I_0 are the zero order modified Bessel functions of the second and first kind, respectively, and u_n and v_n are coefficients to be determined.

Because of equation A2, $v_n(p)=0$ and, consequently,

$$\bar{f}_n = u_n(p)K_0(q_n r_D) \qquad \text{(A11)}$$

Substitution of equation A11 into A6 yields

$$\bar{h}_D = \sum_{n=0}^{\infty} u_n(p)K_0(q_n r_D)\cos(\varepsilon_n z_D) \qquad \text{(A12)}$$

The coefficients $u_n(p)$ are determined from equations A3a and A3b. First substitute equation A12 into A3a and let $r_D=1$ to get

$$-\sum_{n=0}^{\infty} u_n(p) q_n K_1(q_n) \cos(\varepsilon_n z_D) = \bar{q}_s \qquad 1-\ell_D \le z_D \le 1-d_D \tag{A13}$$

where

$$\bar{q}_s = -\frac{2}{p(\ell_D - d_D)} + W_D p \bar{h}_{wD} \tag{A14}$$

Likewise, use equation A3b to get

$$-\sum_{n=0}^{\infty} u_n(p) q_n K_1(q_n) \cos(\varepsilon_n z_D) = 0 \qquad \begin{matrix} z_D < 1-\ell_D \\ z_D > 1-d_D \end{matrix} \tag{A15}$$

Multiplying equation A13 through by $\cos(\varepsilon_m z_D)$, where m is an integer, and integrating over the indicated interval one obtains

$$\begin{aligned} -\sum_{n=0}^{\infty} u_n(p) q_n K_1(q_n) \int_{1-\ell_D}^{1-d_D} \cos(\varepsilon_n z_D)\cos(\varepsilon_m z_D) dz_D \\ = \bar{q}_s \int_{1-\ell_D}^{1-d_D} \cos(\varepsilon_m z_D) dz_D \end{aligned} \tag{A16}$$

Multiplying equation A15 by $\cos(\varepsilon_m z_D)$ and integrating over the interval below the screen one obtains

$$-\sum_{n=0}^{\infty} u_n(p) q_n K_1(q_n) \int_{0}^{1-\ell_D} \cos(\varepsilon_n z_D)\cos(\varepsilon_m z_D) dz_D = 0 \tag{A17}$$

Also, by performing the same operation over the interval above the screen one obtains

$$-\sum_{n=0}^{\infty} u_n(p) q_n K_1(q_n) \int_{1-d_D}^{1} \cos(\varepsilon_n z_D)\cos(\varepsilon_m z_D) dz_D = 0 \tag{A18}$$

Adding equations A17 and A18 to the left hand side of equation A16 one obtains

$$-\sum_{n=0}^{\infty} u_n(p) q_n K_1(q_n) \int_0^1 \cos(\varepsilon_n z_D)\cos(\varepsilon_m z_D) dz_D = \overline{q}_s \int_{1-\ell_D}^{1-d_D} \cos(\varepsilon_m z_D) dz_D \quad \text{(A19)}$$

It can be shown quite simply by use of fundamental trigonometric identities, equation A7, and direct integration that all terms in the sum on the left-hand-side of equation A19 are zero except those for which n=m. Thus, the set $\cos(\varepsilon_n z_D)\cos(\varepsilon_m z_D)$ is orthogonal over the interval 0,1 and equation A19 becomes

$$-u_n(p) q_n K_1(q_n) \int_0^1 \cos^2(\varepsilon_n z_D) dz_D = \overline{q}_s \int_{1-\ell_D}^{1-d_D} \cos(\varepsilon_n z_D) dz_D \quad \text{(A20)}$$

Performing the integration and rearranging terms, one obtains

$$u_n(p) = -\frac{2\overline{q}_s \{\sin[\varepsilon_n(1-d_D)] - \sin[\varepsilon_n(1-\ell_D)]\}}{q_n K_1(q_n)[\varepsilon_n + 0.5\sin(2\varepsilon_n)]} \quad \text{(A21)}$$

Thus, the solution (equation A12) becomes

$$\overline{h}_D(r_D, z_D, p) = -\overline{q}_s E \quad \text{(A22)}$$

where E is defined by equation 17.

The Laplace transform of the hydraulic head in the pumped well is obtained by inserting equation A22 into A3d. Thus, at r_D=1, one obtains

$$\overline{h}_D^* = -\overline{q}_s A \quad \text{(A23)}$$

where A is defined by equation 16. From equations A3c and A23

$$\overline{h}_{wD} = -\overline{q}_s A - S_w \overline{q}_s \quad \text{(A24)}$$

Substitution of equation A14 into A24 yields the solution (equation 14) for the Laplace transform of the dimensionless head in the pumped well.

Substitution of equation A24 into A14 and combining the result with A22 yields the solution (equation 15) for the Laplace transform of the dimensionless head in the aquifer.

APPENDIX II

Drawdown data plots for well test and data selected for parameter estimation

FIGURE CAPTIONS FOR APPENDIX II

Figure A. Drawdown data for the pumped well F507-080. Open diamonds represent values of drawdown selected for parameter estimation. Dots represent drawdown measured by pressure transducer.

Figure B. Drawdown data for piezometers F505-080 and F504-080. Open diamonds represent values of drawdown selected for parameter estimation. Small dots represent drawdown measured by pressure transducer. Large dots represent drawdown measured manually.

Figure C. Drawdown data for wells F505-059 and F504-060. Open diamonds represent values of drawdown selected for parameter estimation. Small dots represent drawdown measured by pressure transducer. Large dots represent drawdown measured manually.

Figure D. Drawdown data for piezometers F505-032 and F504-032. Open diamonds represent values of drawdown selected for parameter estimation. Small dots represent drawdown measured by pressure transducer. Large dots represent drawdown measured manually.

Figure E. Drawdown data for piezometers F377-037 and F347-031. Open diamonds represent values of drawdown selected for parameter estimation. Small dots represent drawdown measured by pressure transducer. Large dots and pluses represent drawdown measured manually.

Figure F. Drawdown data for piezometers F383-061 and F383-032. Open boxes and circles represent drawdown selected for parameter estimation. Dots and pluses represent drawdown measured manually.

Figure G. Drawdown data for piezometers F383-082 and F383-129. Open boxes and circles represent drawdown selected for parameter estimation. Dots and pluses represent drawdown measured manually.

Figure H. Drawdown data for piezometers F384-033 and F385-032. Open boxes and circles represent drawdown selected for parameter estimation. Dots and pluses represent drawdown measured manually.

Figure I. Drawdown data for piezometers F381-056 and F376-037. Open boxes and circles represent drawdown selected for parameter estimation. Dots and pluses represent drawdown measured manually.

Figure J. Drawdown data for wells F434-060 and F450-061. Open boxes and circles represent drawdown selected for parameter estimation. Dots and pluses represent drawdown measured manually.

Figure K. Drawdown data for wells F476-061 and F478-061. Open boxes and circles represent drawdown selected for parameter estimation. Dots and pluses represent drawdown measured manually.

Fig. A

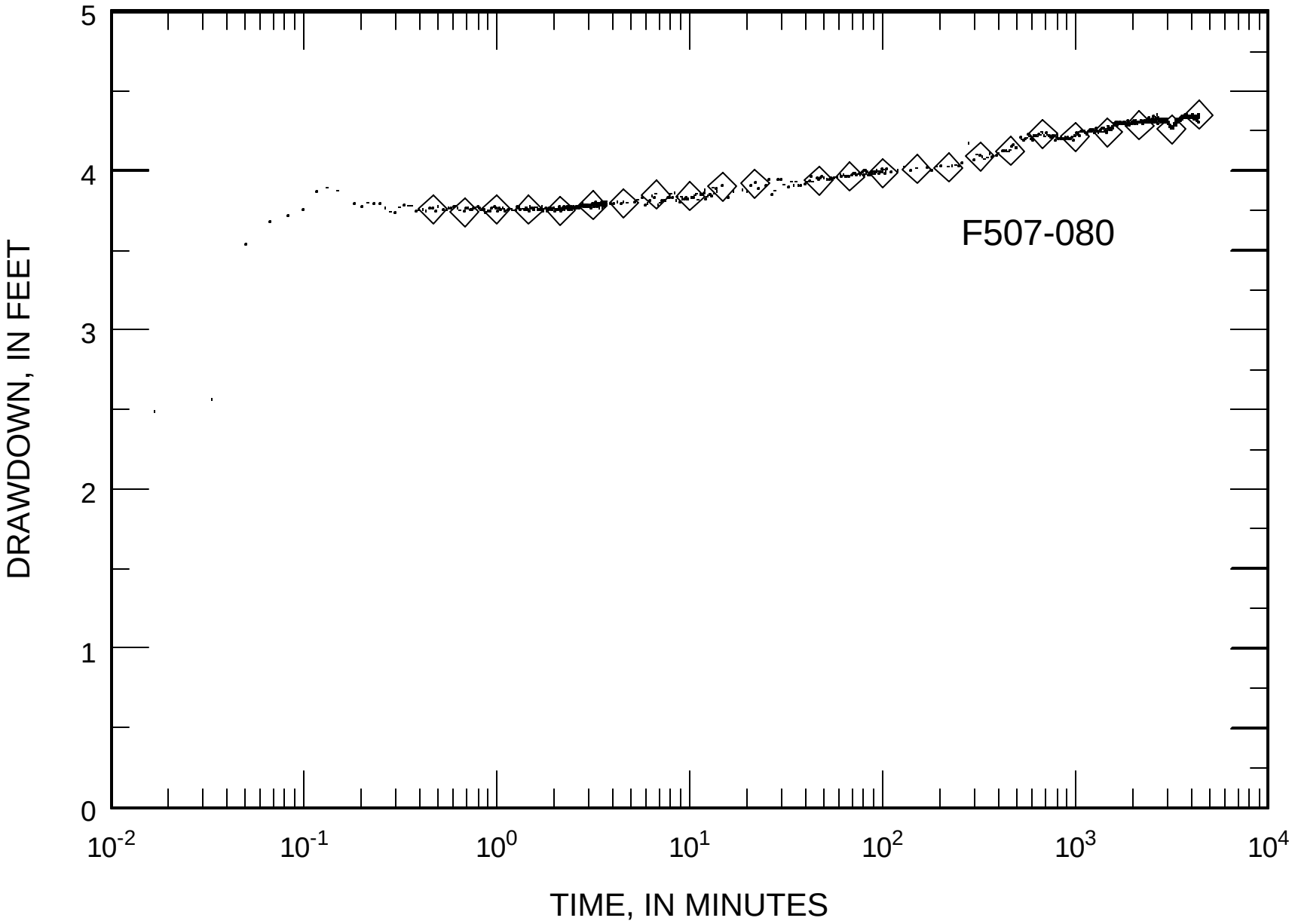
5
4
3
2
1
0
DRAWDOWN, IN FEET
F507-080
10^{-2}
10^{-1}
10^{0}
10^{1}
10^{2}
10^{3}
10^{4}
TIME, IN MINUTES

Fig. B

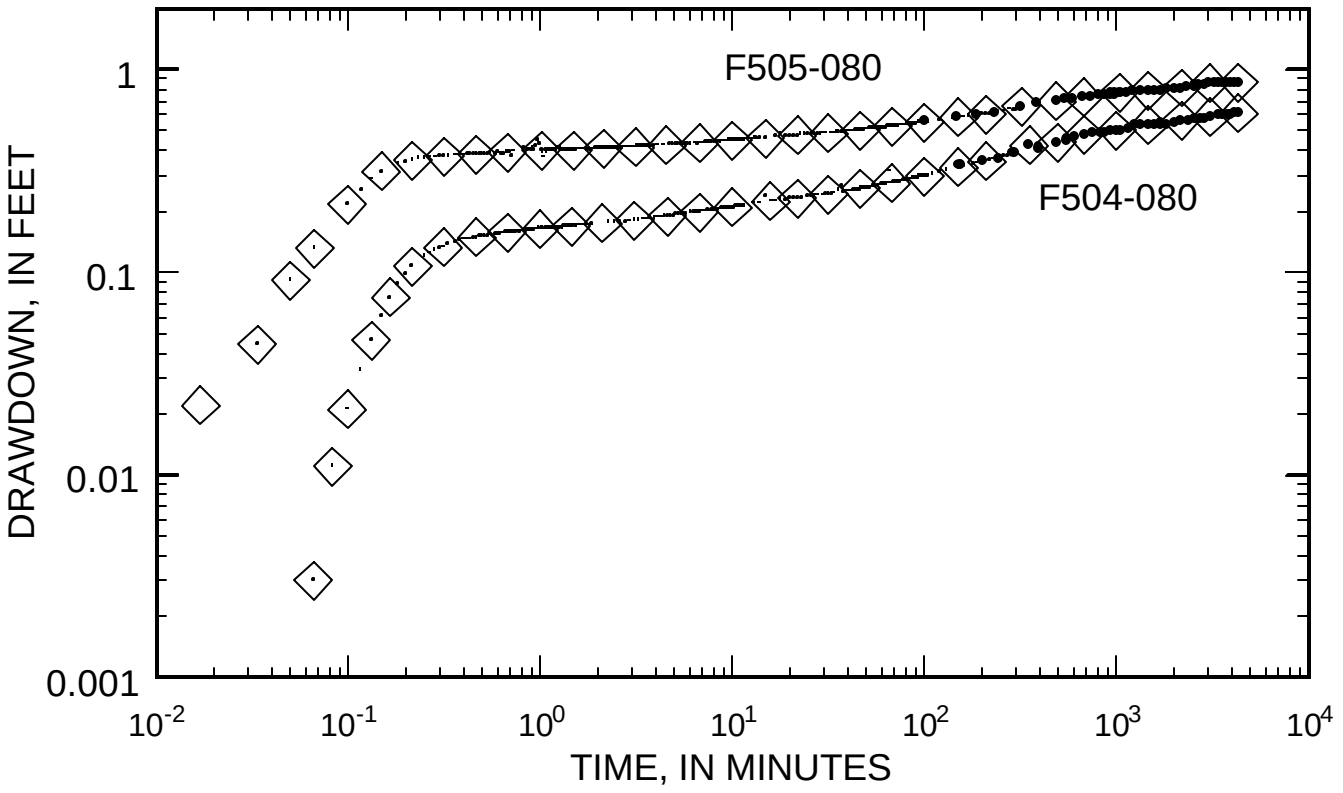
F505-080
F504-080
DRAWDOWN, IN FEET
TIME, IN MINUTES
1
0.1
0.01
0.001
10^{-2}
10^{-1}
10^{0}
10^{1}
10^{2}
10^{3}
10^{4}

Fig. C

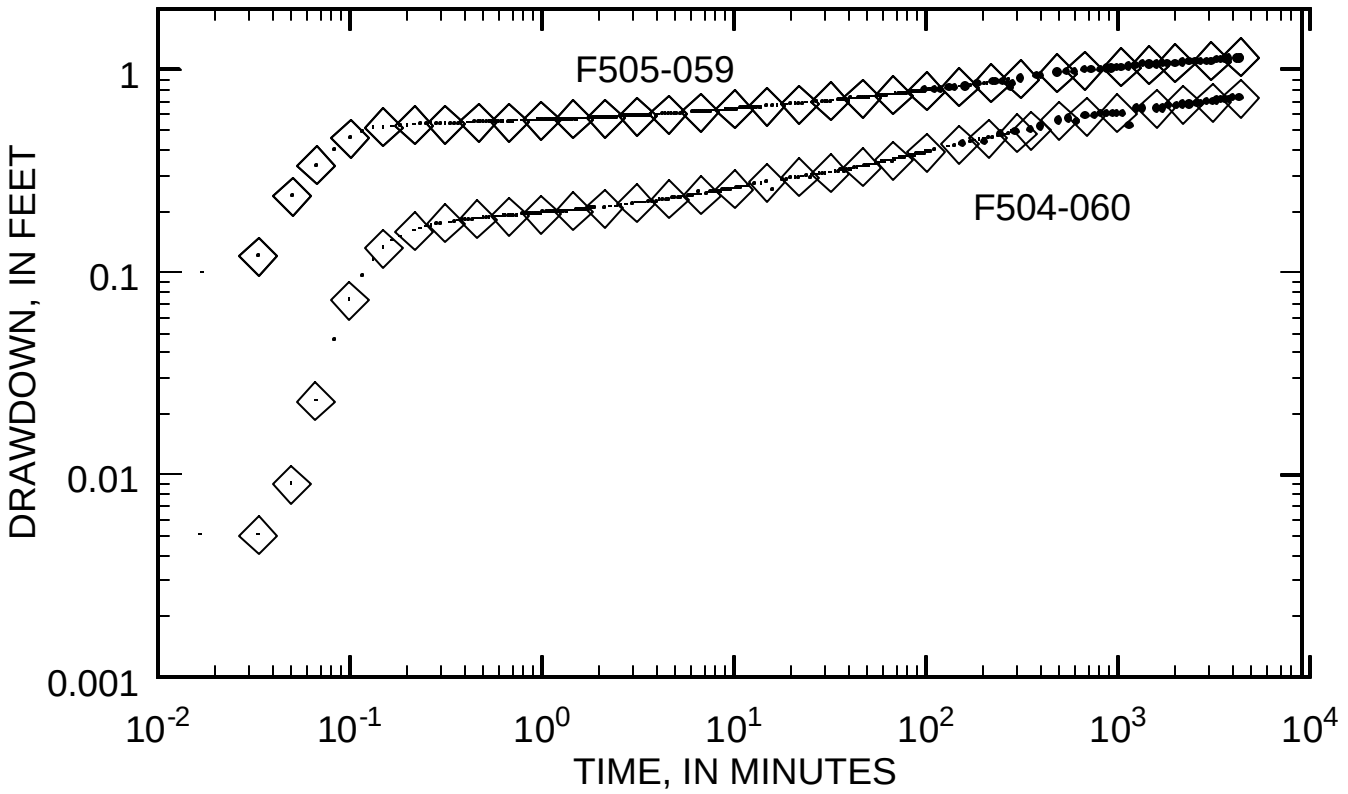
F505-059
F504-060
DRAWDOWN, IN FEET
TIME, IN MINUTES
1
0.1
0.01
0.001
10^{-2}
10^{-1}
10^{0}
10^{1}
10^{2}
10^{3}
10^{4}

Fig. D

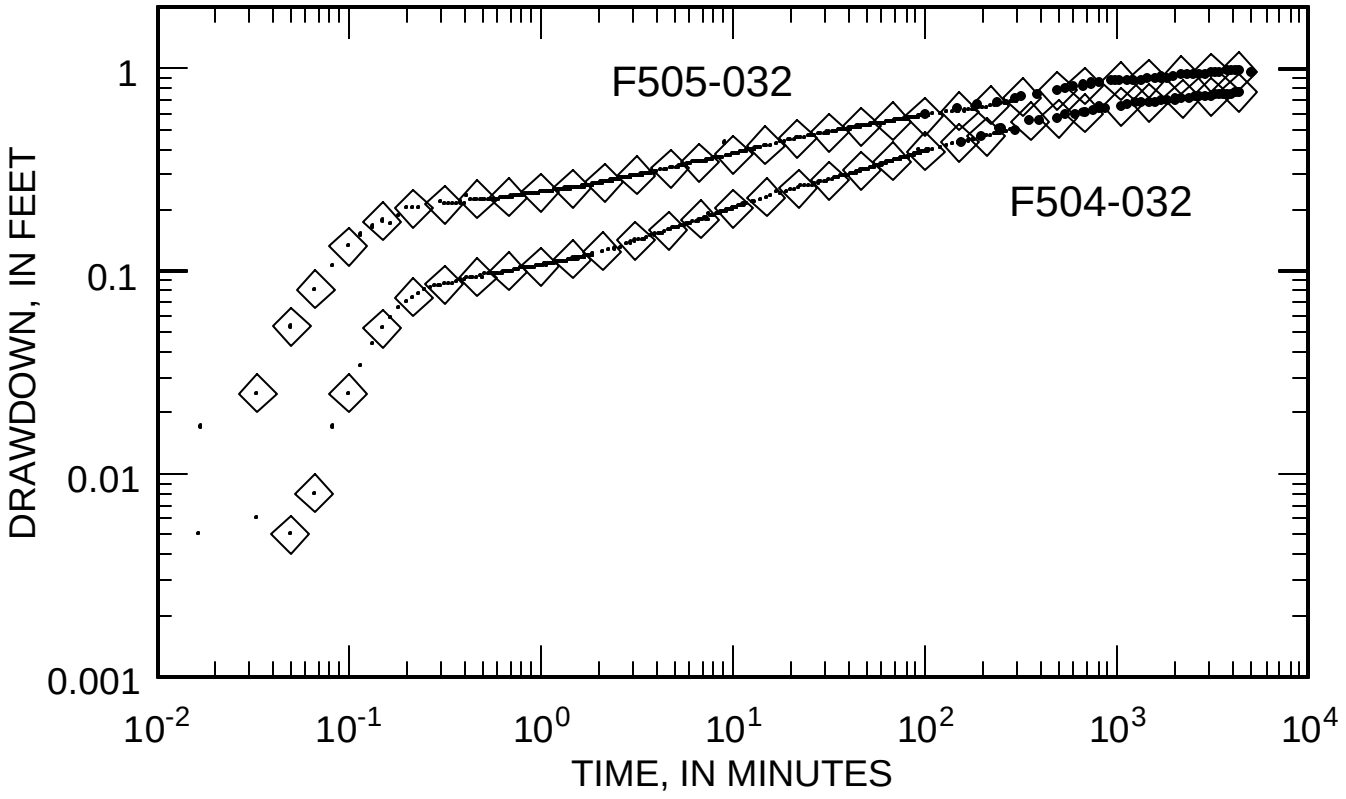
F505-032
F504-032
DRAWDOWN, IN FEET
1
0.1
0.01
0.001
10^{-2}
10^{-1}
10^{0}
10^{1}
10^{2}
10^{3}
10^{4}
TIME, IN MINUTES

Fig. E

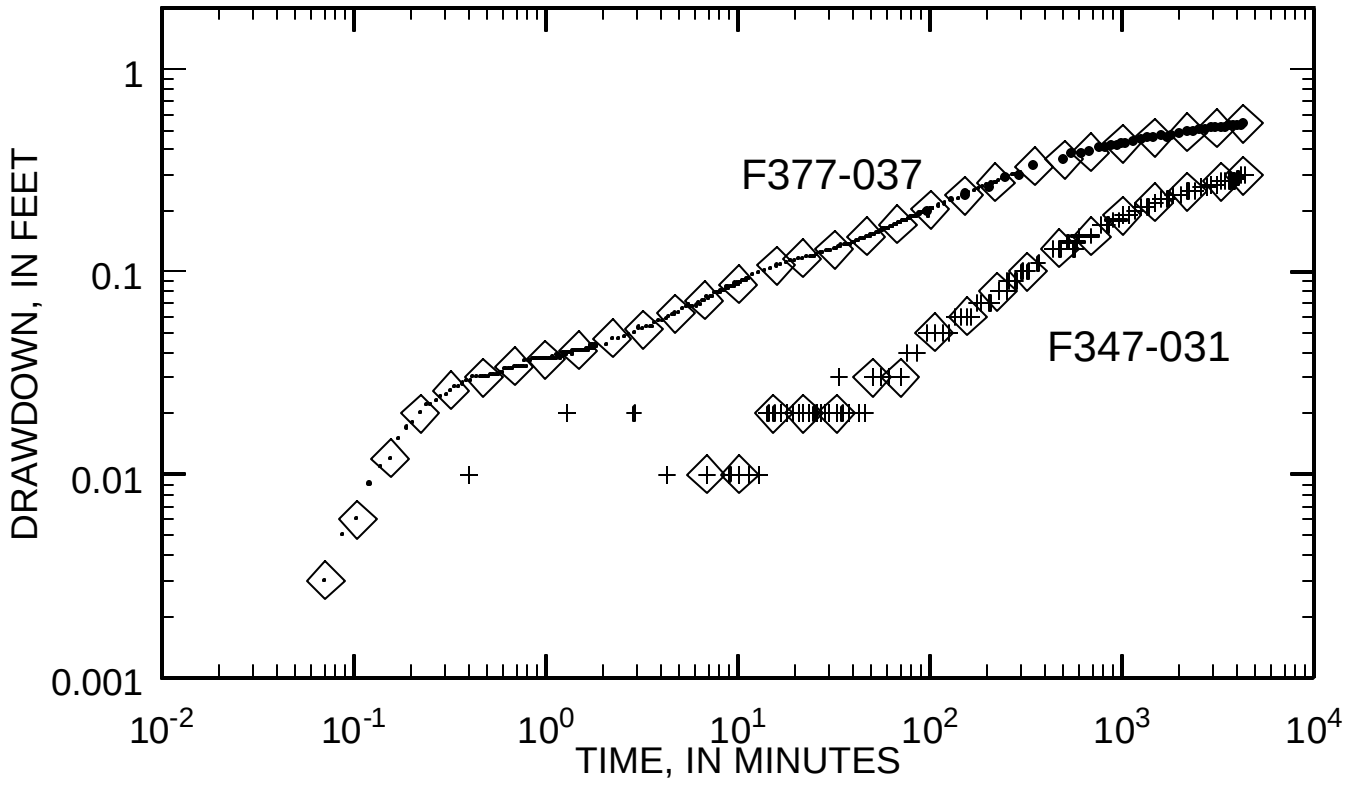
F377-037
F347-031
DRAWDOWN, IN FEET
1
0.1
0.01
0.001
10^{-2}
10^{-1}
10^{0}
10^{1}
10^{2}
10^{3}
10^{4}
TIME, IN MINUTES

Fig. F

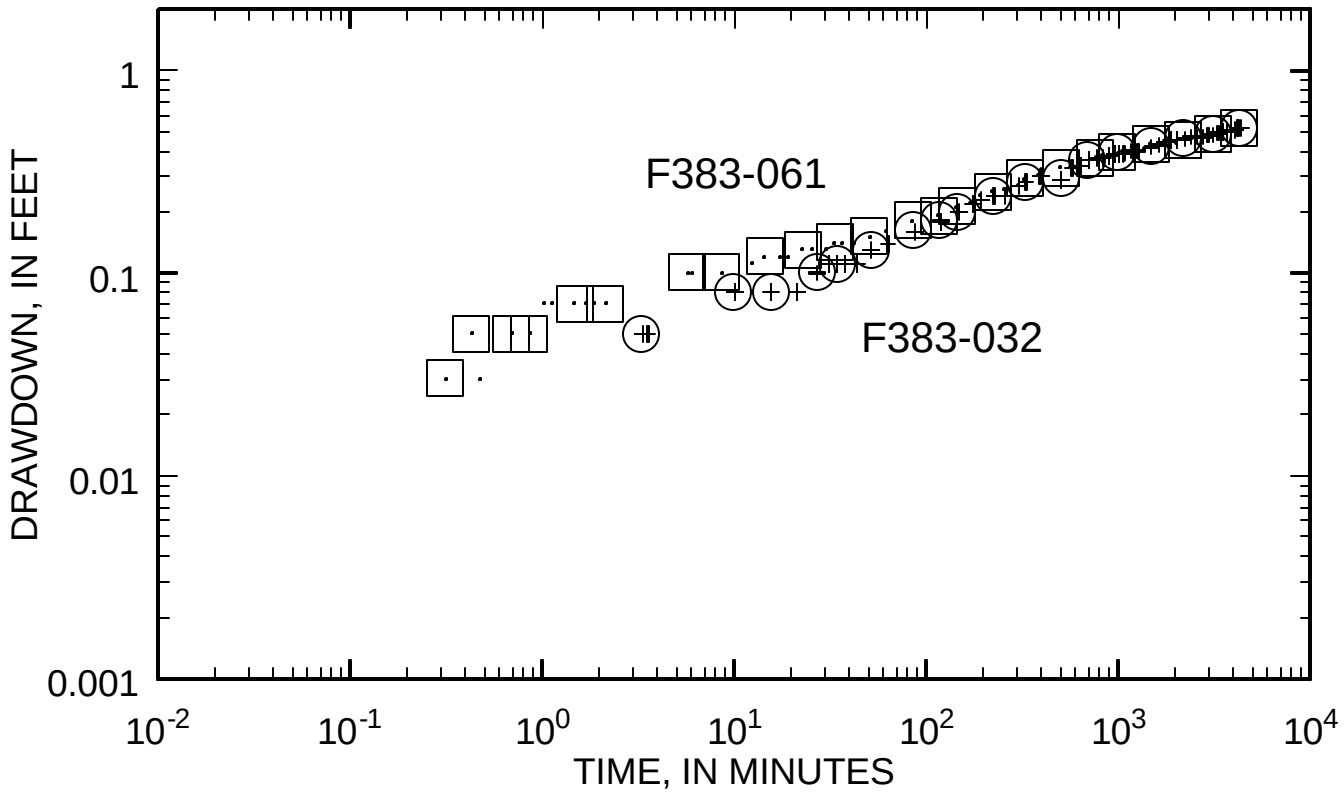
DRAWDOWN, IN FEET
1
0.1
0.01
0.001
F383-061
F383-032
10^{-2}
10^{-1}
10^{0}
10^{1}
10^{2}
10^{3}
10^{4}
TIME, IN MINUTES

Fig. G

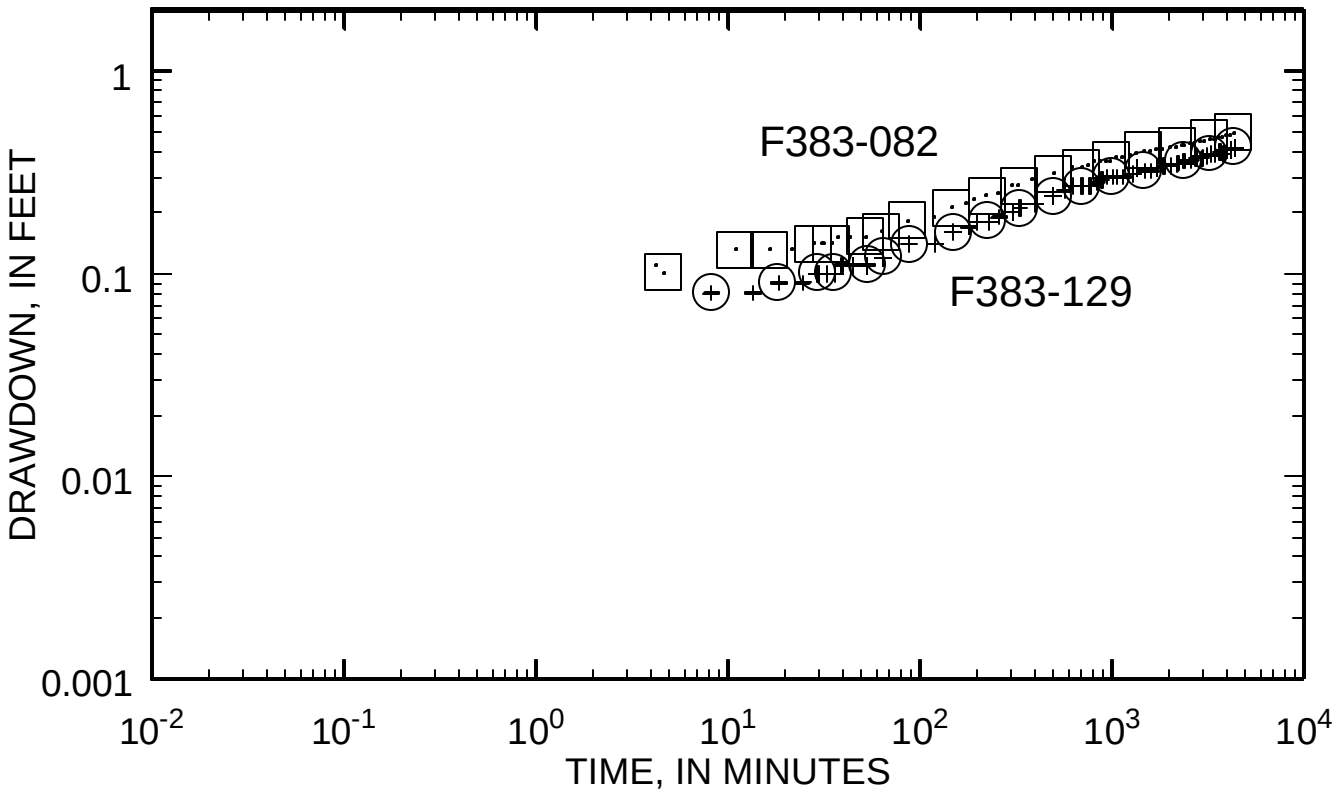
DRAWDOWN, IN FEET
1
0.1
0.01
0.001
F383-082
F383-129
10^{-2}
10^{-1}
10^{0}
10^{1}
10^{2}
10^{3}
10^{4}
TIME, IN MINUTES

Fig. H

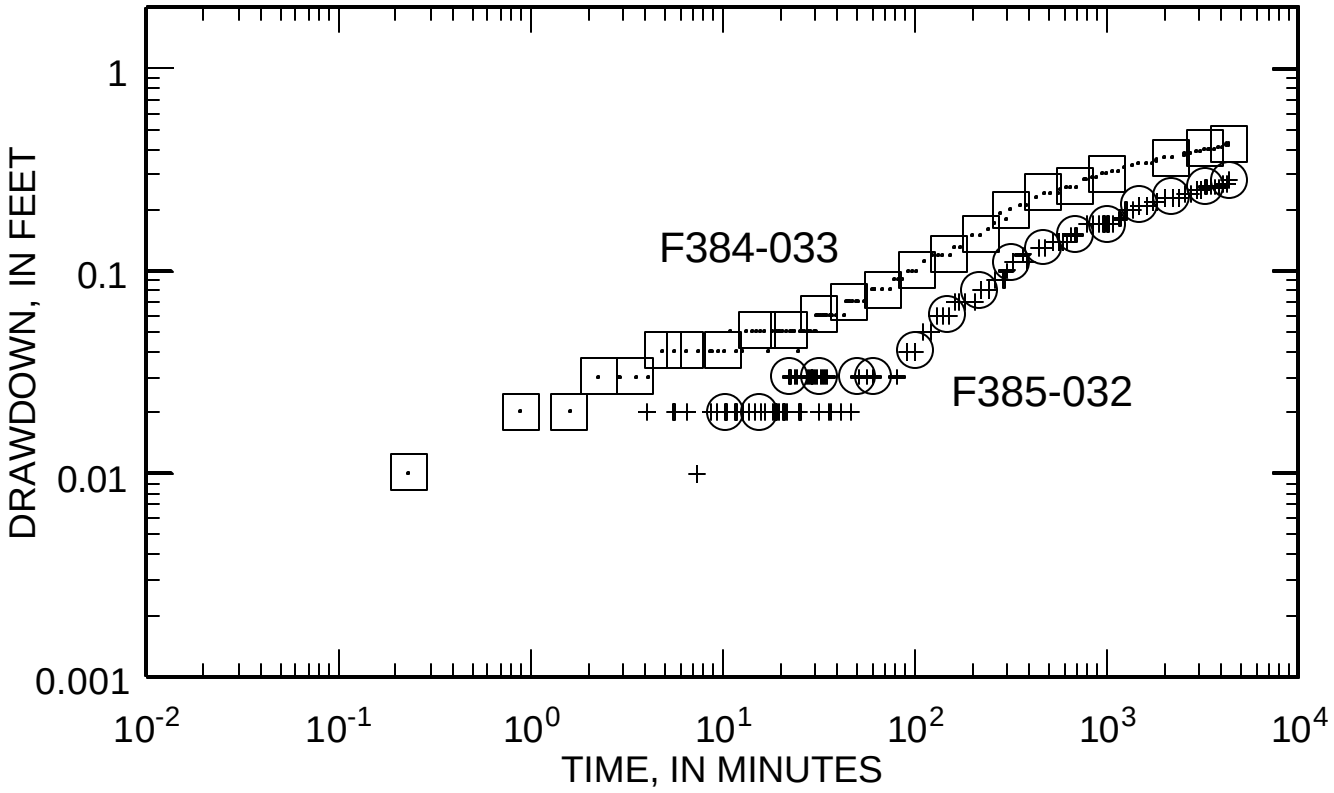
DRAWDOWN, IN FEET
1
0.1
0.01
0.001
F384-033
F385-032
10^{-2}
10^{-1}
10^{0}
10^{1}
10^{2}
10^{3}
10^{4}
TIME, IN MINUTES

Fig. I

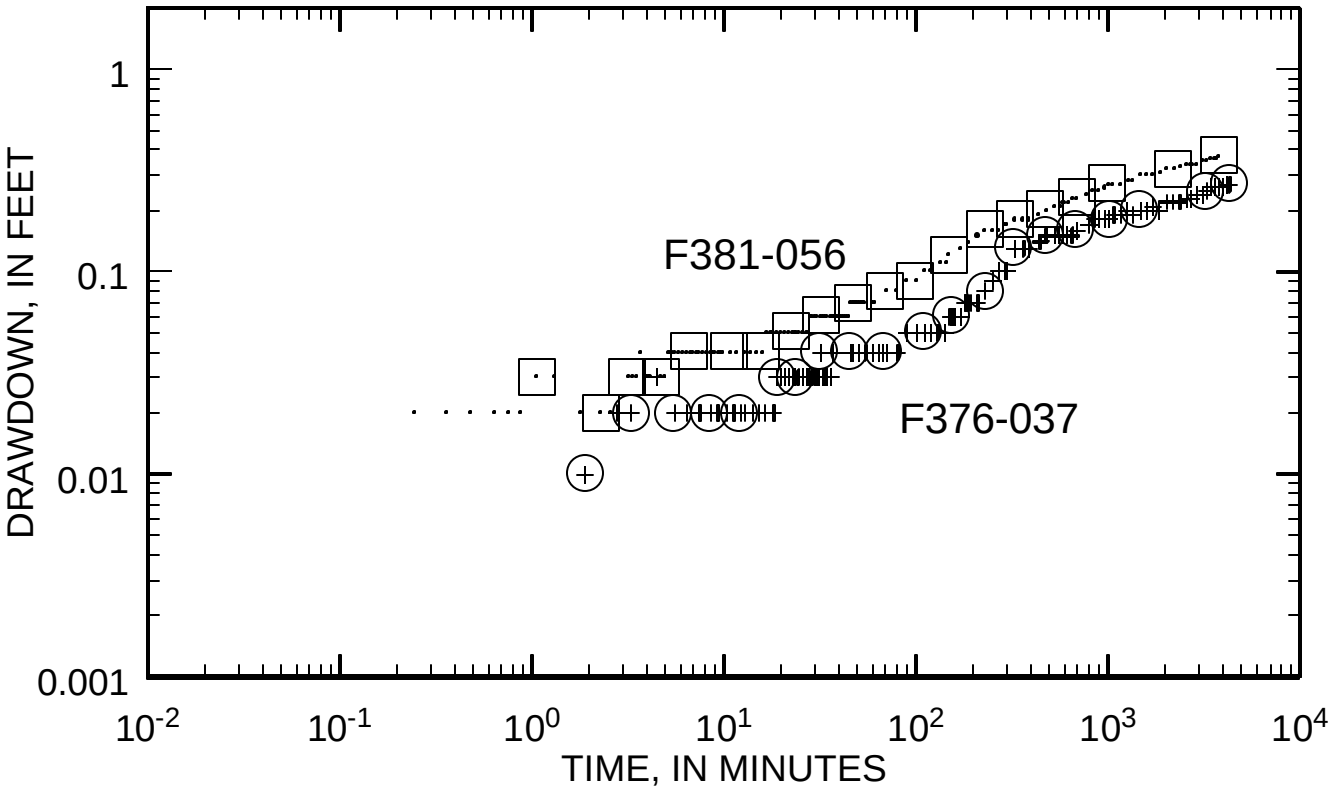
DRAWDOWN, IN FEET
1
0.1
0.01
0.001
F381-056
F376-037
10^{-2}
10^{-1}
10^{0}
10^{1}
10^{2}
10^{3}
10^{4}
TIME, IN MINUTES

Fig. J

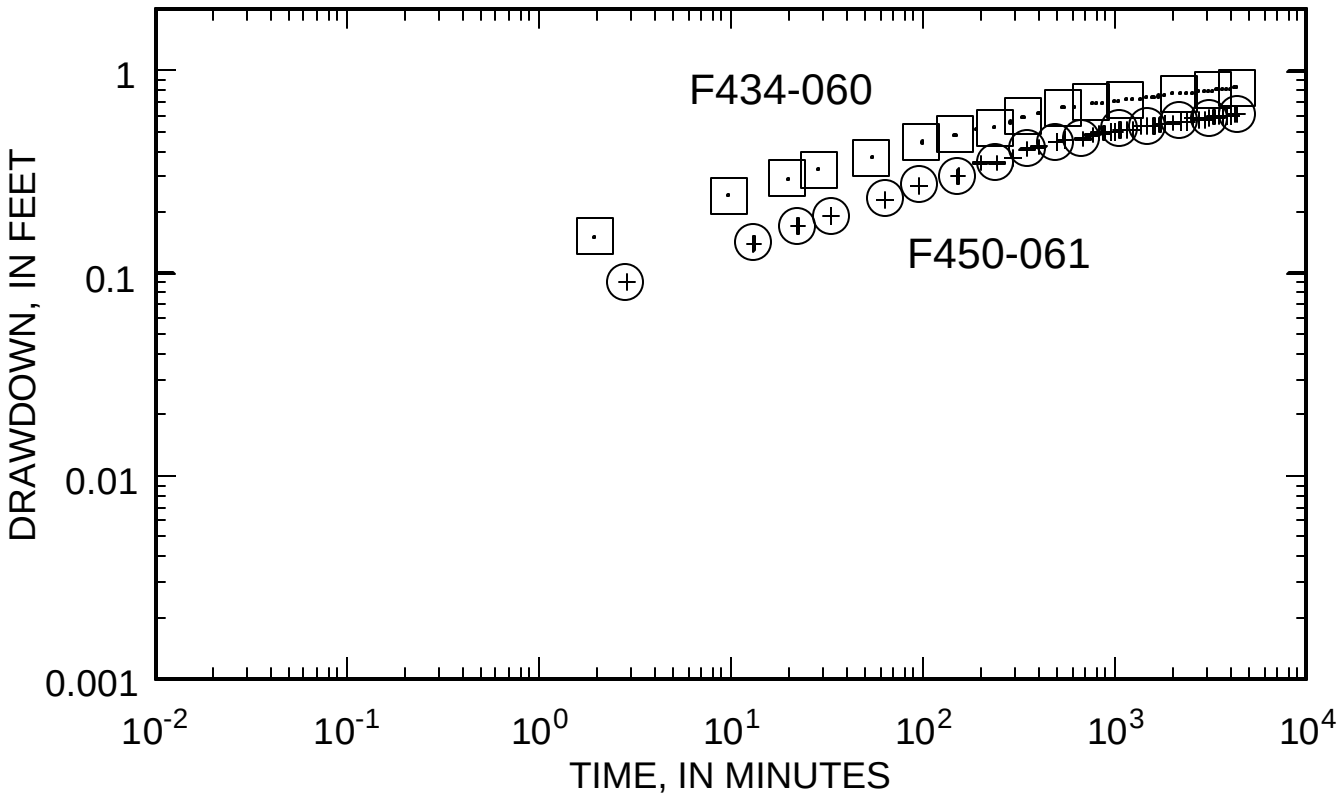
F434-060
F450-061
DRAWDOWN, IN FEET
TIME, IN MINUTES
1
0.1
0.01
0.001
10-2
10-1
100
101
102
103
104

Fig. K

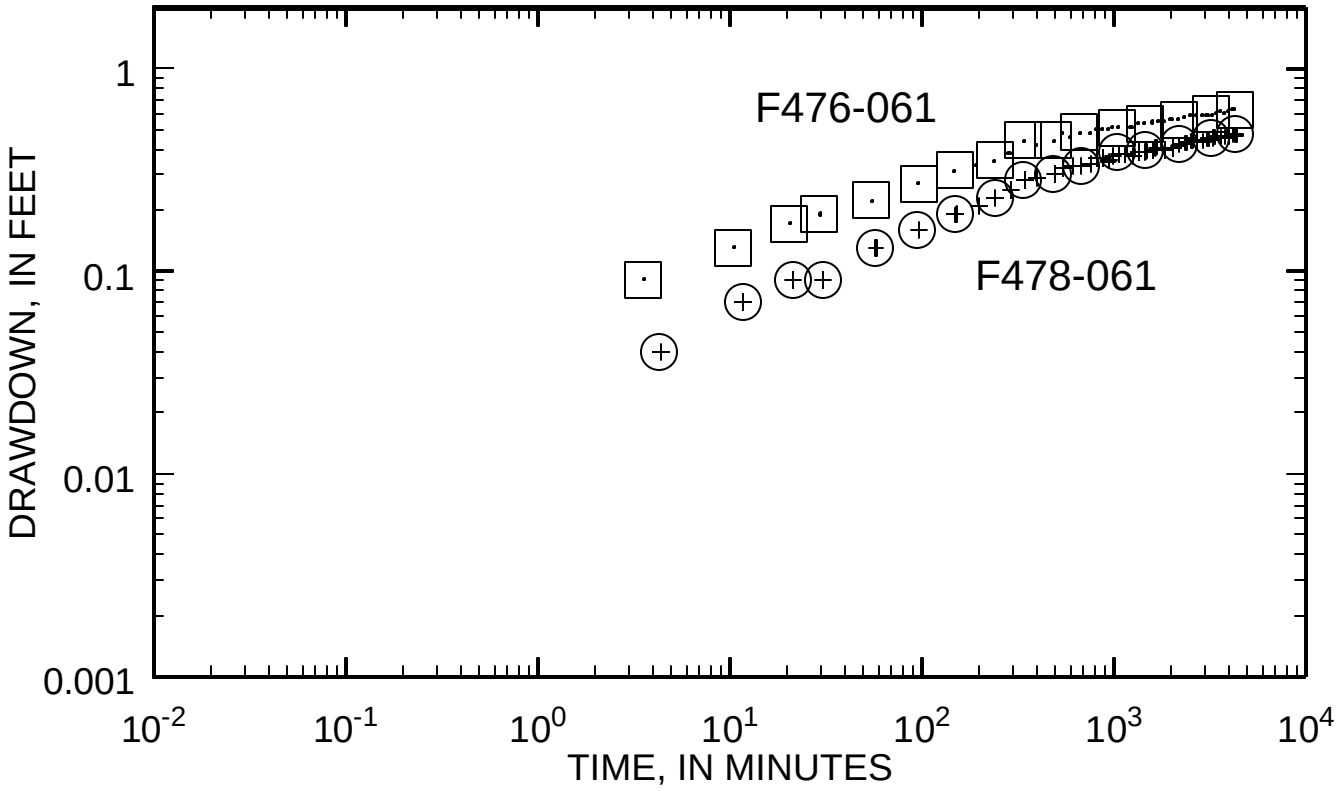
F476-061
F478-061
DRAWDOWN, IN FEET
TIME, IN MINUTES
1
0.1
0.01
0.001
10-2
10-1
100
101
102
103
104

Table A. Data selected for parameter estimation, with PEST observation numbers.

F507-080		PEST
t (min)	h(ft)	Obs. #
0.0337	2.560	1 *
0.0504	3.530	2 *
0.0670	3.680	3 *
0.1000	3.750	4 *
0.1500	3.870	5 *
0.2170	3.790	6 *
0.3170	3.760	7 *
0.4670	3.760	8
0.6840	3.740	9
1.0000	3.760	10
1.4700	3.750	11
2.1500	3.750	12
3.1700	3.780	13
4.5800	3.790	14
6.7500	3.850	15
10.100	3.840	16
14.900	3.900	17
21.900	3.920	18
46.900	3.940	19
67.900	3.960	20
101.00	3.990	21
151.00	4.010	22
221.00	4.020	23
321.00	4.090	24
461.00	4.120	25
681.00	4.230	26
1000.0	4.210	27
1470.0	4.240	28
2150.0	4.290	29
3160.0	4.260	30
4360.0	4.350	31

F505-032		PEST
t (min)	h(ft)	Obs. #
0.0337	0.0250	32
0.0504	0.0530	33
0.0670	0.0810	34
0.1000	0.1320	35
0.1500	0.1770	36
0.2170	0.2040	37
0.3170	0.2140	38
0.4670	0.2250	39
0.6840	0.2310	40
1.0000	0.2440	41
1.4700	0.2570	42
2.1500	0.2750	43
3.1700	0.2960	44
4.7500	0.3210	45
6.7500	0.3450	46
10.100	0.3770	47
14.900	0.4150	48
21.900	0.4510	49
31.900	0.4820	50
46.900	0.5160	51
67.900	0.5450	52
99.900	0.5820	53
151.00	0.6130	54
221.00	0.6540	55
325.00	0.7200	56
492.00	0.7800	57
675.00	0.8200	58
1050.0	0.8600	59
1470.0	0.8900	60
2190.0	0.9200	61
3100.0	0.9500	62
4330.0	0.9700	63

F505-059		PEST
t (min)	h(ft)	Obs. #
0.0337	0.1190	64
0.0504	0.2370	65
0.0670	0.3350	66
0.1000	0.4550	67
0.1500	0.5160	68
0.2170	0.5310	69
0.3170	0.5350	70
0.4670	0.5450	71
0.6840	0.5500	72
1.0000	0.5590	73
1.4700	0.5670	74
2.1500	0.5760	75
3.1700	0.5890	76
4.5800	0.6020	77
6.7500	0.6140	78
10.100	0.6340	79
14.900	0.6560	80
21.900	0.6740	81
31.900	0.6930	82
46.900	0.7200	83
67.900	0.7460	84
101.00	0.7810	85
151.00	0.8190	86
221.00	0.8580	87
312.00	0.9000	88
488.00	0.9600	89
672.00	0.9900	90
1050.0	1.0200	91
1470.0	1.0500	92
2010.0	1.0700	93
3090.0	1.1000	94
4350.0	1.1400	95

F505-080		PEST
t (min)	h(ft)	Obs. #
0.0170	0.0220	96
0.0337	0.0440	97
0.0504	0.0910	98
0.0670	0.1310	99
0.1000	0.2160	100
0.1500	0.3130	101
0.2170	0.3560	102
0.3170	0.3720	103
0.4670	0.3820	104
0.6840	0.3900	105
1.0200	0.3980	106
1.5000	0.4020	107
2.1500	0.4070	108
3.1500	0.4150	109
4.5800	0.4230	110
6.7500	0.4330	111
10.100	0.4460	112
14.900	0.4590	113
21.900	0.4730	114
31.900	0.4860	115
46.900	0.5020	116
68.900	0.5230	117
101.00	0.5470	118
151.00	0.5780	119
211.00	0.6020	120
321.00	0.6600	121
491.00	0.7000	122
674.00	0.7300	123
1050.0	0.7700	124
1470.0	0.7900	125
2190.0	0.8100	126
3090.0	0.8500	127
4330.0	0.8700	128

* Values not used

Table A (con't)

F504-032		PEST
t (min)	h(ft)	Obs. #
0.0500	0.0050	129
0.0667	0.0080	130
0.1000	0.0250	131
0.1500	0.0520	132
0.2170	0.0740	133
0.3170	0.0860	134
0.4670	0.0930	135
0.6830	0.1000	136
1.0000	0.1060	137
1.4700	0.1150	138
2.1200	0.1250	139
3.1200	0.1410	140
4.6200	0.1580	141
6.7800	0.1790	142
10.100	0.2040	143
14.900	0.2310	144
21.900	0.2560	145
31.900	0.2810	146
46.900	0.3130	147
67.900	0.3470	148
101.00	0.3880	149
151.00	0.4290	150
211.00	0.4620	151
356.00	0.5500	152
497.00	0.5700	153
682.00	0.6000	154
1060.0	0.6500	155
1480.0	0.6800	156
2200.0	0.7100	157
3100.0	0.7300	158
4330.0	0.7600	159

F504-060		PEST
t (min)	h(ft)	Obs. #
0.0333	0.0050	160
0.0500	0.0090	161
0.0667	0.0230	162
0.1000	0.0720	163
0.1500	0.1310	164
0.2170	0.1590	165
0.3170	0.1740	166
0.4670	0.1820	167
0.6830	0.1890	168
1.0000	0.1940	169
1.4700	0.1990	170
2.1200	0.2070	171
3.1200	0.2180	172
4.6200	0.2280	173
6.7800	0.2390	174
10.100	0.2570	175
14.900	0.2760	176
21.900	0.2930	177
31.900	0.3080	178
46.900	0.3300	179
67.900	0.3560	180
101.00	0.3880	181
151.00	0.4260	182
211.00	0.4550	183
301.00	0.4870	184
354.00	0.5000	185
498.00	0.5600	186
684.00	0.5900	187
1000.0	0.6100	188
1600.0	0.6400	189
2200.0	0.6700	190
3100.0	0.6900	191
4340.0	0.7200	192

F504-080		PEST
t (min)	h(ft)	Obs. #
0.0667	0.0030	193
0.0833	0.0110	194
0.1000	0.0210	195
0.1330	0.0460	196
0.1670	0.0750	197
0.2170	0.1060	198
0.3170	0.1330	199
0.4670	0.1480	200
0.6830	0.1570	201
1.0000	0.1630	202
1.4700	0.1680	203
2.1200	0.1740	204
3.1200	0.1810	205
4.6200	0.1890	206
6.7800	0.1980	207
10.100	0.2080	208
15.900	0.2240	209
21.900	0.2320	210
31.900	0.2420	211
46.900	0.2580	212
67.900	0.2740	213
101.00	0.2980	214
151.00	0.3280	215
211.00	0.3530	216
353.00	0.4200	217
499.00	0.4400	218
686.00	0.4800	219
1000.0	0.5000	220
1480.0	0.5300	221
2200.0	0.5600	222
3100.0	0.5800	223
4330.0	0.6100	224

F377-037		PEST
t (min)	h(ft)	Obs. #
0.0720	0.0030	225
0.1050	0.0060	226
0.1550	0.0120	227
0.2220	0.0200	228
0.3220	0.0260	229
0.4720	0.0300	230
0.6880	0.0340	231
1.0050	0.0370	232
1.4720	0.0410	233
2.2380	0.0470	234
3.2380	0.0520	235
4.7380	0.0620	236
6.7380	0.0720	237
10.072	0.0870	238
15.905	0.1070	239
21.905	0.1160	240
31.905	0.1290	241
46.905	0.1490	242
67.905	0.1710	243
100.91	0.2030	244
150.91	0.2390	245
220.91	0.2760	246
351.90	0.3300	247
500.90	0.3600	248
687.90	0.3900	249
1001.9	0.4300	250
1481.9	0.4600	251
2202.9	0.4900	252
3103.9	0.5100	253
4336.9	0.5400	254

Table A (con't)

F383-032		PEST
t (min)	h(ft)	Obs. #
3.3200	0.0500	255
10.000	0.0800	256
15.600	0.0800	257
27.000	0.1000	258
34.500	0.1100	259
51.800	0.1300	260
86.700	0.1600	261
119.00	0.1800	262
147.00	0.2000	263
226.00	0.2400	264
329.00	0.2800	265
506.00	0.2900	266
706.00	0.3600	267
1000.0	0.3900	268
1490.0	0.4200	269
2210.0	0.4600	270
3120.0	0.4800	271
4350.0	0.5200	272

F383-061		PEST
t (min)	h(ft)	Obs. #
0.3170	0.0300	273
0.4330	0.0500	274
0.7000	0.0500	275
0.8670	0.0500	276
1.5000	0.0700	277
2.1700	0.0700	278
5.7800	0.1000	279
8.7300	0.1000	280
14.500	0.1200	281
22.900	0.1300	282
33.700	0.1400	283
51.100	0.1500	284
85.600	0.1800	285
118.00	0.1900	286
146.00	0.2100	287
224.00	0.2500	288
328.00	0.2900	289
507.00	0.3300	290
773.00	0.3700	291
1010.0	0.3900	292
1490.0	0.4300	293
2210.0	0.4500	294
3120.0	0.4800	295
4350.0	0.5100	296

F383-082		PEST
t (min)	h(ft)	Obs. #
4.7000	0.1000	297
11.100	0.1300	298
16.800	0.1300	299
28.500	0.1400	300
35.300	0.1400	301
52.800	0.1500	302
64.100	0.1600	303
87.700	0.1800	304
149.00	0.2100	305
227.00	0.2400	306
331.00	0.2700	307
505.00	0.3100	308
708.00	0.3300	309
1000.0	0.3600	310
1490.0	0.4000	311
2210.0	0.4200	312
3300.0	0.4600	313
4350.0	0.4900	314

F383-129		PEST
t (min)	h(ft)	Obs. #
8.2300	0.0800	315
18.500	0.0900	316
29.500	0.1000	317
36.000	0.1000	318
53.600	0.1100	319
64.900	0.1200	320
88.700	0.1400	321
151.00	0.1600	322
228.00	0.1800	323
333.00	0.2100	324
501.00	0.2400	325
703.00	0.2700	326
1010.0	0.3000	327
1490.0	0.3200	328
2390.0	0.3600	329
3300.0	0.3900	330
4350.0	0.4200	331

Table A (con't)

F384-033		PEST
t (min)	h (ft)	Obs. #
0.2330	0.0100	332
0.9000	0.0200	333
1.6200	0.0200	334
2.3000	0.0300	335
3.5700	0.0300	336
4.9000	0.0400	337
6.5200	0.0400	338
10.3000	0.0400	339
15.2000	0.0500	340
22.6000	0.0500	341
32.1000	0.0600	342
46.3000	0.0700	343
68.8000	0.0800	344
104.0000	0.1000	345
154.0000	0.1200	346
223.0000	0.1500	347
321.0000	0.2000	348
474.0000	0.2400	349
695.0000	0.2600	350
1010.0000	0.3000	351
2210.0000	0.3600	352
3300.0000	0.4000	353
4340.0000	0.4200	354

F381-056		PEST
t (min)	h (ft)	Obs. #
1.0800	0.0300	355
2.3200	0.0200	356
3.2200	0.0300	357
4.7300	0.0300	358
6.7300	0.0400	359
10.9000	0.0400	360
15.9000	0.0400	361
22.9000	0.0500	362
32.9000	0.0600	363
47.9000	0.0700	364
70.9000	0.0800	365
101.0000	0.0900	366
151.0000	0.1200	367
231.0000	0.1600	368
332.0000	0.1800	369
483.0000	0.2000	370
699.0000	0.2300	371
1010.0000	0.2700	372
2220.0000	0.3200	373
3850.0000	0.3700	374

F347-031		PEST
t (min)	h (ft)	Obs. #
6.9000	0.0100	375
10.2000	0.0100	376
15.4000	0.0200	377
22.0000	0.0200	378
32.6000	0.0200	379
50.3000	0.0300	380
70.6000	0.0300	381
106.0000	0.0500	382
157.0000	0.0600	383
227.0000	0.0800	384
324.0000	0.1000	385
475.0000	0.1300	386
694.0000	0.1500	387
1010.0000	0.1900	388
1490.0000	0.2200	389
2210.0000	0.2500	390
3290.0000	0.2800	391
4340.0000	0.3000	392

Table A (con't)

F434-060		PEST
t (min)	h(ft)	Obs. #
1.97	0.1500	393
9.92	0.2400	394
20.00	0.2900	395
29.00	0.3200	396
54.90	0.3700	397
100.00	0.4400	398
149.00	0.4800	399
240.00	0.5200	400
337.00	0.5900	401
545.00	0.6500	402
765.00	0.6900	403
1150.00	0.7100	404
2200.00	0.7600	405
3280.00	0.7900	406
4330.00	0.8200	407

F450-061		PEST
t (min)	h(ft)	Obs. #
2.88	0.0900	408
13.2	0.1400	409
22.4	0.1700	410
33.3	0.1900	411
64.2	0.2300	412
96.0	0.2700	413
152.0	0.3000	414
243.0	0.3500	415
350.0	0.4100	416
496.0	0.4400	417
681.0	0.4600	418
1060.0	0.5100	419
1480.0	0.5300	420
2200.0	0.5600	421
3100.0	0.5800	422
4330.0	0.6100	423

F476-061		PEST
t (min)	h(ft)	Obs. #
3.62	0.0900	424
10.6	0.1300	425
20.7	0.1700	426
30.0	0.1900	427
55.7	0.2200	428
97.9	0.2700	429
150.0	0.3100	430
242.0	0.3500	431
343.0	0.4400	432
494.0	0.4400	433
678.0	0.4800	434
1060.0	0.5100	435
1470.0	0.5300	436
2200.0	0.5600	437
3280.0	0.5900	438
4330.0	0.6200	439

F478-061		PEST
t (min)	h(ft)	Obs. #
4.37	0.0400	440
11.8	0.0700	441
21.5	0.0900	442
30.8	0.0900	443
57.8	0.1300	444
96.9	0.1600	445
151.0	0.1900	446
243.0	0.2300	447
346.0	0.2800	448
495.0	0.3000	449
680.0	0.3300	450
1060.0	0.3800	451
1480.0	0.3900	452
2200.0	0.4200	453
3280.0	0.4500	454
4330.0	0.4700	455

Table A (con't)

F385-032		PEST
t (min)	h(ft)	Obs. #
10.400	0.0200	456
15.700	0.0200	457
22.400	0.0300	458
32.400	0.0300	459
51.300	0.0300	460
61.200	0.0300	461
101.00	0.0400	462
151.00	0.0600	463
221.00	0.0800	464
326.00	0.1100	465
477.00	0.1300	466
692.00	0.1500	467
1020.0	0.1700	468
1480.0	0.2100	469
2210.0	0.2300	470
3290.0	0.2600	471
4340.0	0.2800	472

F376-037		PEST
t (min)	h(ft)	Obs. #
1.9000	0.0100	473
3.3000	0.0200	474
5.5700	0.0200	475
8.5500	0.0200	476
12.300	0.0200	477
19.000	0.0300	478
23.600	0.0300	479
32.200	0.0400	480
45.700	0.0400	481
68.100	0.0400	482
111.00	0.0500	483
156.00	0.0600	484
231.00	0.0800	485
327.00	0.1300	486
478.00	0.1500	487
690.00	0.1600	488
1020.0	0.1800	489
1480.0	0.2000	490
3290.0	0.2500	491
4340.0	0.2700	492

Table 1. Dimensionless Expressions

d_D	d/b
h_D	$4\pi K_r b(h_i-h)/Q$
h_{mD}	$4\pi K_r b(h_i-h_m)/Q$
h_{wD}	$4\pi K_r b(h_i-h_w)/Q$
K_D	K_z/K_r
ℓ_D	ℓ/b
r_D	r/r_w
r_{wD}	r_w/b
S_w	$K_r d_s/K_s r_w$
t_D	$K_r t/r_w^2 S_s$
t_{Dy}	$K_r bt/r_w^2 S_y$
W_D	$\pi r_c^2/[2\pi r_w^2 S_s(\ell-d)]$
W_D'	$\pi r_p^2/(2\pi r_w^2 S_s F')$
z_D	z/b
z_{D1}	z_1/b
z_{D2}	z_2/b
β_w	$K_D r_{wD}^2$
β	$\beta_w r_D^2$
σ	$S_s b/S_y$
γ_m	$\alpha_m b S_y/K_z$
τ	$K_r t'/r_w^2 S_s$

Table 2. Locations of observation piezometers, number of PEST values and measurement numbers.

Location number	Well number (feet)	Radial distance[1] (feet)	Depth[2] (ft)	Screen length (feet)	No. of obs. values for PEST	Measure-ment numbers for PEST
1	F507-080	0.333	13.2	47.	24	8-31 [3]
2	F505-032	23.9	10.7	2.	32	32-63
3	F505-059	19.5	30.6	9.	32	64-95
4	F505-080	21.6	58.4	2.	33	96-128
5	F504-032	46.6	9.6	2.	31	129-159
6	F504-060	49.8	30.0	9.	33	160-192
7	F504-080	53.1	57.5	2.	32	193-224
8	F377-037	85.1	13.3	2.	30	225-254
9	F383-032	93.0	12.1	2.	18	255-272
10	F383-061	92.9	39.9	2.	24	273-296
11	F383-082	94.8	61.8	2.	18	297-314
12	F383-129	96.7	107.8	2.	17	315-331
13	F384-033	137.3	15.8	2.	23	332-354
14	F381-056	159.8	20.0	2.	20	355-374
15	F347-031	225.7	14.8	2.	18	375-392
16	F434-060	38.6	2.0	39.	15	393-407
17	F450-061	66.3	1.7	39.	16	408-423
18	F476-061	65.6	2.2	39.	16	424-439
19	F478-061	101.3	2.2	39.	16	440-455
20	F385-032	224.6	10.0	2.	17	456-472
21	F376-037	227.6	13.2	2.	20	473-492

[1] Distance from center of pumped well

[2] Depth below the initial water table to the top of the screen

[3] First seven values eliminated (see text)

Table 3. Parameters obtained from preliminary analysis of hand-measured drawdown data, where S_y = specific yield, b = saturated thickness, K_r = hydraulic conductivity in the horizontal direction, and K_z = hydraulic conductivity in the vertical direction.

Parameter	Estimated value
S_y	0.23
b (ft)	160.
K_r (ft/min)	0.24
K_z (ft/min)	0.12

Table 4. Parameters obtained from late-time data exclusively using PEST with b=160 feet, where S_y = specific yield, K_r = hydraulic conductivity in the horizontal direction, and K_z = hydraulic conductivity in the vertical direction.

Parameter	Estimated value	95 percent confidence limits		Initial value
		lower limit	upper limit	
S_y	0.2868	0.2790	0.2947	0.1
K_r (ft/min)	0.2318	0.2299	0.2337	0.01
K_z (ft/min)	0.1325	0.1277	0.1375	0.01

Table 5.Parameters obtained from late-time data exclusively using PEST with b as an estimated parameter, where S_y = specific yield, b = saturated thickness, K_r = hydraulic conductivity in the horizontal direction, and K_z = hydraulic conductivity in the vertical direction.

Parameter	Estimated value	95 percent confidence limits		Initial value
		lower limit	upper limit	
S_y	0.2536	0.2356	0.2730	0.1
b (ft)	171.3	165.3	177.4	100.
K_r (ft/min)	0.2289	0.2265	0.2313	0.01
K_z (ft/min)	0.1369	0.1316	0.1424	0.01

Table 6. Parameters estimated from early and late-time data exclusively, using PEST, where S_s = specific storage, S_y = specific yield, b = saturated thickness, K_r = hydraulic conductivity in the horizontal direction, and K_z = hydraulic conductivity in the vertical direction.

Parameter	Estimated value	95 percent confidence limits		Initial value
		lower limit	upper limit	
S_s (ft^{-1})	1.299E-05	1.239E-05	1.362E-05	1.E-06
S_y	0.2645	0.2402	0.2913	0.1
b (ft)	168.3	160.6	176.3	100.
K_r (ft/min)	0.2303	0.2272	0.2334	0.01
K_z (ft/min)	0.1295	0.1235	0.1357	0.01

Table 7. Parameters estimated from the complete data set using PEST, where S_s = specific storage, S_y = specific yield, b = saturated thickness, K_r = hydraulic conductivity in the horizontal direction, K_z = hydraulic conductivity in the vertical direction, and α_1, α_2, and α_3 are empirical constants for gradual drainage from the unsaturated zone.

Parameter	Estimated Value	95% Confidence Limits		Initial Value
		lower limit	upper limit	
S_s (ft^{-1})	1.305E-05	1.205E-05	1.414E-05	1.E-06
S_y	0.2660	0.2525	0.2802	0.1
b (ft)	168.9	162.5	175.4	200.
K_r (ft/min)	0.2331	0.2299	0.2362	0.01
K_z (ft/min)	0.1418	0.1365	0.1474	0.01
α_1 (min^{-1})	2.78E-04	1.50E-04	5.14E-04	1.E-03
α_2 (min^{-1})	1.68E-02	1.27E-02	2.22E-02	1.E-02
α_3 (min^{-1})	0.416	0.318	0.545	1.E-01

Table 8. Correlation Coefficient Matrix for Table 7, where S_s = specific storage, S_y = specific yield, b = saturated thickness, K_r = hydraulic conductivity in the horizontal direction, K_z = hydraulic conductivity in the vertical direction, and α_1, α_2, and α_3 are empirical constants for gradual drainage from the unsaturated zone.

	S_s	S_y	b	K_r	K_z	α_1	α_2	α_3
S_s	1.							
S_y	.006	1						
b	-.058	-.195	1					
K_r	.213	-.217	-.406	1				
K_z	-.290	-.002	.173	-.703	1			
α_1	-.035	-.380	-.627	.025	.065	1		
α_2	.012	-.797	.142	.103	-.070	.378	1	
α_3	-.093	-.180	-.020	.294	-.539	.092	.160	1

Table 9. Parameters estimated from the complete data set using PEST with alternative initial values, where S_s = specific storage, S_y = specific yield, b = saturated thickness, K_r = hydraulic conductivity in the horizontal direction, K_z = hydraulic conductivity in the vertical direction, and α_1, α_2, and α_3 are empirical constants for gradual drainage from the unsaturated zone.

Parameter	Estimated Value	95% Confidence Limits		Initial Value
		lower limit	upper limit	
S_s (ft^{-1})	1.306E-05	1.206E-05	1.415E-05	1.E-07
S_y	0.2623	0.2500	0.2752	0.05
b (ft)	172.8	165.3	180.7	80.
K_r (ft/min)	0.2336	0.2304	0.2368	0.005
K_z (ft/min)	0.1409	0.1356	0.1465	0.005
α_1 (min^{-1})	1.92E-04	9.94E-05	3.72E-04	1.E-04
α_2 (min^{-1})	1.79E-02	1.37E-02	2.33E-02	1.E-02
α_3 (min^{-1})	0.441	0.333	0.584	1.E00

Table 10a. Estimates of the variance and standard deviation of head in the aquifer for three-dimensional and one-dimensional flow using equations 27 and 28, where α_f^2 = variance of ln K_r, J = horizontal hydraulic gradient, λ_1 = horizontal log hydraulic conductivity correlation scale, and λ_2 = vertical log hydraulic conductivity correlation scale. Metric units are used.

α_f^2	J	λ_1(m)	λ_3(m)	α_{3Dh}^2 (m^2)	α_{3Dh} (m)	α_{1Dh}^2 (m^2)	α_{1Dh} (m)
0.24	0.01	3.5	0.19	$6.3x10^{-6}$	0.0024	$1.5x10^{-3}$	0.039
0.24	0.01	8.0	0.38	$2.9x10^{-5}$	0.0054	$8.0x10^{-3}$	0.089
0.24	0.001	3.5	0.19	$6.3x10^{-8}$	$2.4x10^{-4}$	$1.5x10^{-5}$	$3.9x10^{-3}$
0.24	0.001	8.0	0.38	$2.9x10^{-7}$	$5.4x10^{-4}$	$8.0x10^{-5}$	$8.9x10^{-3}$

Table 10b. Estimates of the variance and standard deviation of head in the aquifer for three-dimensional and one-dimensional flow using equations 27 and 28, where α_f^2 = variance of ln K_r, J = horizontal hydraulic gradient, λ_1 = horizontal log hydraulic conductivity correlation scale, and λ_2 = vertical log hydraulic conductivity correlation scale. English units are used.

α_f^2	J	λ_1(ft)	λ_3(ft)	α_{3Dh}^2 (ft^2)	α_{3Dh} (ft)	α_{1Dh}^2 (ft^2)	α_{1Dh} (ft)
0.24	0.01	11.5	0.62	$6.8x10^{-5}$	0.0079	$1.6x10^{-2}$	0.13
0.24	0.01	26.2	1.25	$3.1x10^{-4}$	0.018	$8.6x10^{-2}$	0.29
0.24	0.001	11.5	0.62	$6.8x10^{-7}$	$7.9x10^{-4}$	$1.6x10^{-4}$	$1.3x10^{-2}$
0.24	0.001	26.2	1.25	$3.1x10^{-6}$	$1.8x10^{-3}$	$8.6x10^{-4}$	$2.9x10^{-2}$

Table 11. Column headings for Tables 12-15

Column	Piezometers	Description
A	F505-080 F504-080 F383-082 F383-129	Deep-seated piezometers
B	F505-059 F504-060 F383-061	Mid-depth piezometer and wells
C	F505-032 F504-032 F377-037 F383-032	Shallow, close-in piezometers
D	F384-033 F381-056 F347-031 F385-032 F376-037	Shallow, distant piezometers
E	F434-060 F450-061 F476-061 F478-061	Long-screened wells
F	F505-032 F505-059 F505-080	Piezometer cluster F505 (20-24 ft from pumped well)
G	F504-032 F504-060 F504-080	Piezometer cluster F504 (47-53 ft from pumped well)
H	F383-032 F383-061 F383-082 F383-129	Piezometer cluster F383 (93-97 ft from pumped well)

Table 12. Analysis of selected piezometer groups assuming gradual drainage and adjustable saturated thickness, where S_s = specific storage, S_y = specific yield, b = saturated thickness, K_r = hydraulic conductivity in the horizontal direction, K_z = hydraulic conductivity in the vertical direction, and α_1, α_2, and α_3 are empirical constants for gradual drainage from the unsaturated zone.

Parameter	**Table 7**	A	B	C	D	E	F	G	H
S_s ft^{-1}	**1.3E-05**	1.4E-05	1.3E-05	1.9E-05	1.3E-05 *	1.3E-05 *	1.2E-05	1.8E-05	1.3E-05 *
S_y	**0.266**	0.249	0.248	0.280	0.241	0.278	0.217	0.240	0.360
b ft	**169**	176	157	198	217	178	159	202	253
K_r ft/min	**0.233**	0.243	0.248	0.230	0.203	0.226	0.249	0.227	0.157
K_z ft/min	**0.142**	0.135	0.123	0.110	0.104	0.144	0.135	0.134	0.152
α_1 min^{-1}	**2.8E-04**	2.8E-05	1.7E-04	4.9E-05	8.2E-04	2.3E-04	8.7E-05	1.7E-06	8.0E-04
α_2 min^{-1}	**1.7E-02**	2.8E-02	2.6E-02	1.2E-02	2.2E-02	2.4E-02	1.8E-02	1.9E-02	8.8E-03
α_3 min^{-1}	**0.42**	1.4	3.2	0.65	6.6E-02	21.	0.60	0.32	6.6E-02

* -fixed value

Table 13. Analysis of selected piezometer groups assuming delayed drainage and fixed saturated thickness, where S_s = specific storage, S_y = specific yield, b = saturated thickness, K_r = hydraulic conductivity in the horizontal direction, K_z = hydraulic conductivity in the vertical direction, and α_1, α_2, and α_3 are empirical constants for gradual drainage from the unsaturated zone.

Parameter	**Table 7**	A	B	C	D	E	F	G	H
S_s ft^{-1}	**1.3E-05**	1.4E-05	1.3E-05	2.0E-05	1.3E-05 *	1.3E-05 *	1.1E-05	2.0E-05	1.3E-05 *
S_y	**0.266**	0.260	0.235	0.277	0.252	0.275	0.217	0.206	0.331
b ft	**169**	170 *	170 *	170 *	170 *	170 *	170 *	170 *	170 *
K_r ft/min	**0.233**	0.243	0.247	0.230	0.256	0.227	0.246	0.252	0.211
K_z ft/min	**0.142**	0.132	0.124	0.135	0.0693	0.147	0.137	0.127	0.129
α_1 min^{-1}	**2.8E-04**	4.6-05	3.8E-05	2.1E-04	7.3E-04	4.1E-04	1.1E-05	1.5E-05	6.3E-04
α_2 min^{-1}	**1.7E-02**	2.6E-02	3.0E-02	1.2E-02	3.2E-02	2.7E-02	2.1E-02	2.4E-02	1.2E-02
α_3 min^{-1}	**0.42**	4.1	3.2	0.30	0.35	15.	0.61	0.43	0.17

* -fixed value

Table 14. Analysis of selected piezometer groups assuming instantaneous drainage for times greater than 430 minutes and adjustable saturated thickness, where S_s = specific storage, S_y = specific yield, b = saturated thickness, K_r = hydraulic conductivity in the horizontal direction, and K_z = hydraulic conductivity in the vertical direction.

Parameter	**Table 5**	All	A	B	C	D	E	F	G	H
S_y	**0.254**	0.175	0.152	0.164	0.264	0.181	0.190	0.251	0.241	0.310
b ft	**171**	198	188	172	260	243	228	229	266	403
K_r ft/min	**0.229**	0.227	0.238	0.285	0.222	0.232	0.218	0.209	0.208	0.124
K_z ft/min	**0.137**	0.137	0.140	0.0591	0.0712	0.0682	0.123	0.154	0.101	0.186

Table 15. Analysis of selected piezometer groups assuming instantaneous drainage for times greater than 430 minutes with fixed saturated thickness, where S_s = specific storage, S_y = specific yield, b = saturated thickness, K_r = hydraulic conductivity in the horizontal direction, K_z = hydraulic conductivity in the vertical direction.

Parameter	**Table 5**	All	A	B	C	D	E	F	G	H
S_y	**0.254**	0.208	0.171	0.169	0.230	0.193	0.211	0.124	0.148	0.197
b ft	**171**	170 *	170 *	170 *	170 *	170 *	170 *	170 *	170 *	170 *
K_r ft/min	**0.229**	0.237	0.247	0.286	0.228	0.335	0.252	0.250	0.258	0.238
K_z ft/min	**0.137**	0.125	0.121	0.0584	0.132	0.274	0.0923	0.131	0.0963	0.142

* -fixed value

Table 16a Analysis of time-limited tests for all piezometers and deep-seated piezometers. , where S_s = specific storage, S_y = specific yield, b = saturated thickness, K_r = hydraulic conductivity in the horizontal direction, K_z = hydraulic conductivity in the vertical direction, and α_1, α_2, and α_3 are empirical constants for gradual drainage from the unsaturated zone.

Parameter	All Piezometers				Deep Piezometers F505-080 F504-080 F383-082 F383-129			
	72-hour #	24-hour	16-hour	8-hour	72-hour *	24-hour	16-hour	8-hour
S_s ft^{-1}	1.3E-05	1.3E-05	1.3E-05	1.3E-05	1.4E-05	1.3E-05	1.4E-05	1.4E-05
S_y	0.263	0.255	0.258	0.239	0.249	0.261	0.266	0.270
b ft	174	179	177	186	176	169	166	163
K_r ft/min	0.233	0.236	0.237	0.240	0.243	0.242	0.242	0.245
K_z ft/min	0.141	0.140	0.140	0.139	0.135	0.134	0.132	0.130
α_1 min^{-1}	1.7E-04	6.6E-05	3.1E-05	9.2E-05	2.8E-05	6.1E-05	5.2E-05	6.5E-05
α_2 min^{-1}	1.7E-02	1.8E-02	1.7E-02	2.0E-02	2.8E-02	2.8E-02	2.8E-02	2.4E-02
α_3 min^{-1}	0.42	0.45	0.42	0.43	1.4	4.4	3.7	8.8

Values slightly different from those in Tables 7 & 9 because of different initial values (consistent with others used in generating this table).

* Values taken from Table 12 column A.

Table 16b Analysis of time-limited tests for long-screened piezometers and piezometer clusters, where S_s = specific storage, S_y = specific yield, b = saturated thickness, K_r = hydraulic conductivity in the horizontal direction, K_z = hydraulic conductivity in the vertical direction, and α_1, α_2, and α_3 are empirical constants for gradual drainage from the unsaturated zone.

Parameter	Long-Screened Piezometers F434-060 F450-061 F476-061 F478-061				Piezometer Clusters F505 F504 F383			
	72-hour *	24-hour	16-hour	8-hour	72-hour	24-hour	16-hour	8-hour
S_s ft^{-1}	no data	no data	no data	no data	1.3E-05	1.3E-05	1.3E-05	1.3E-05
S_y	0.278	0.278	0.294	0.294	0.235	0.241	0.234	0.215
b ft	178	167	146	132	183	178	181	199
K_r ft/min	0.226	0.233	0.235	0.248	0.235	0.239	0.240	0.244
K_z ft/min	0.144	0.149	0.152	0.150	0.139	0.139	0.137	0.136
α_1 min^{-1}	2.3E-04	8.0E-05	2.5E-04	2.4E-05	1.4E-05	2.1E-05	3.1E-05	1.3E-04
α_2 min^{-1}	2.4E-02	2.2E-02	1.8E-02	1.8E-02	2.2E-02	1.7E-02	1.9E-02	2.1E-02
α_3 min^{-1}	21.	6.1	5.2	22.	0.44	0.45	0.47	0.52

* Values taken from Table 12 column E.

Table 17. Various data analyses for piezometers F505-059, F505-080, F504-080, and F383-129, where S_s = specific storage, S_y = specific yield, b = saturated thickness, K_r = hydraulic conductivity in the horizontal direction, K_z = hydraulic conductivity in the vertical direction, and α_1, α_2, and α_3 are empirical constants for gradual drainage from the unsaturated zone.

Parameter	Delayed Drainage		Instantaneous Drainage	
	72-hour	8-hour	72-hour	8-hour
Ss ft^{-1}	1.2E-05	1.2E-05	1.3E-05	1.3E-05
Sy	0.298	0.297	0.163	0.160
b ft	170	174	180	178
Kr ft/min	0.233	0.236	0.243	0.246
Kz ft/min	0.136	0.134	0.124	0.121
α_1 min^{-1}	1.5E-04	1.9E-05	--	--
α_2 min^{-1}	2.8E-02	2.3E-02	--	--
α_3 min^{-1}	21	44	--	--

FIGURES

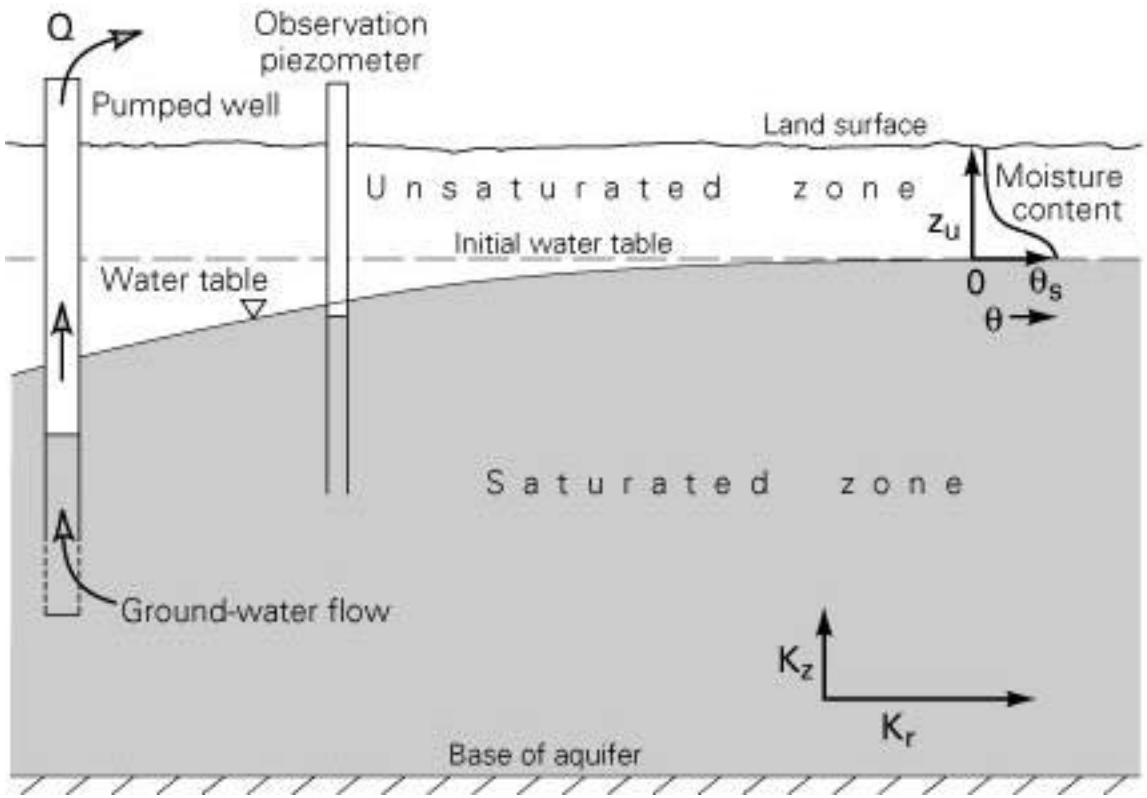

Explanation

- Q Pumping rate
- z_u Vertical distance above water table
- θ Moisture content of unsaturated zone
- θ_s Moisture content above the water table at saturation
- K_z Vertical hydraulic conductivity—Length of arrow indicates relative magnitude
- K_r Horizontal hydraulic conductivty—Length of arrow indicates relative magnitude

Fig. 1b

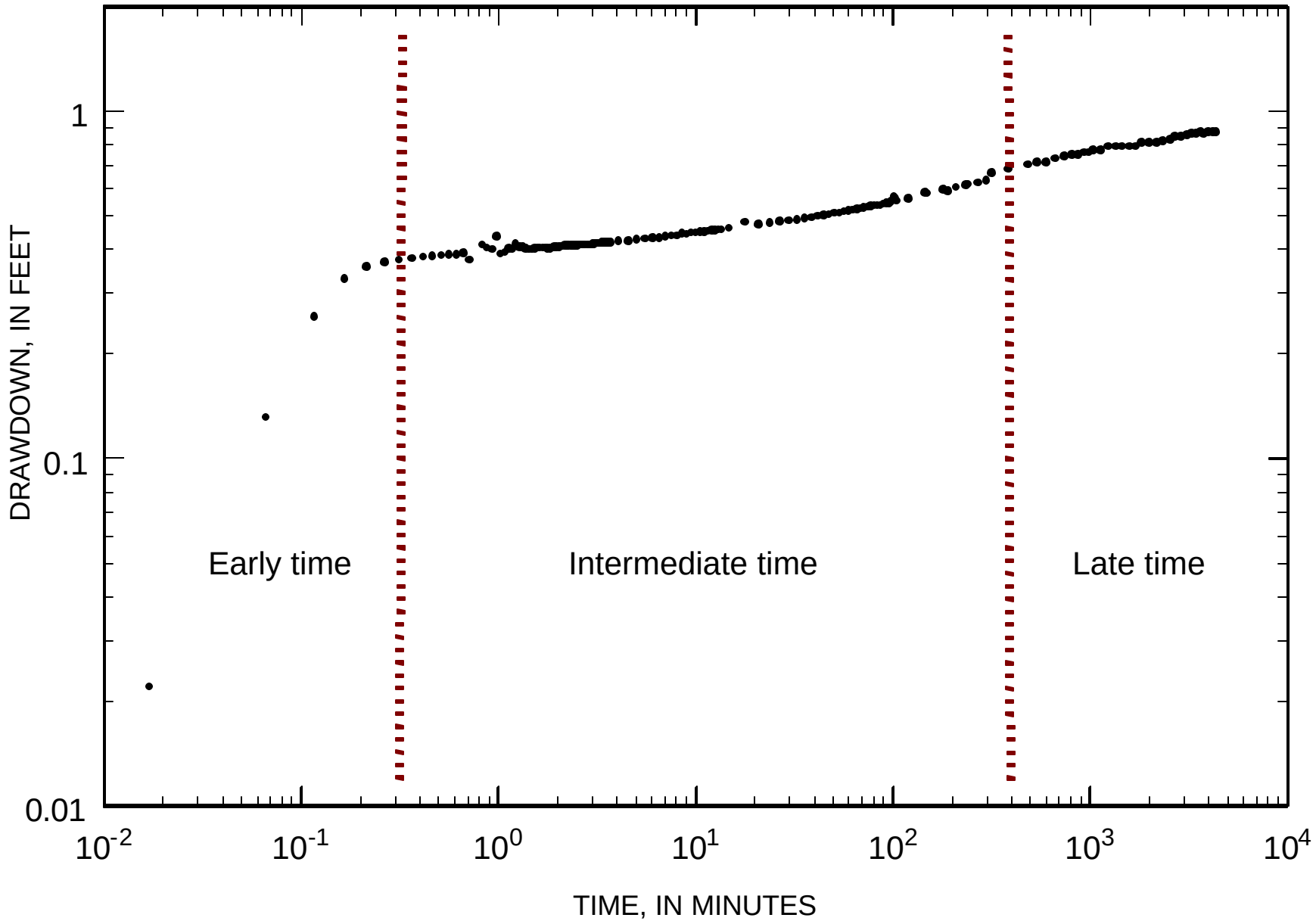
DRAWDOWN, IN FEET
1
0.1
0.01
Early time
Intermediate time
Late time
10^{-2}
10^{-1}
10^{0}
10^{1}
10^{2}
10^{3}
10^{4}
TIME, IN MINUTES

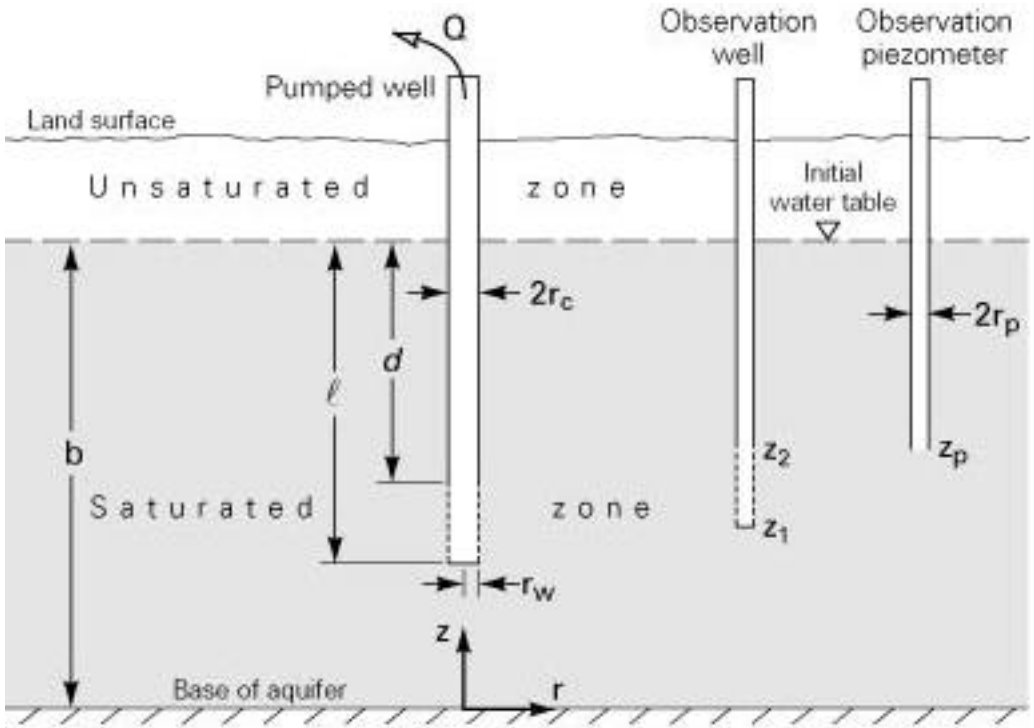

Explanation

Q	Pumping rate
$2r_c$	Effective diameter of pumped well in the interval where water levels are changing
$2r_p$	Diameter of observation piezometer in the interval where water levels are changing
r_w	Outside radius of the pumped well screen
d	Vertical distance from initial water table to top of pumped well screen
ℓ	Vertical distance from initial water table to bottom of pumped well screen
b	Initial saturated thickness of aquifer
z	Vertical distance above base of aquifer
z_1, z_2	Vertical distance above base of aquifer to the bottom and top, respectively, of the observation well screen
z_p	Vertical distance above base of aquifer to the center of the piezometer screen
r	Radial distance from axis of pumped well

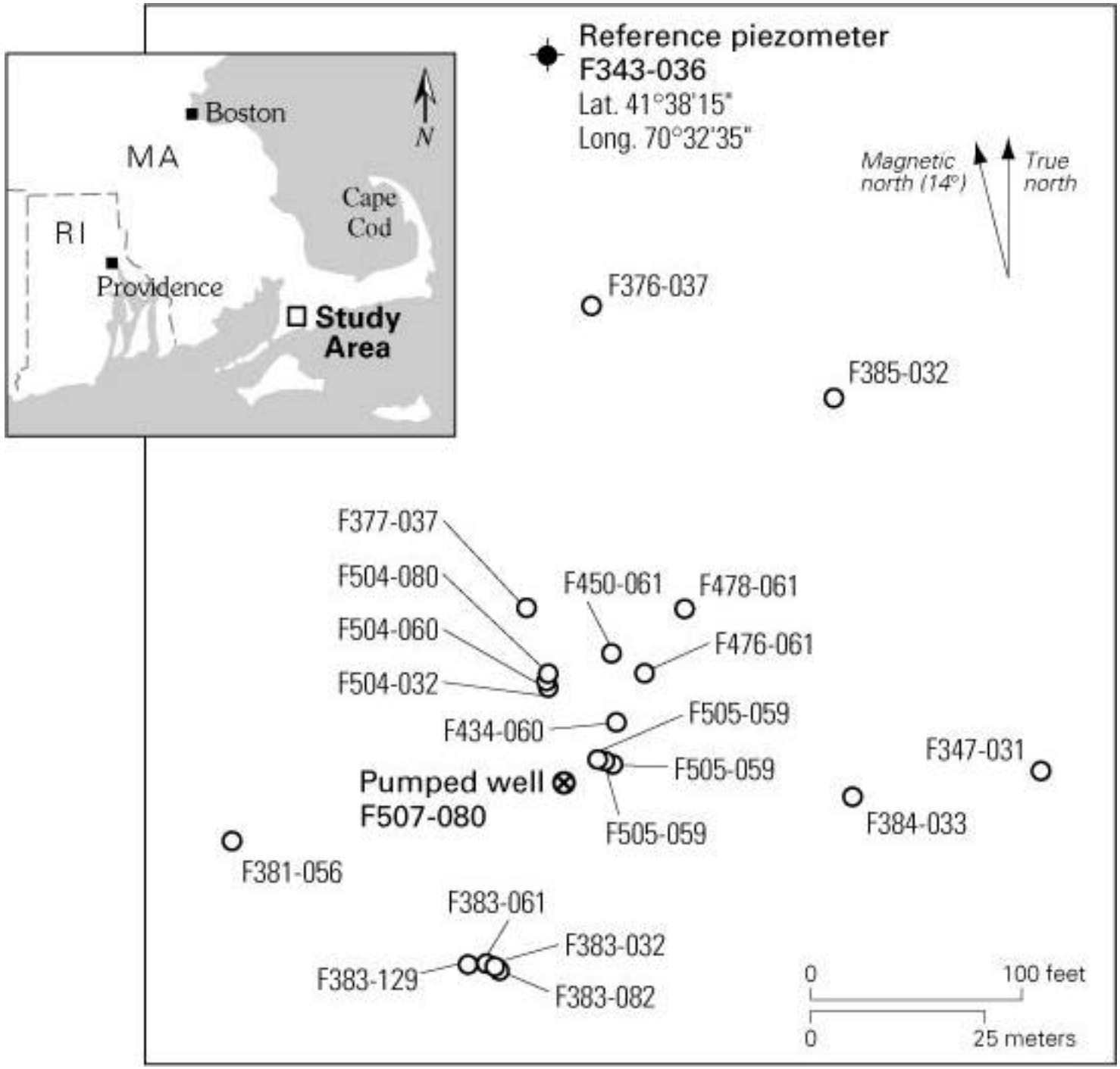
Reference piezometer
F343-036
Lat. 41°38'15"
Long. 70°32'35"
Magnetic north (14°)
True north
Boston
MA
RI
Providence
Cape Cod
N
Study Area
F376-037
F385-032
F377-037
F504-080
F504-060
F504-032
F450-061
F478-061
F476-061
F434-060
F505-059
F505-059
F505-059
Pumped well
F507-080
F347-031
F384-033
F381-056
F383-061
F383-032
F383-129
F383-082
0
100 feet
0
25 meters

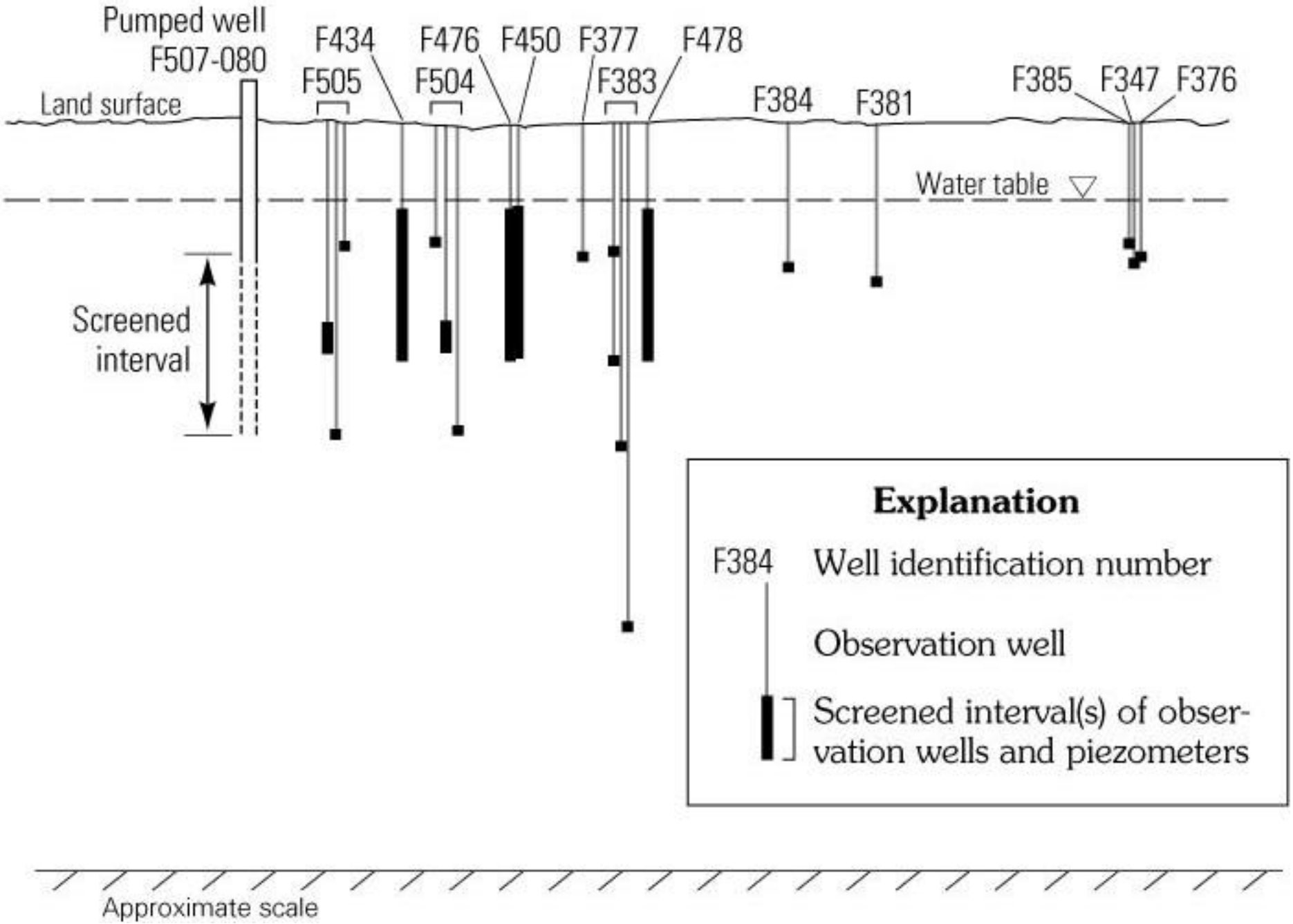
Pumped well
F507-080
F434
F505
F476
F504
F450
F377
F383
F478
F384
F381
F385
F347
F376
Land surface
Water table
Screened interval
Explanation
F384
Well identification number
Observation well
Screened interval(s) of observation wells and piezometers
Approximate scale

Fig. 5

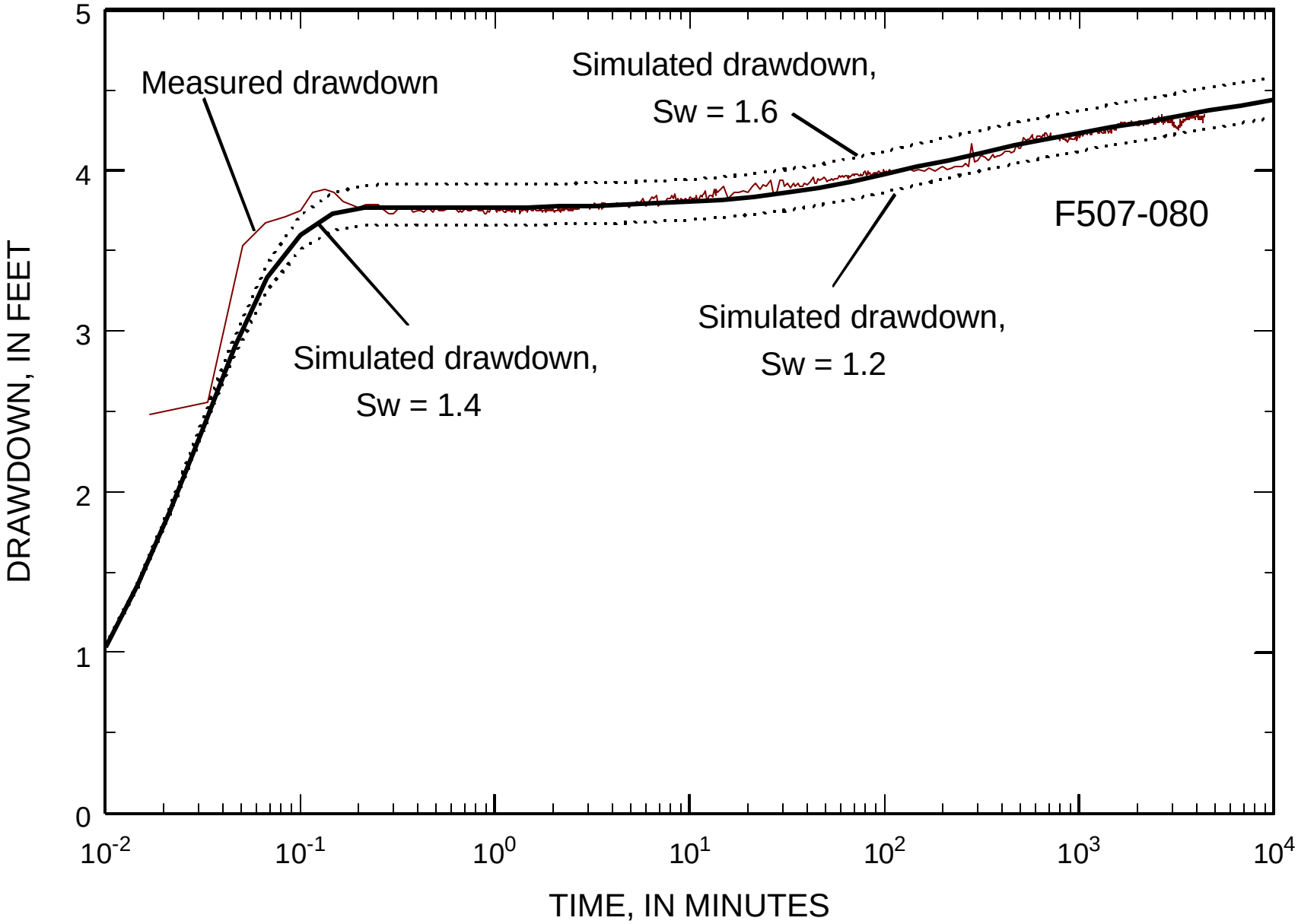
Measured drawdown
Simulated drawdown,
Sw = 1.6
F507-080
Simulated drawdown,
Sw = 1.4
Simulated drawdown,
Sw = 1.2
DRAWDOWN, IN FEET
TIME, IN MINUTES
0
1
2
3
4
5
10-2
10-1
100
101
102
103
104

Fig. 6

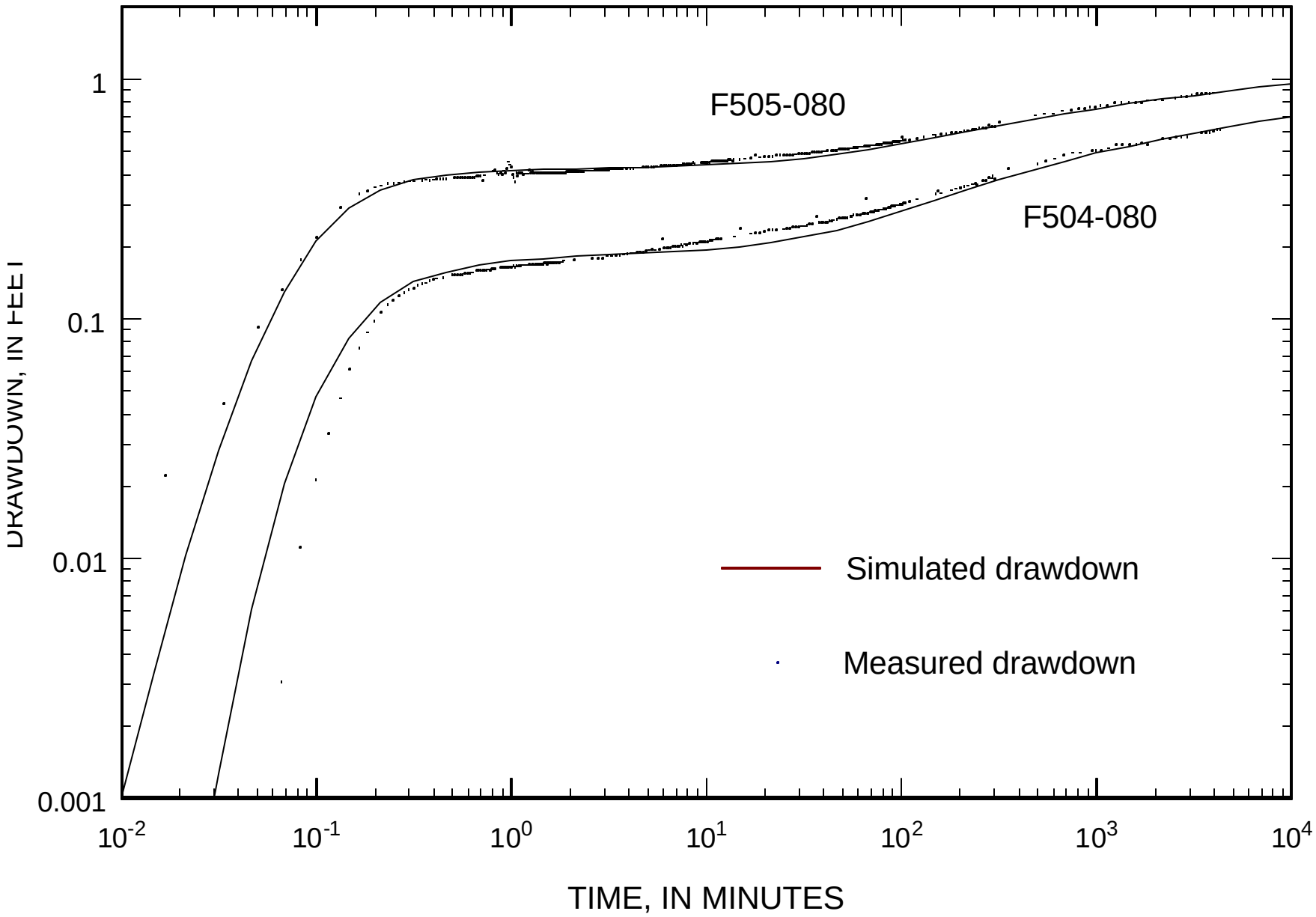
F505-080
F504-080
Simulated drawdown
Measured drawdown
DRAWDOWN, IN FEET
TIME, IN MINUTES
1
0.1
0.01
0.001
10^{-2}
10^{-1}
10^{0}
10^{1}
10^{2}
10^{3}
10^{4}

FIG. 7

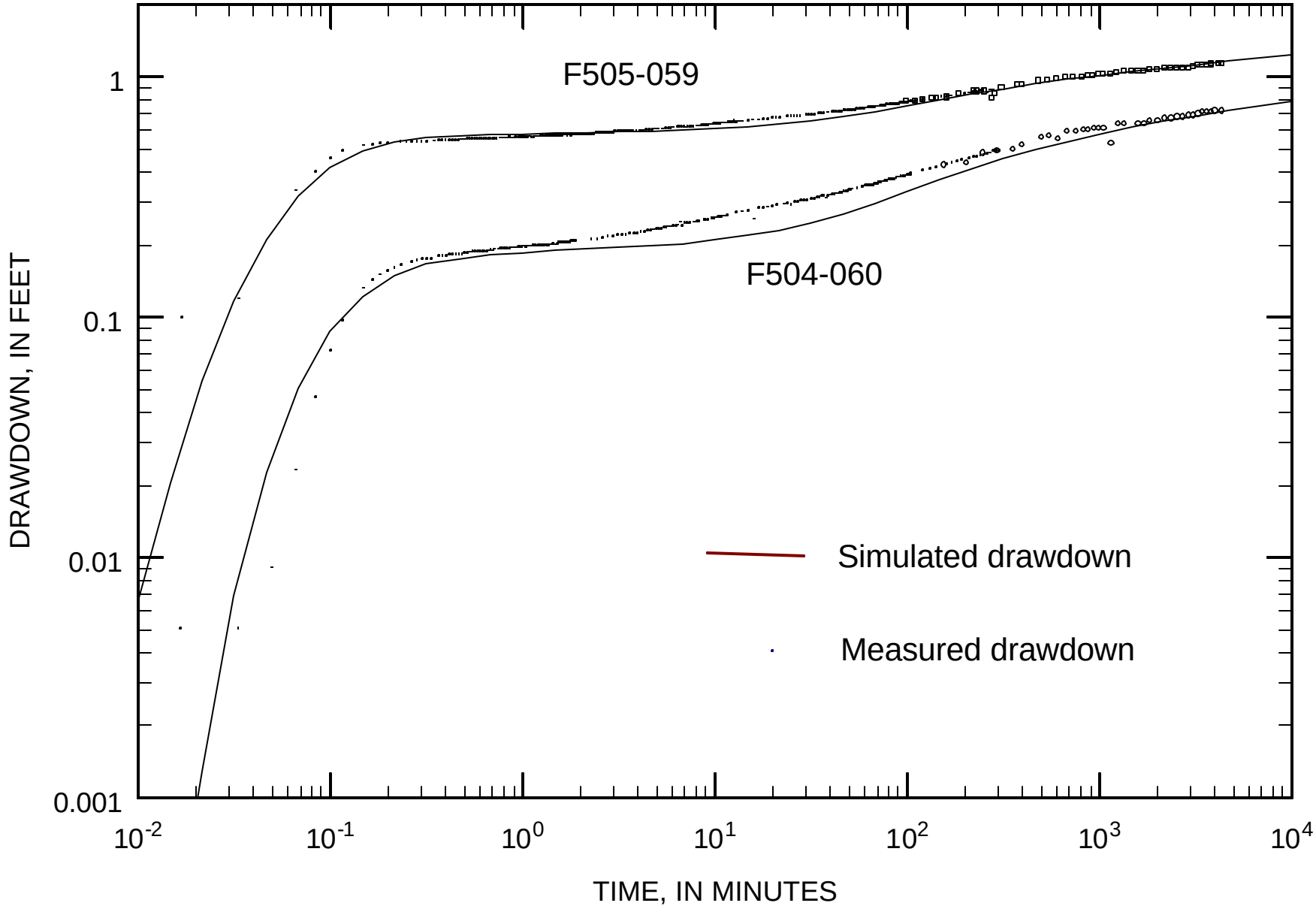
F505-059
F504-060
Simulated drawdown
Measured drawdown
DRAWDOWN, IN FEET
TIME, IN MINUTES
1
0.1
0.01
0.001
10-2
10-1
100
101
102
103
104

Fig. 8

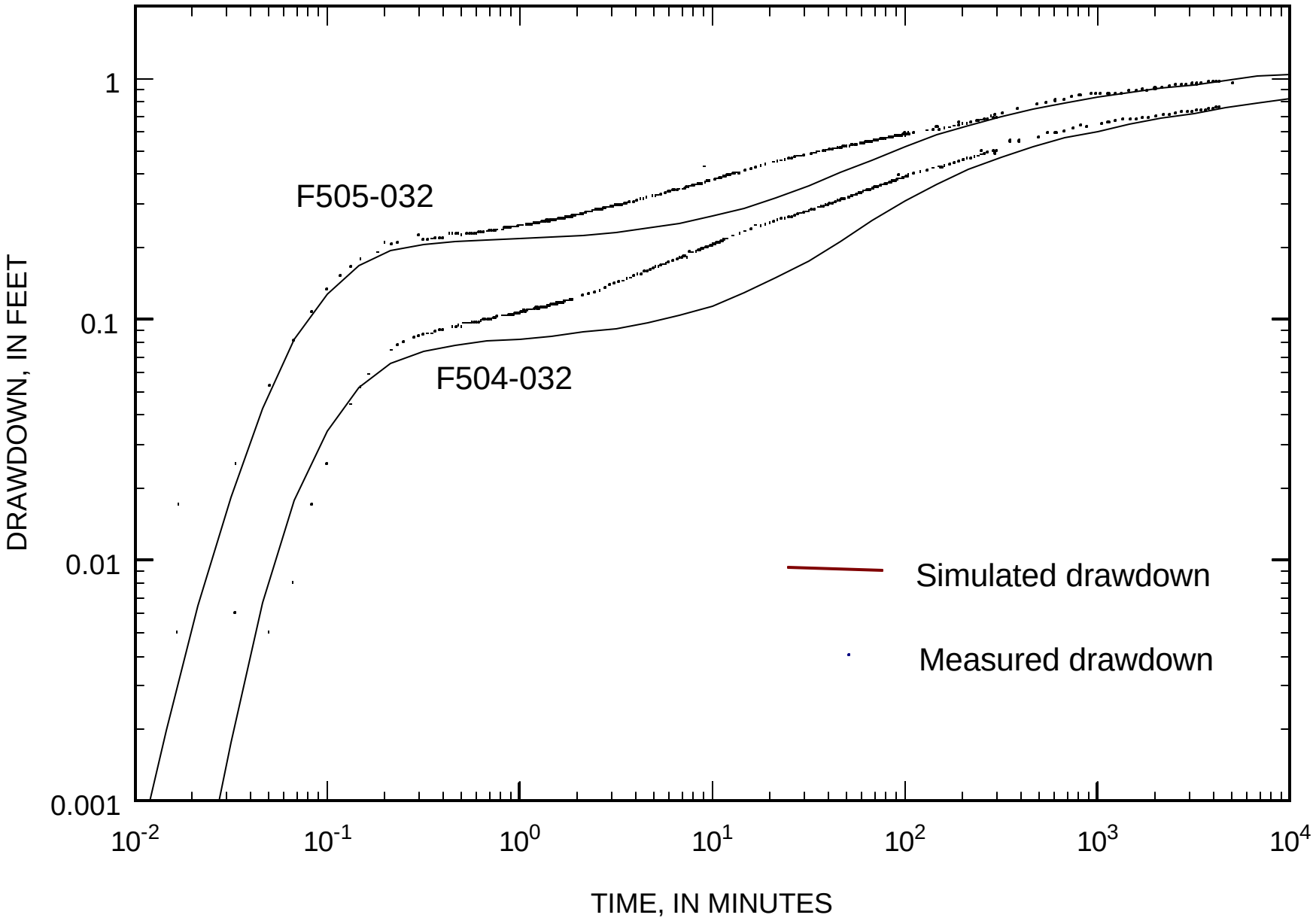
DRAWDOWN, IN FEET
1
0.1
0.01
0.001
F505-032
F504-032
Simulated drawdown
Measured drawdown
10^{-2}
10^{-1}
10^{0}
10^{1}
10^{2}
10^{3}
10^{4}
TIME, IN MINUTES

Fig. 9

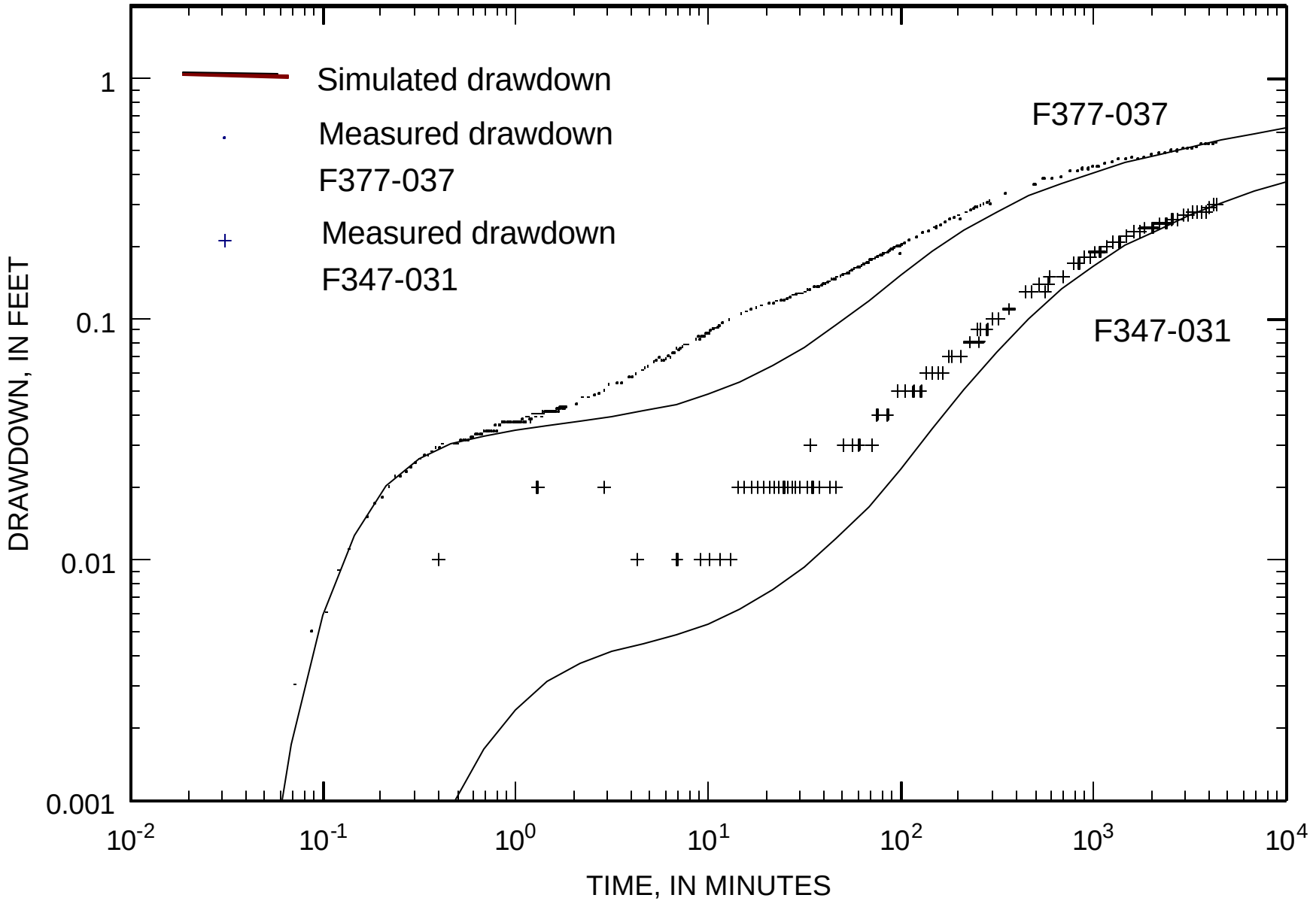
Simulated drawdown
Measured drawdown
F377-037
Measured drawdown
F347-031
F377-037
F347-031
DRAWDOWN, IN FEET
1
0.1
0.01
0.001
10^{-2}
10^{-1}
10^{0}
10^{1}
10^{2}
10^{3}
10^{4}
TIME, IN MINUTES

Fig. 10a

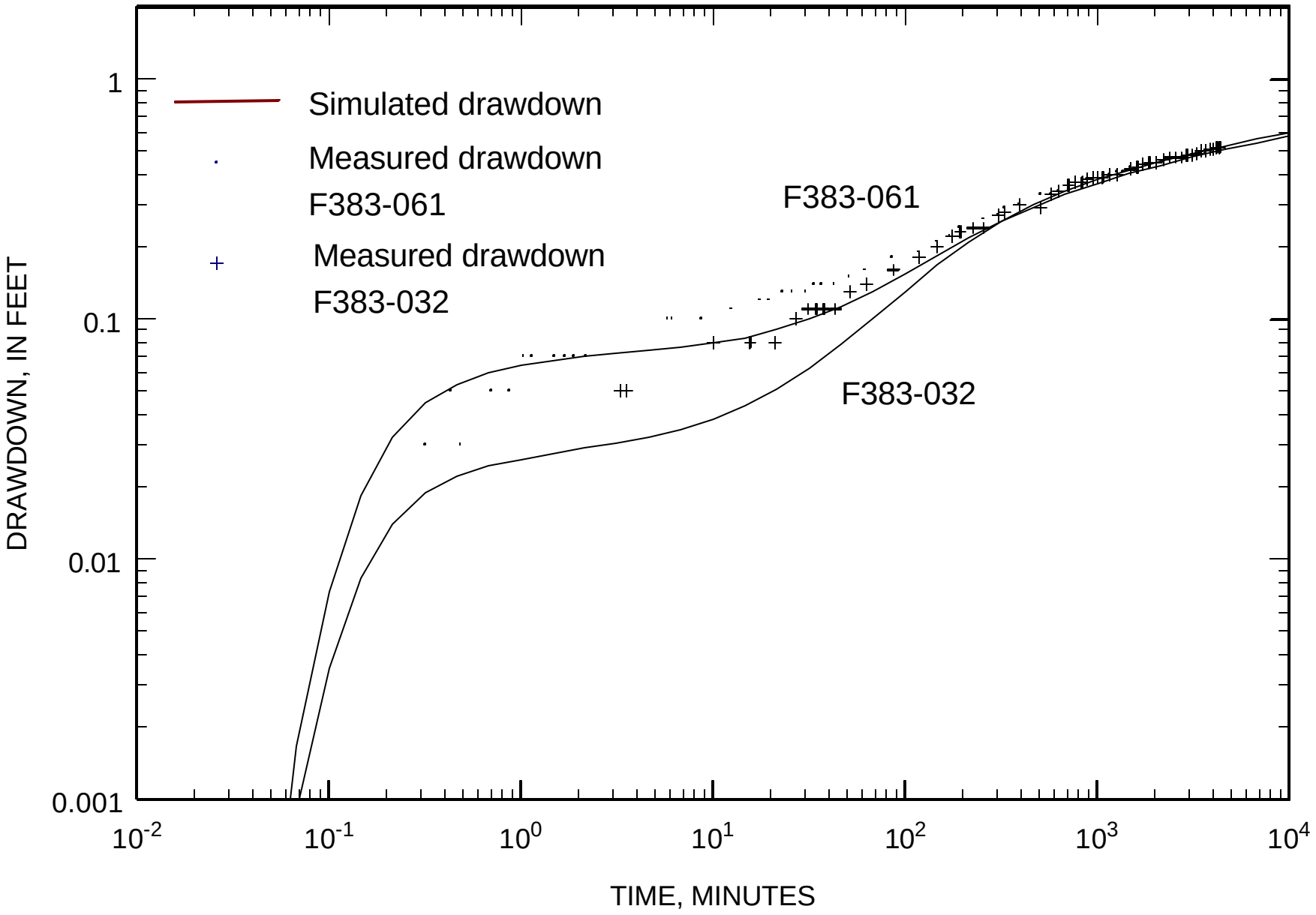
Simulated drawdown
Measured drawdown
F383-061
Measured drawdown
F383-032
F383-061
F383-032
DRAWDOWN, IN FEET
1
0.1
0.01
0.001
10^{-2}
10^{-1}
10^{0}
10^{1}
10^{2}
10^{3}
10^{4}
TIME, MINUTES

Fig. 10b

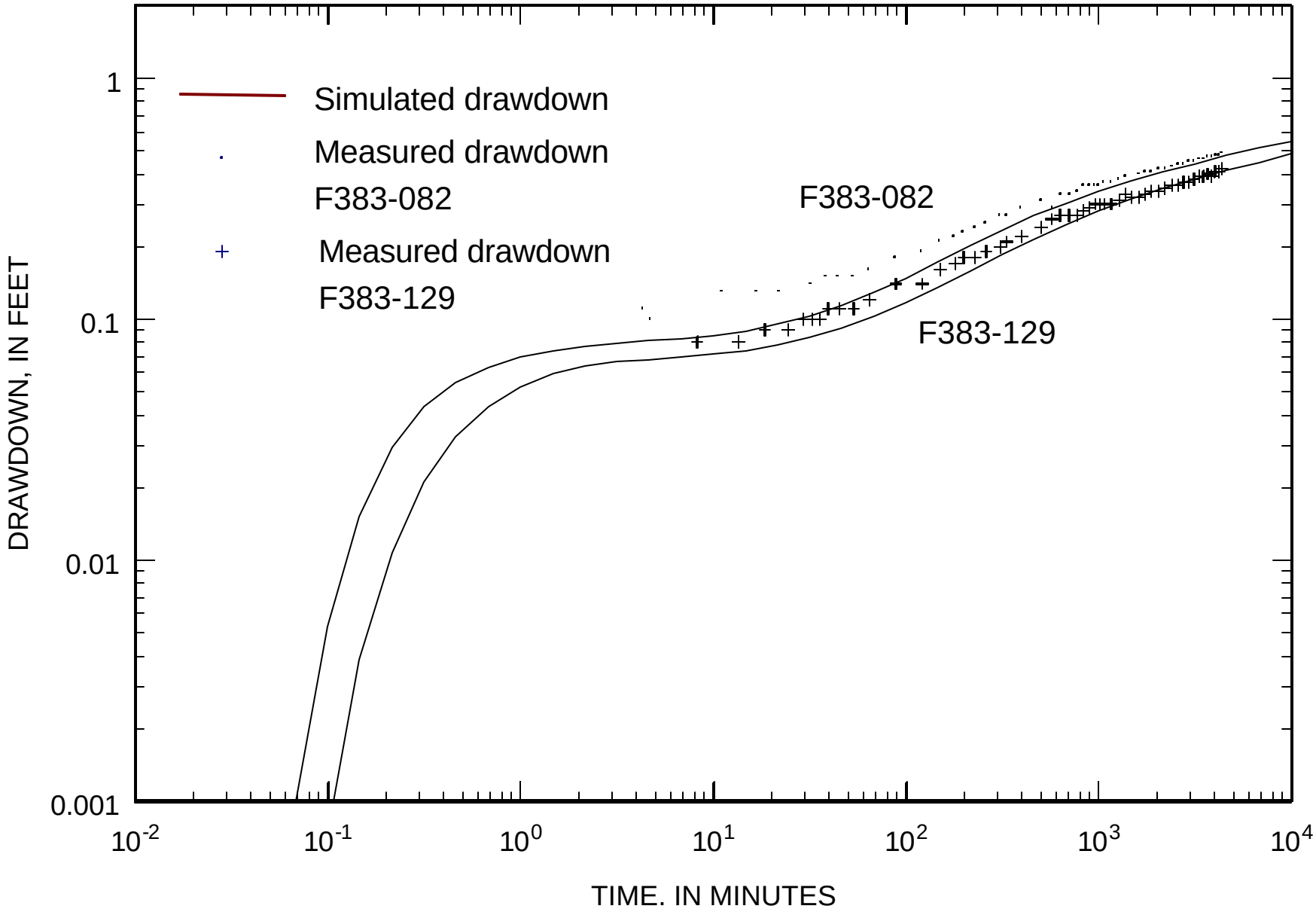
Simulated drawdown
Measured drawdown
F383-082
Measured drawdown
F383-129
F383-082
F383-129
DRAWDOWN, IN FEET
1
0.1
0.01
0.001
10^{-2}
10^{-1}
10^{0}
10^{1}
10^{2}
10^{3}
10^{4}
TIME. IN MINUTES

Fig. 11a

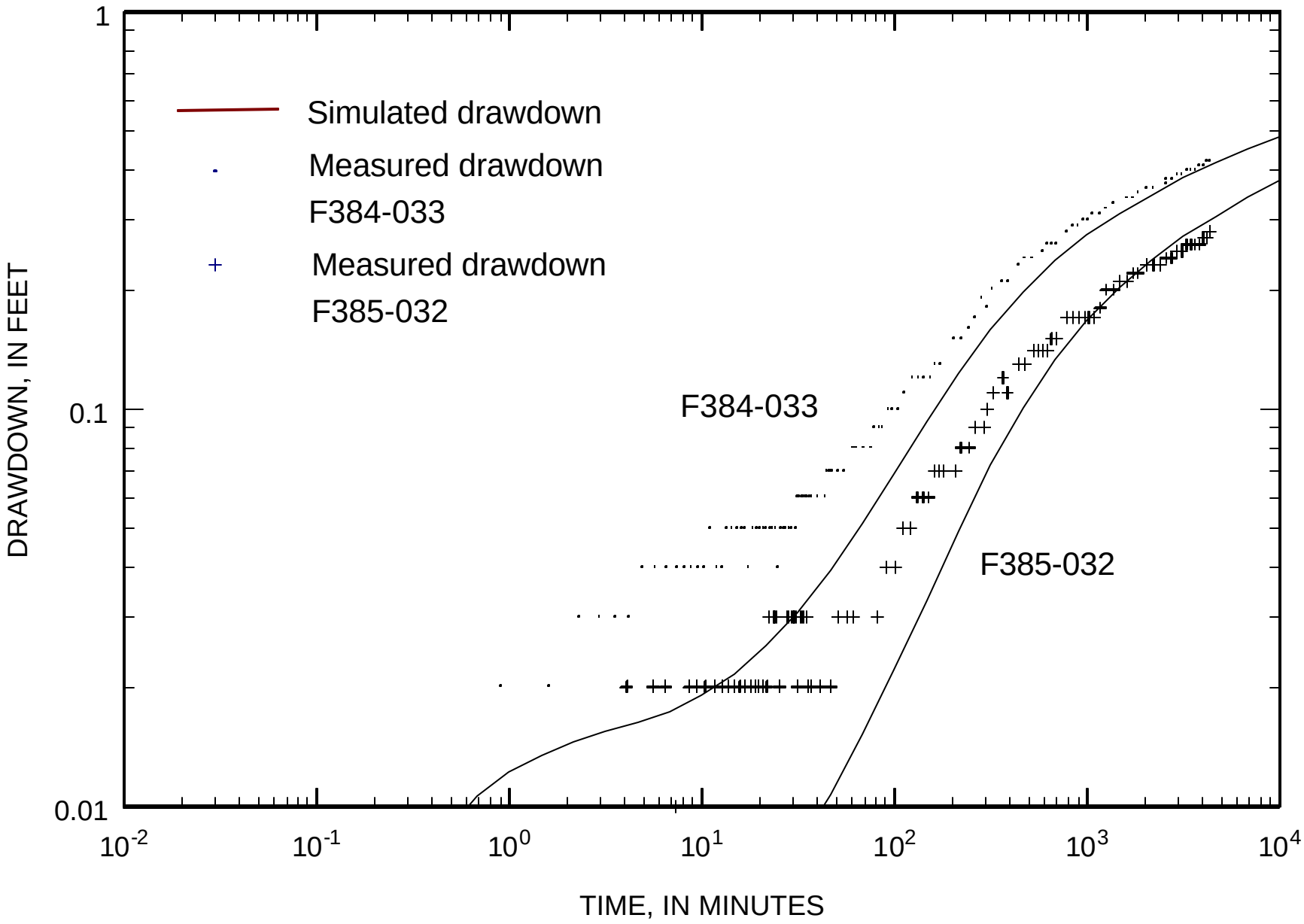
Simulated drawdown
Measured drawdown
F384-033
Measured drawdown
F385-032
F384-033
F385-032
DRAWDOWN, IN FEET
TIME, IN MINUTES
1
0.1
0.01
10-2
10-1
100
101
102
103
104

Fig. 11b

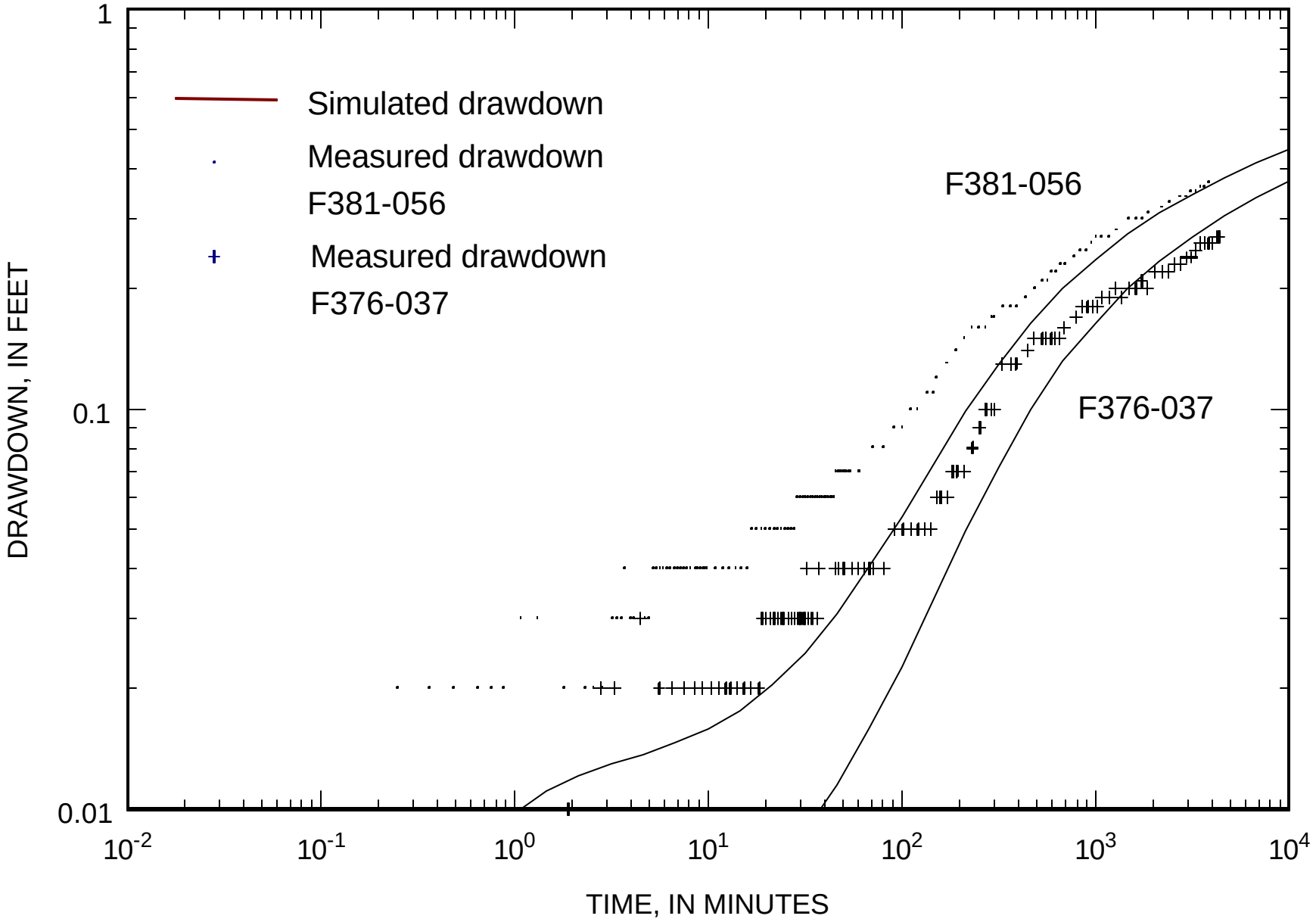
Simulated drawdown
Measured drawdown
F381-056
Measured drawdown
F376-037
F381-056
F376-037
DRAWDOWN, IN FEET
TIME, IN MINUTES
1
0.1
0.01
10-2
10-1
100
101
102
103
104

Fig. 12a

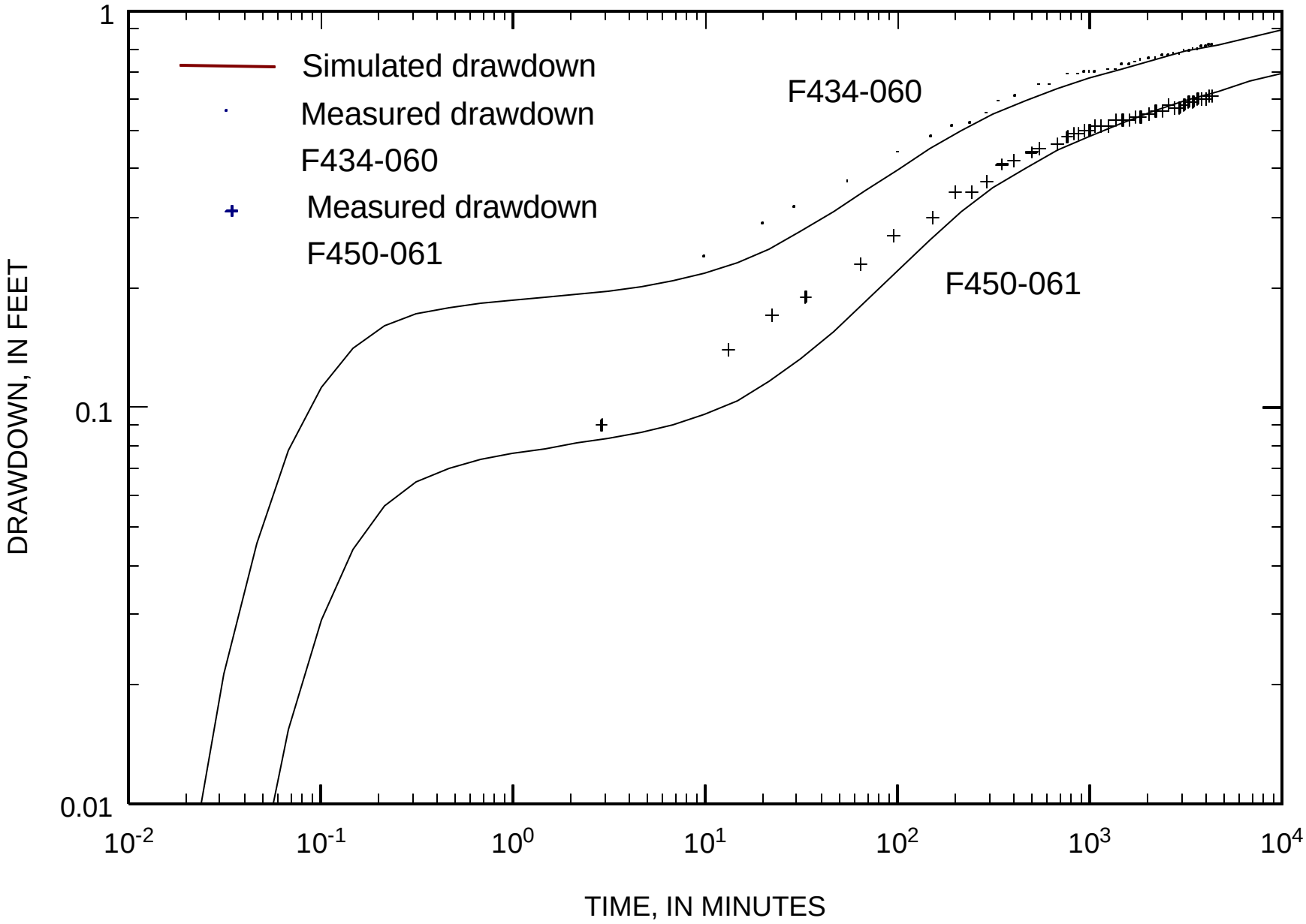
Simulated drawdown
Measured drawdown
F434-060
Measured drawdown
F450-061
F434-060
F450-061
DRAWDOWN, IN FEET
1
0.1
0.01
10^{-2}
10^{-1}
10^{0}
10^{1}
10^{2}
10^{3}
10^{4}
TIME, IN MINUTES

Fig. 12b

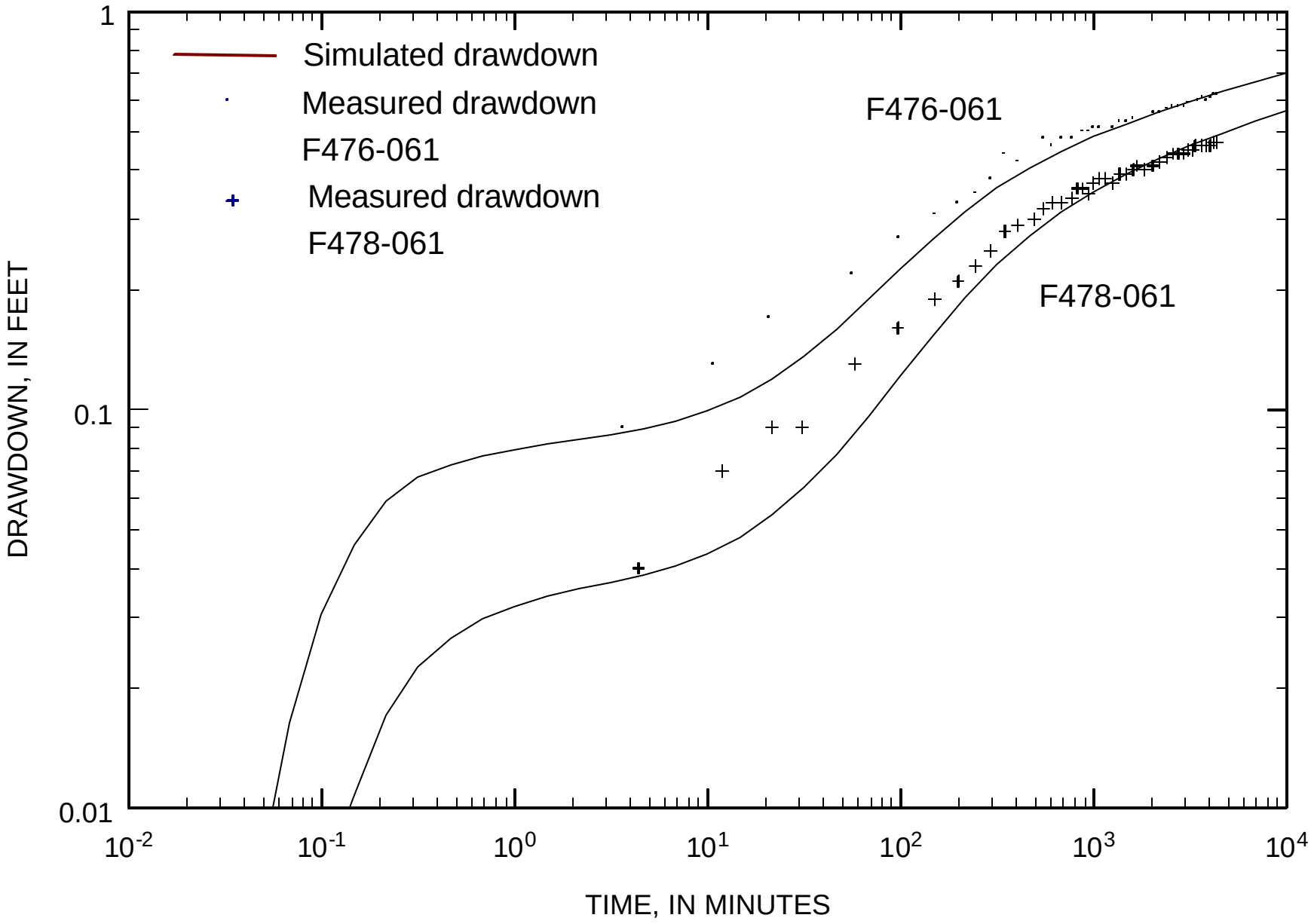
Simulated drawdown
Measured drawdown
F476-061
Measured drawdown
F478-061
F476-061
F478-061
DRAWDOWN, IN FEET
1
0.1
0.01
10^{-2}
10^{-1}
10^{0}
10^{1}
10^{2}
10^{3}
10^{4}
TIME, IN MINUTES

Fig. 13

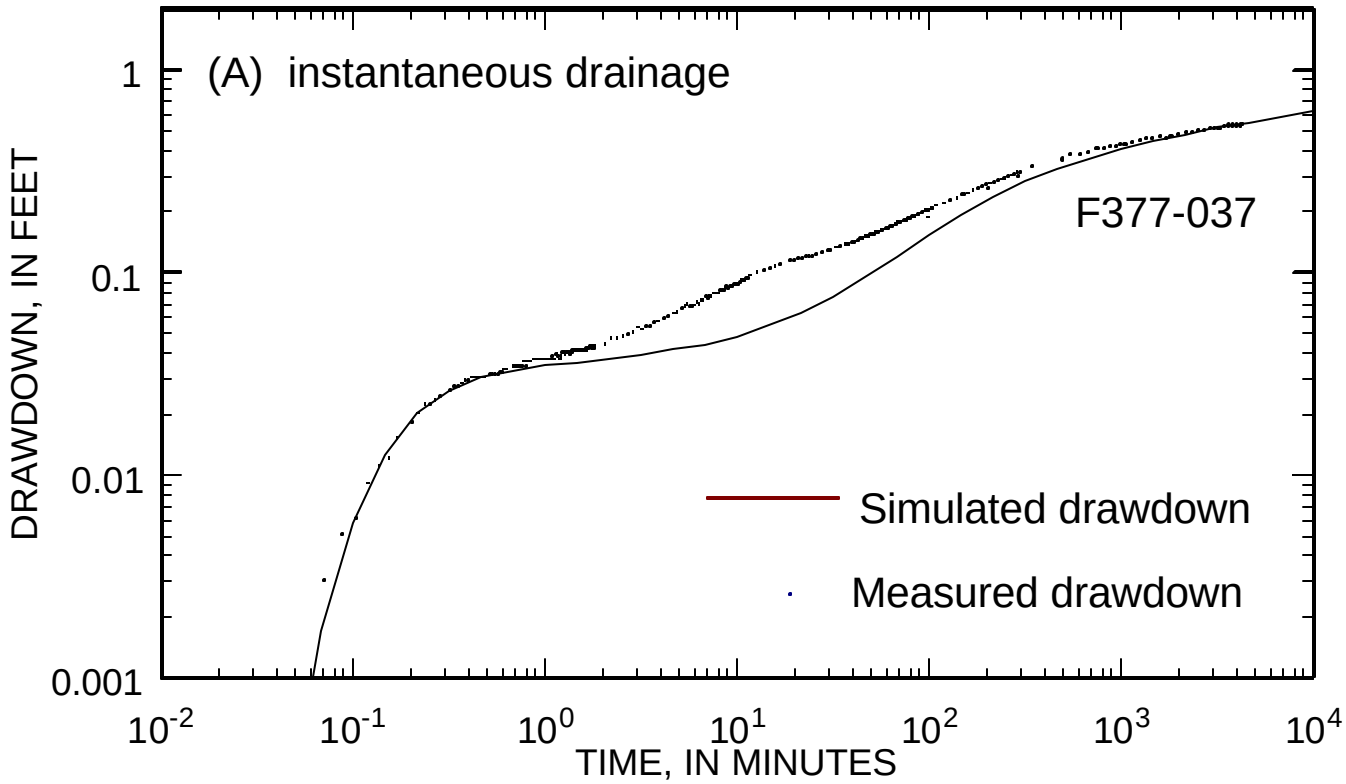
(A) instantaneous drainage
F377-037
Simulated drawdown
Measured drawdown
DRAWDOWN, IN FEET
TIME, IN MINUTES
1
0.1
0.01
0.001
10-2
10-1
100
101
102
103
104

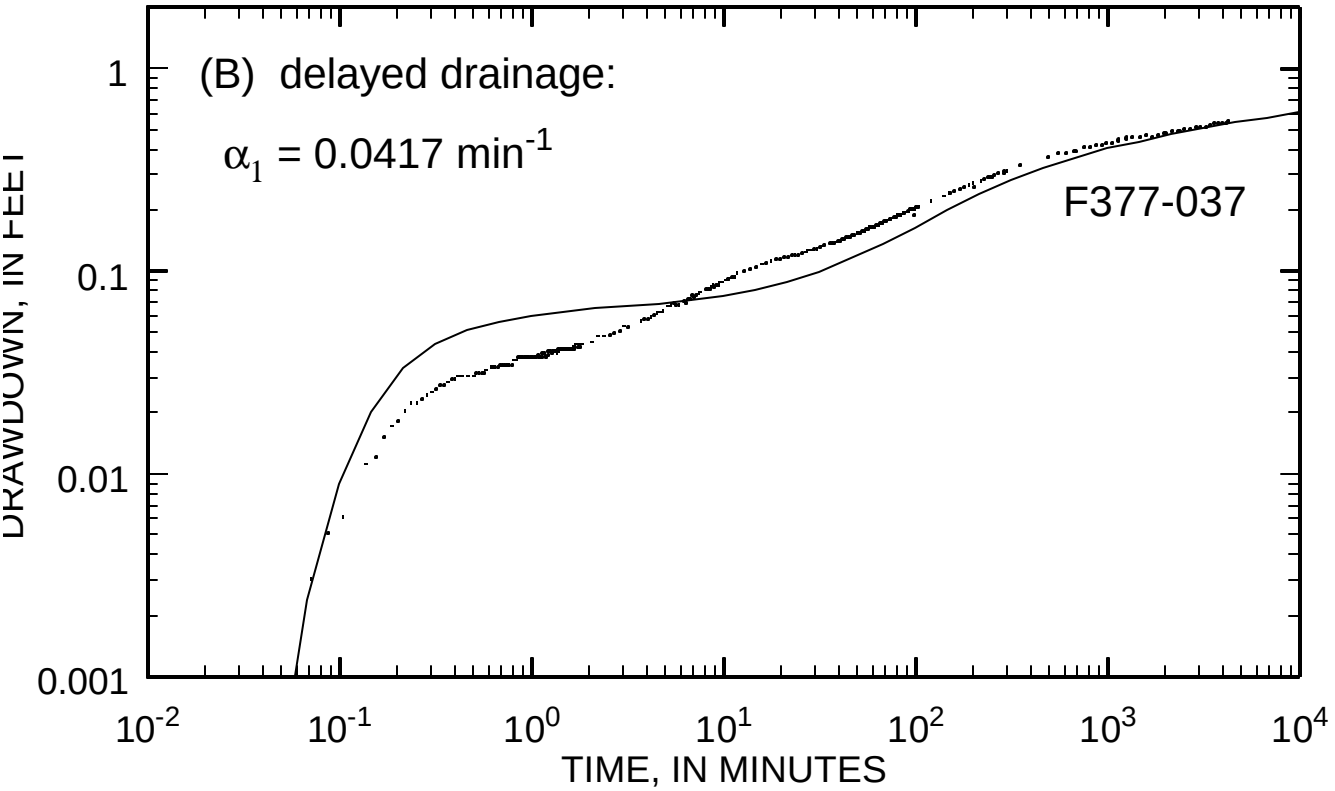
(B) delayed drainage:
α1 = 0.0417 min-1
F377-037
TIME, IN MINUTES
1
0.1
0.01
0.001
10-2
10-1
100
101
102
103
104

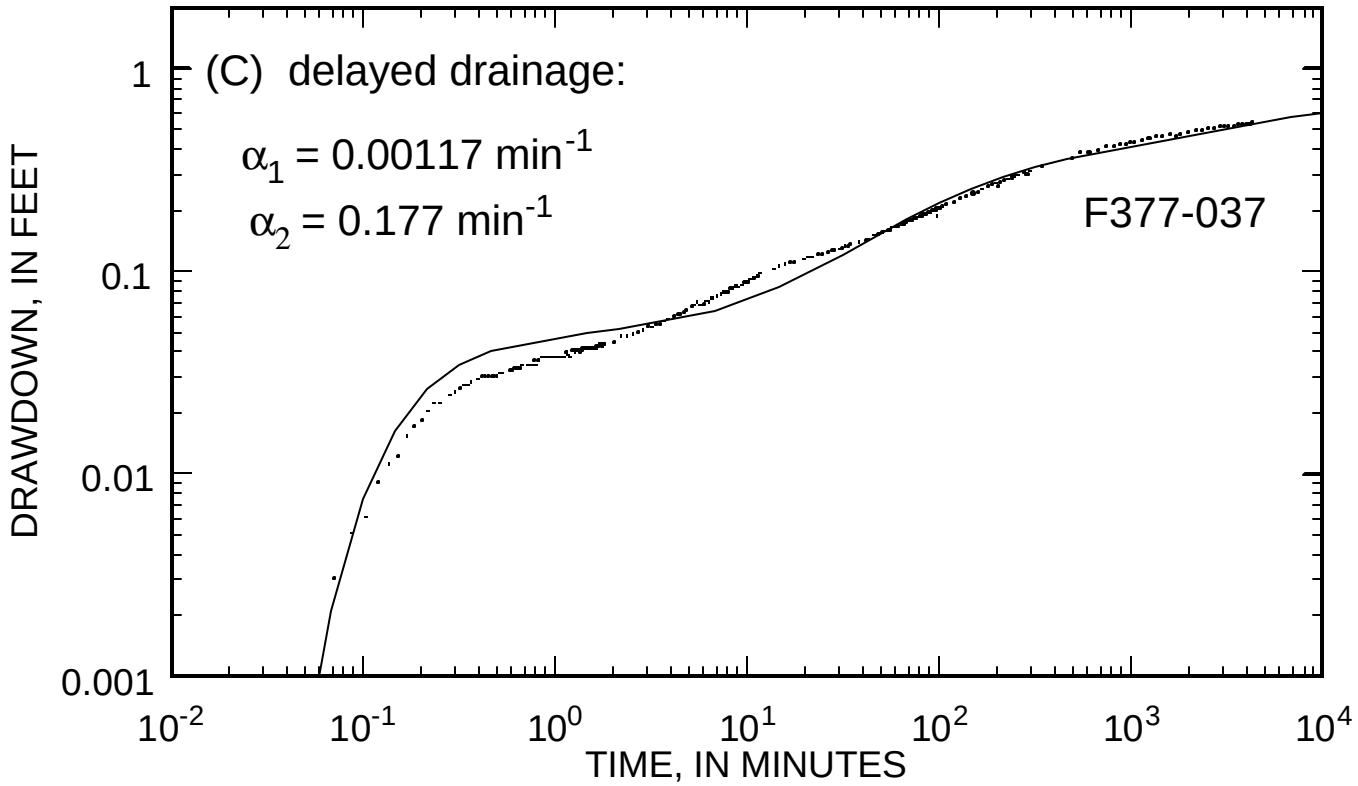
(C) delayed drainage:
α_1 = 0.00117 min^{-1}
α_2 = 0.177 min^{-1}
F377-037
DRAWDOWN, IN FEET
1
0.1
0.01
0.001
10^{-2}
10^{-1}
10^{0}
10^{1}
10^{2}
10^{3}
10^{4}
TIME, IN MINUTES

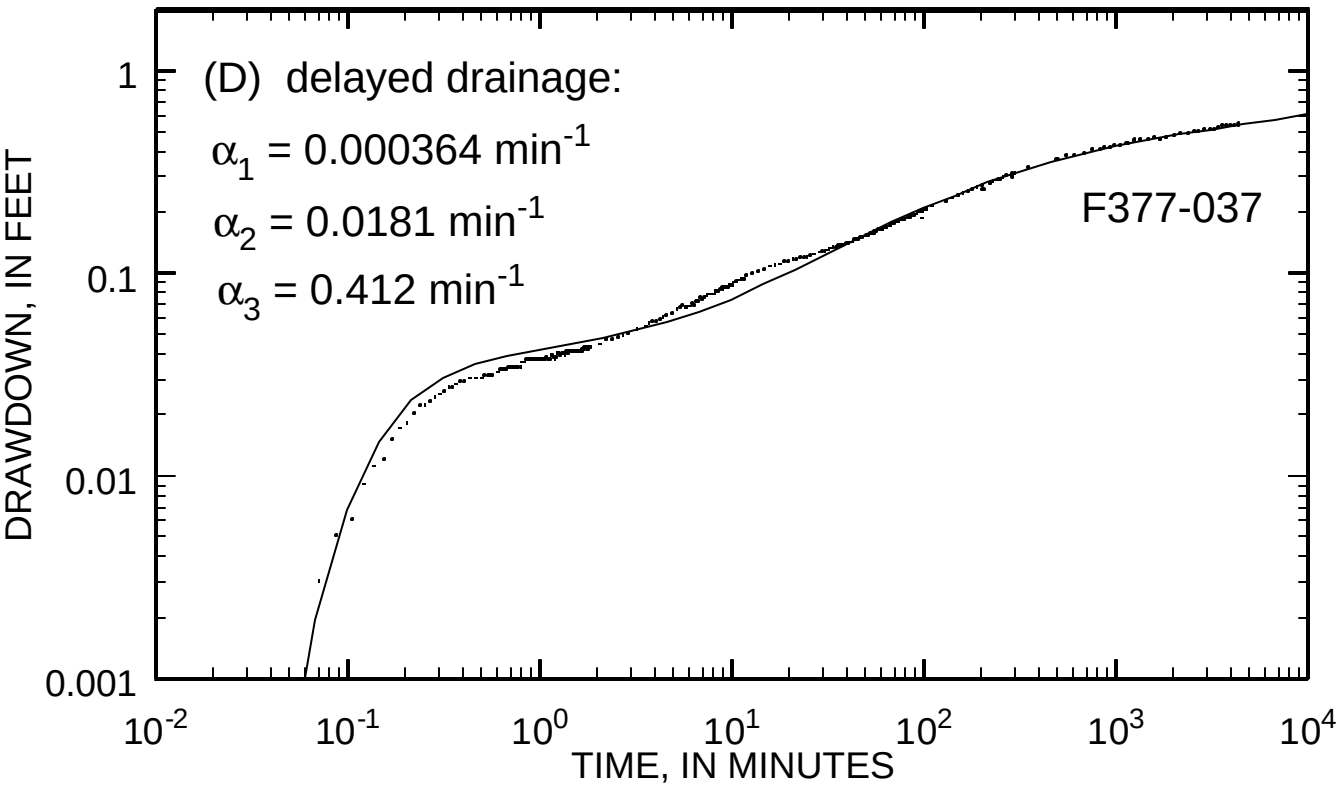
(D) delayed drainage:
α_1 = 0.000364 min^{-1}
α_2 = 0.0181 min^{-1}
α_3 = 0.412 min^{-1}
F377-037
DRAWDOWN, IN FEET
1
0.1
0.01
0.001
10^{-2}
10^{-1}
10^{0}
10^{1}
10^{2}
10^{3}
10^{4}
TIME, IN MINUTES

Fig. 14

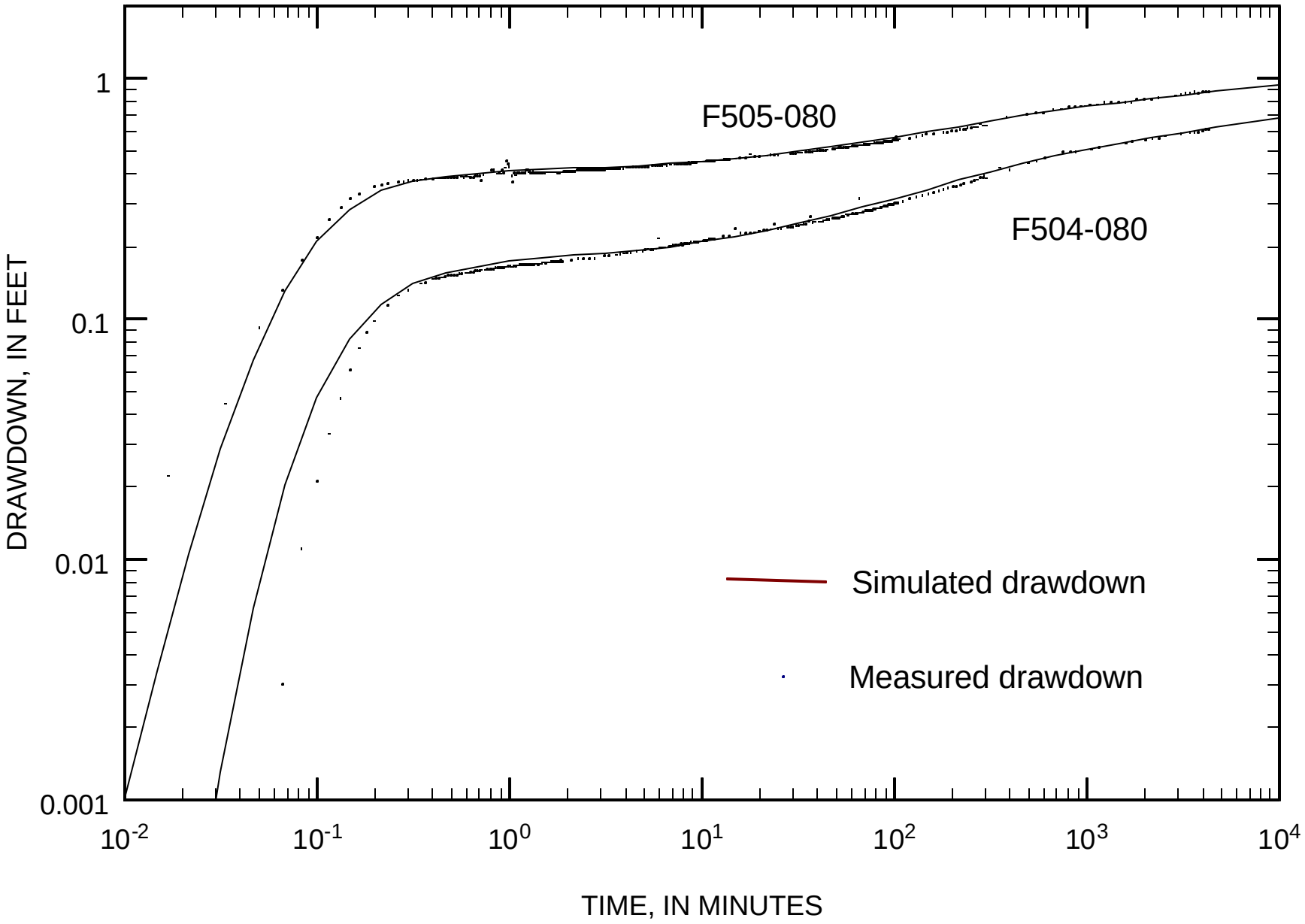
F505-080
F504-080
Simulated drawdown
Measured drawdown
DRAWDOWN, IN FEET
TIME, IN MINUTES
1
0.1
0.01
0.001
10-2
10-1
100
101
102
103
104

Fig. 15

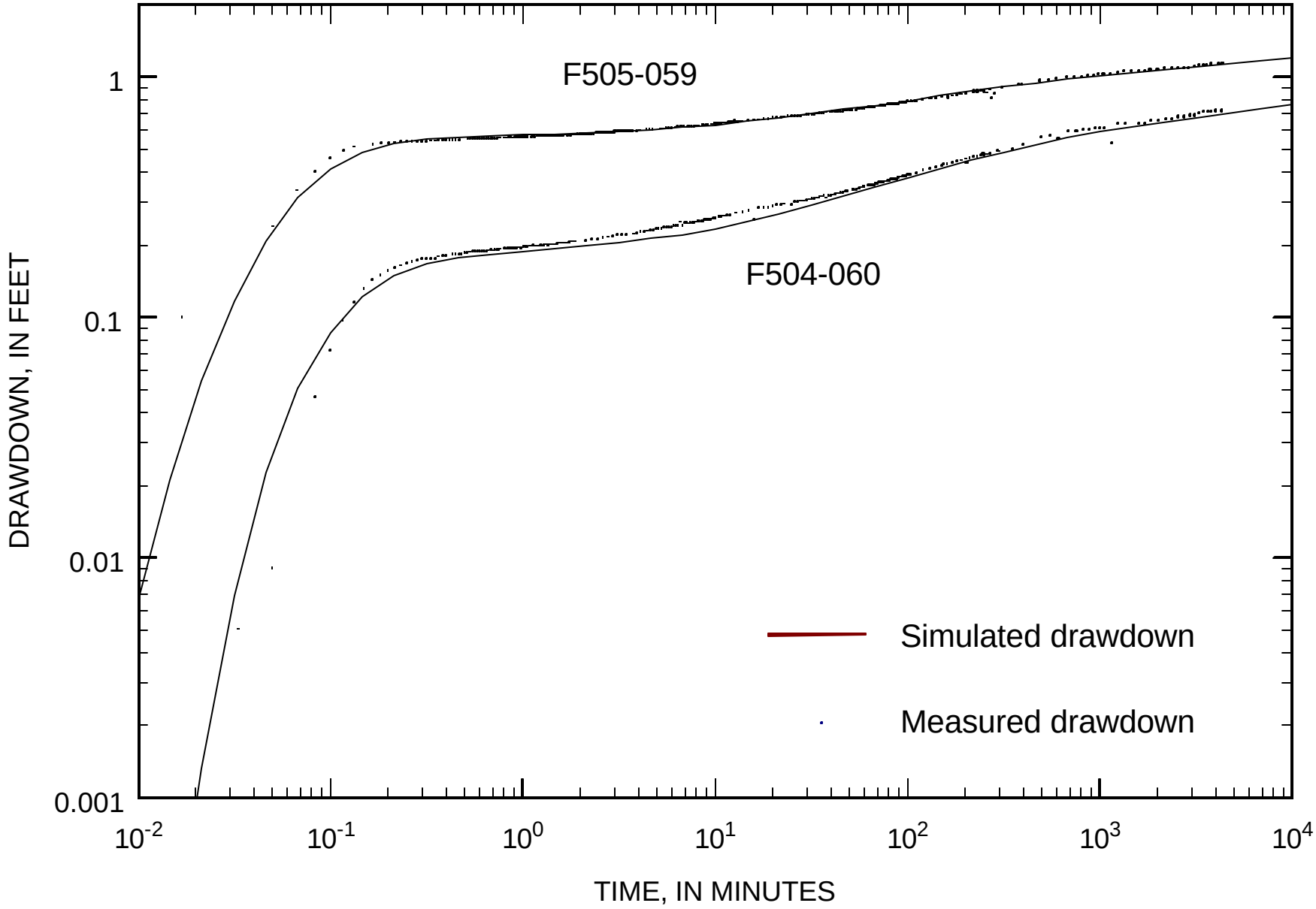
F505-059
F504-060
Simulated drawdown
Measured drawdown
DRAWDOWN, IN FEET
TIME, IN MINUTES
1
0.1
0.01
0.001
10-2
10-1
100
101
102
103
104

Fig. 16

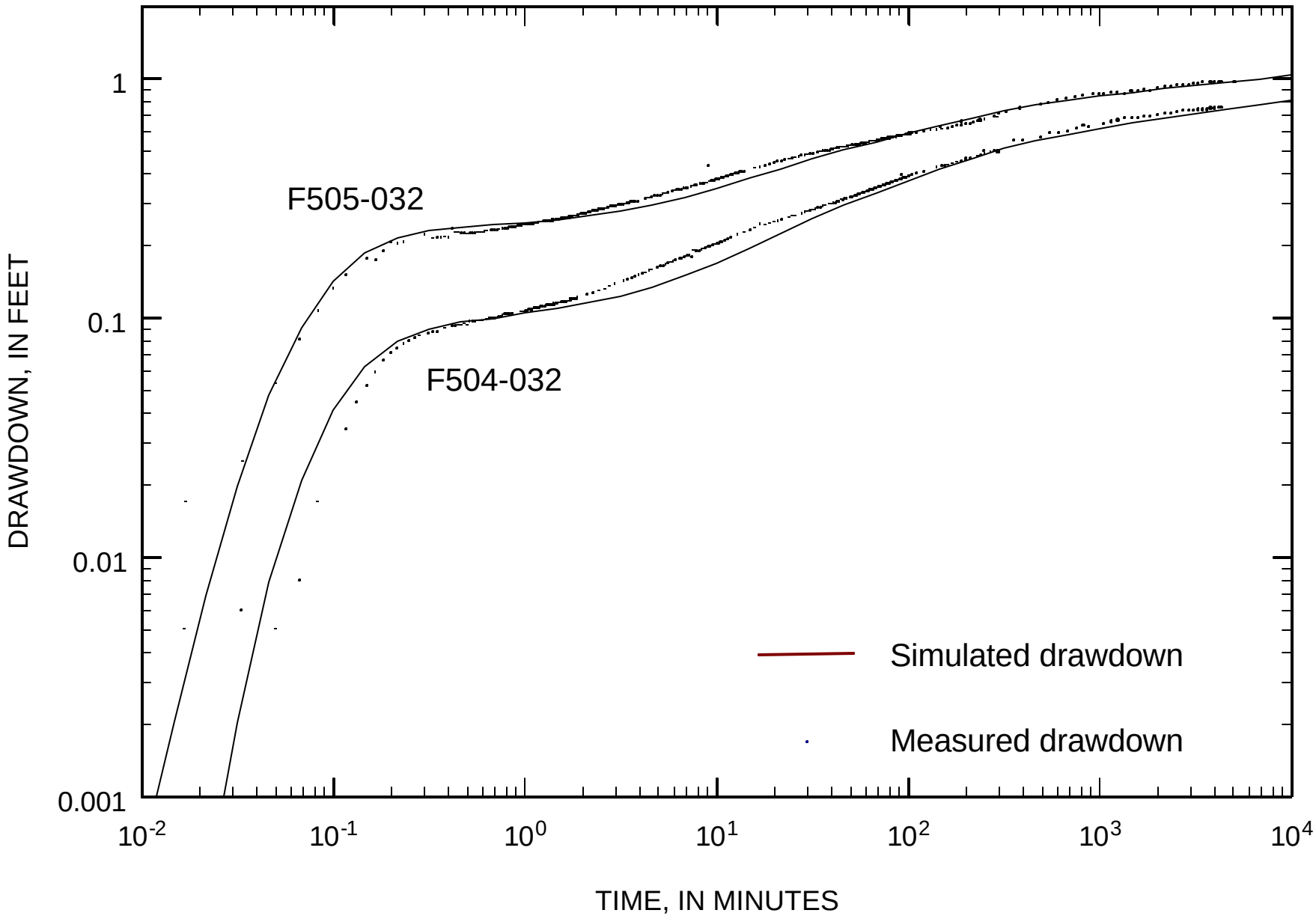
F505-032
F504-032
Simulated drawdown
Measured drawdown
DRAWDOWN, IN FEET
TIME, IN MINUTES
1
0.1
0.01
0.001
10-2
10-1
100
101
102
103
104

Fig. 17

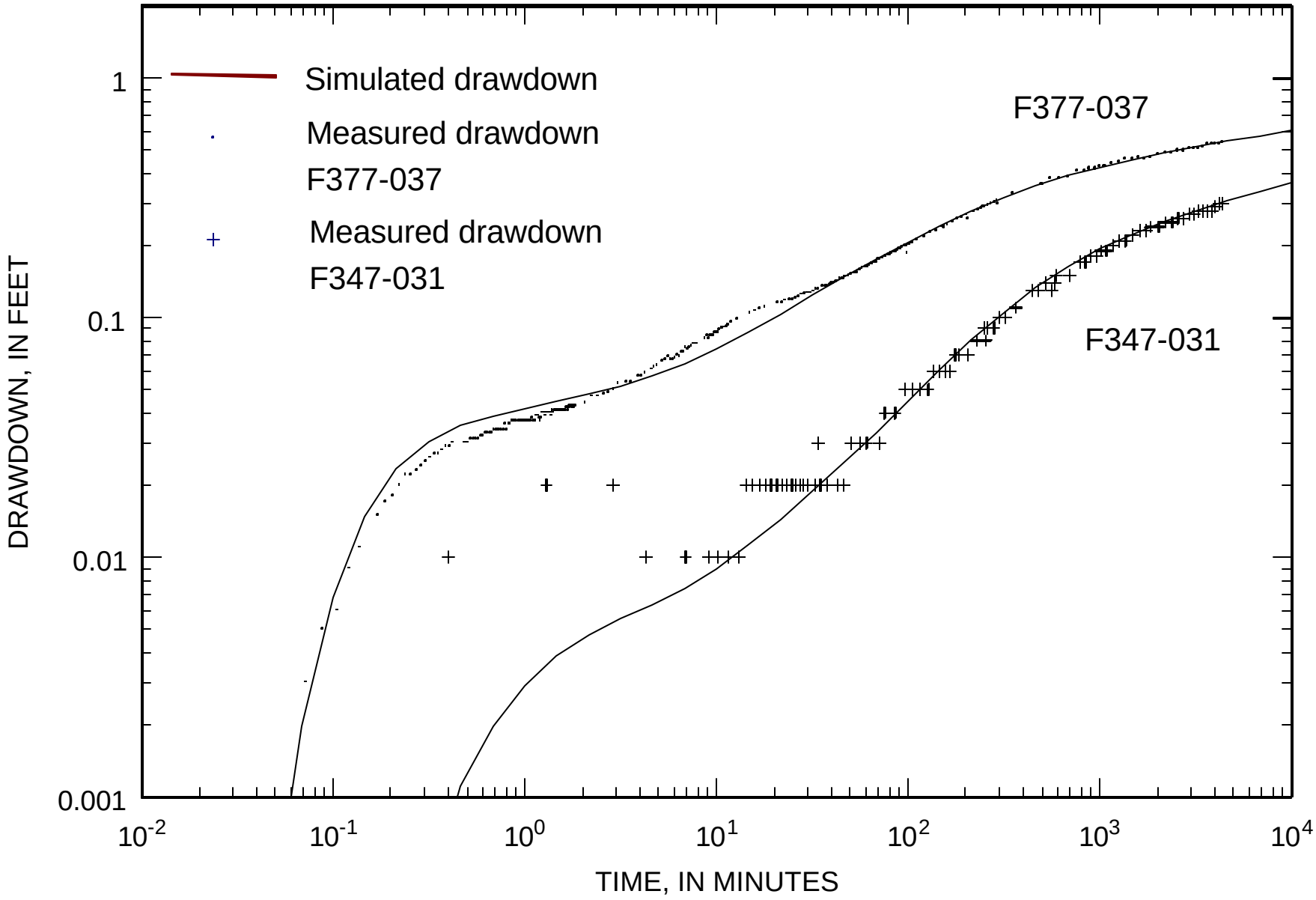
Simulated drawdown
Measured drawdown
F377-037
Measured drawdown
F347-031
F377-037
F347-031
DRAWDOWN, IN FEET
1
0.1
0.01
0.001
10^{-2}
10^{-1}
10^{0}
10^{1}
10^{2}
10^{3}
10^{4}
TIME, IN MINUTES

Fig.18a

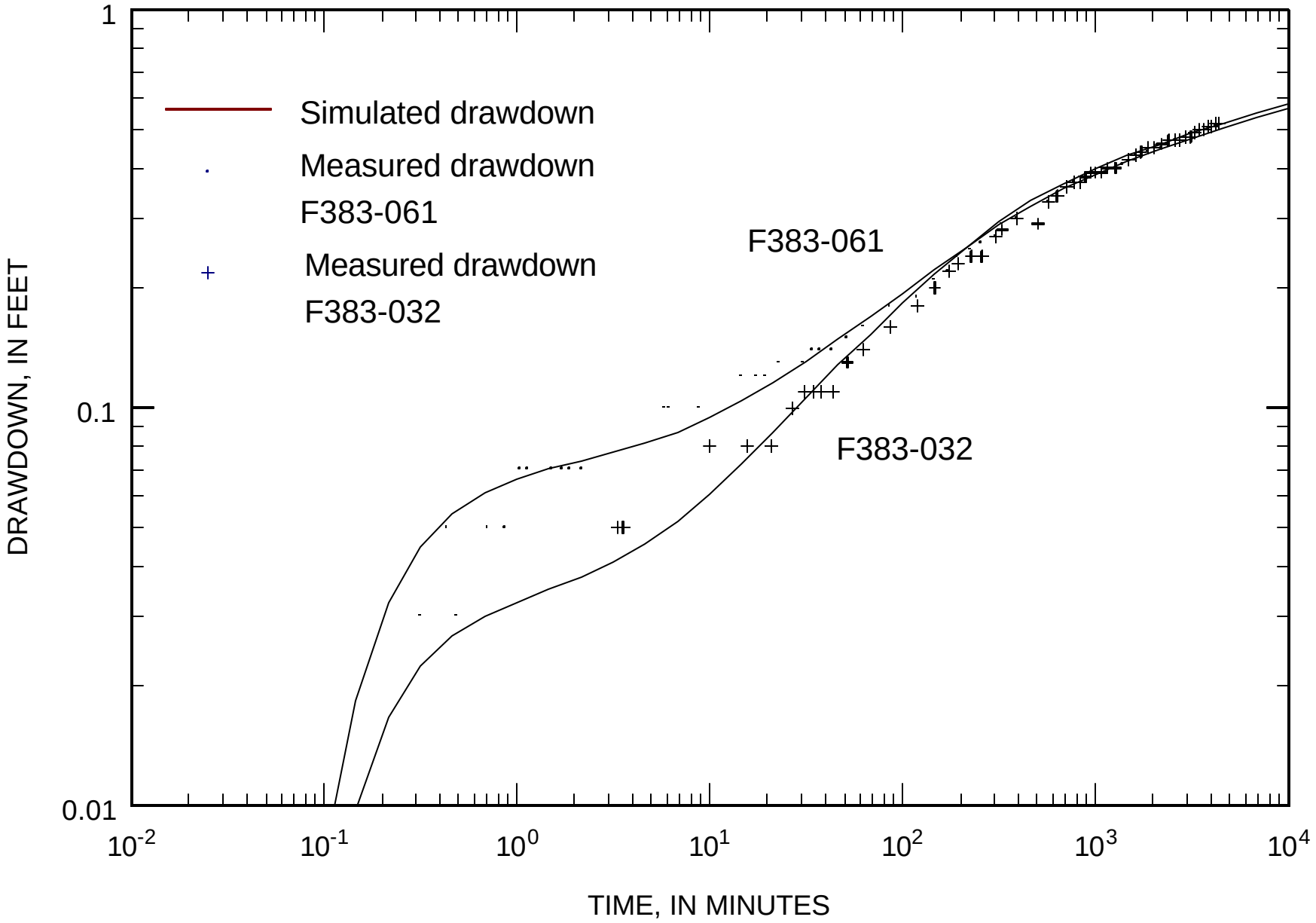
Simulated drawdown
Measured drawdown
F383-061
Measured drawdown
F383-032
F383-061
F383-032
DRAWDOWN, IN FEET
TIME, IN MINUTES
1
0.1
0.01
10^{-2}
10^{-1}
10^{0}
10^{1}
10^{2}
10^{3}
10^{4}

Fig. 18b

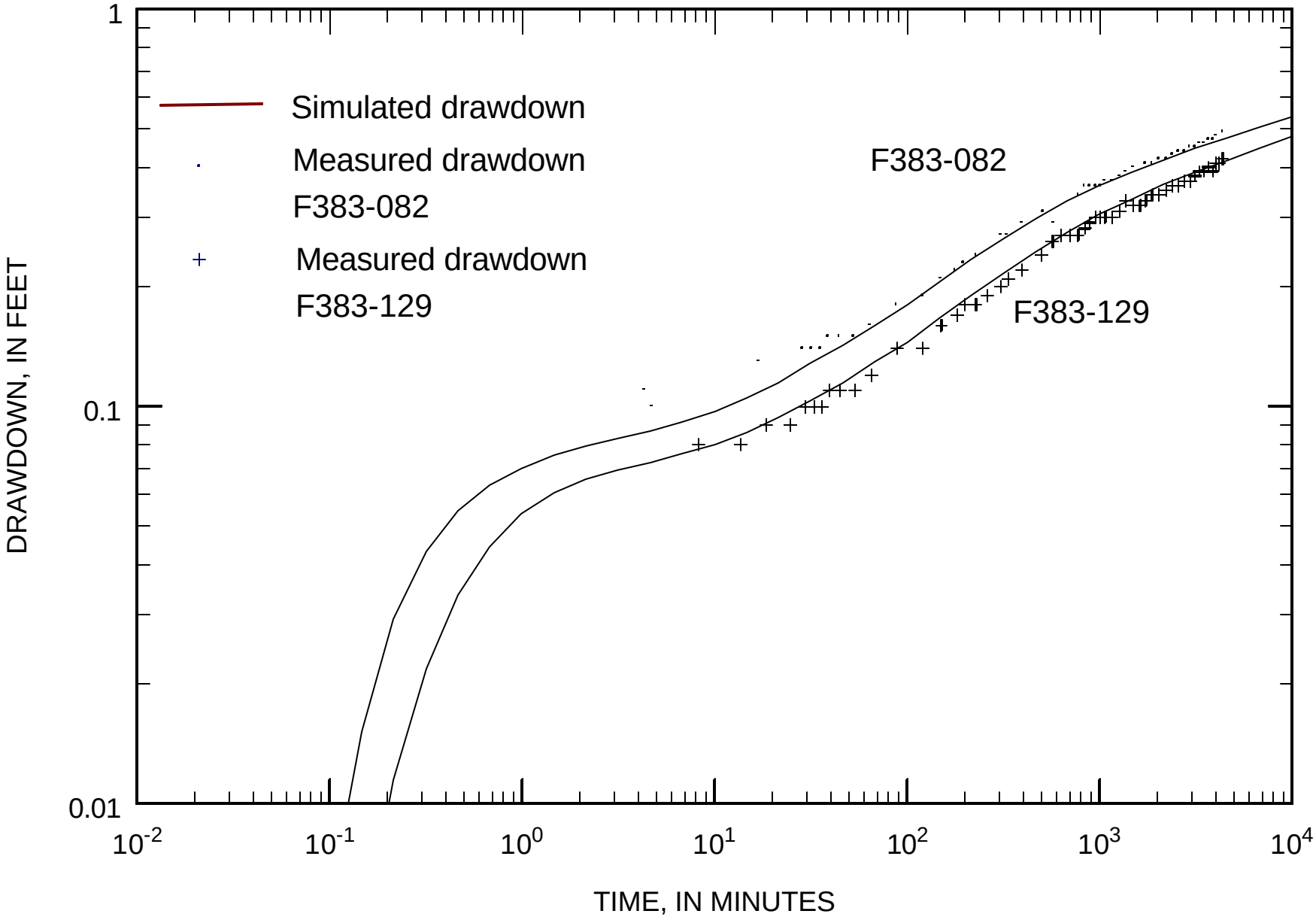
Simulated drawdown
Measured drawdown
F383-082
Measured drawdown
F383-129
F383-082
F383-129
DRAWDOWN, IN FEET
TIME, IN MINUTES
1
0.1
0.01
10-2
10-1
100
101
102
103
104

Fig. 19a

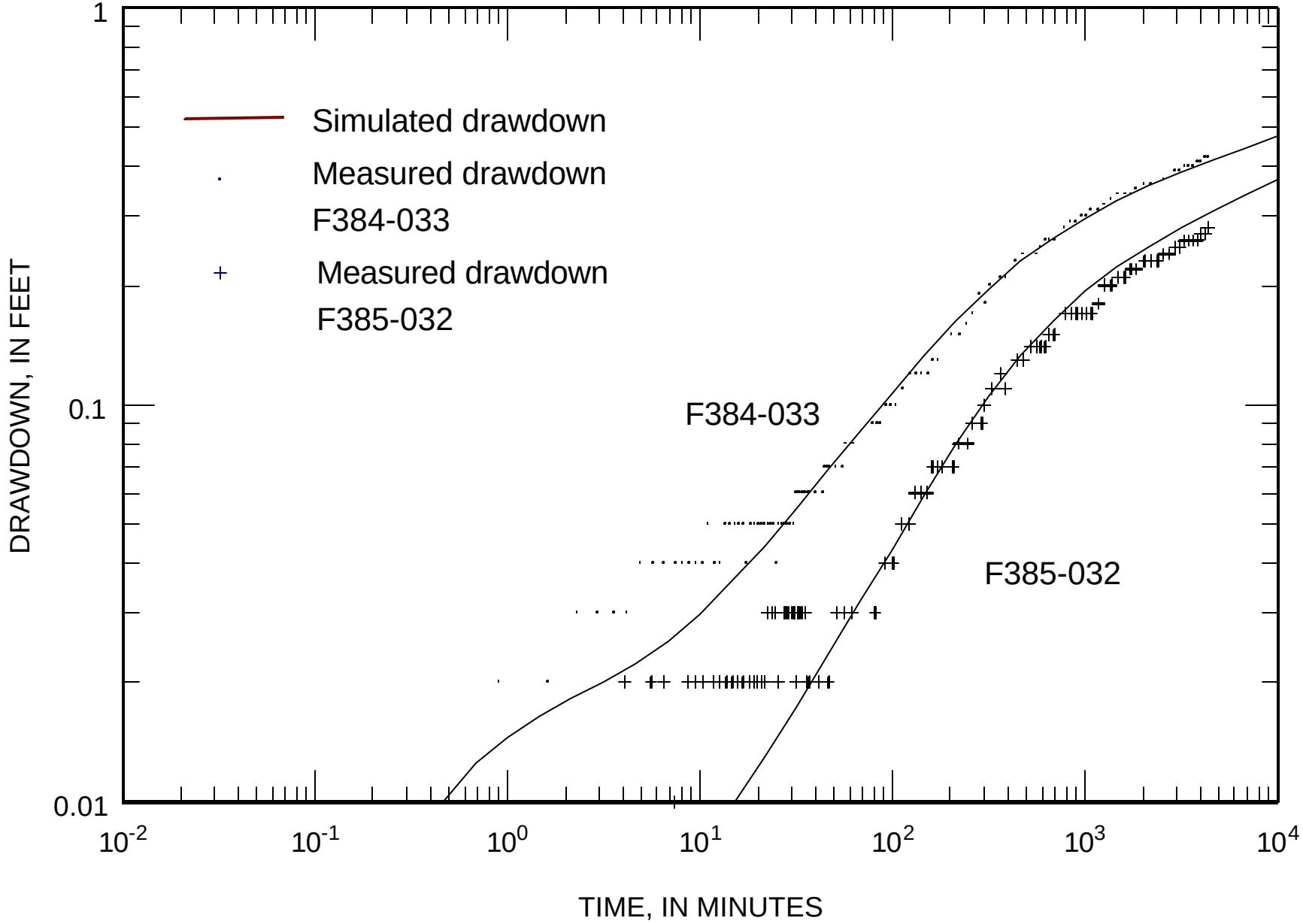
Simulated drawdown
Measured drawdown
F384-033
Measured drawdown
F385-032
F384-033
F385-032
DRAWDOWN, IN FEET
TIME, IN MINUTES
1
0.1
0.01
10^{-2}
10^{-1}
10^{0}
10^{1}
10^{2}
10^{3}
10^{4}

Fig. 19b

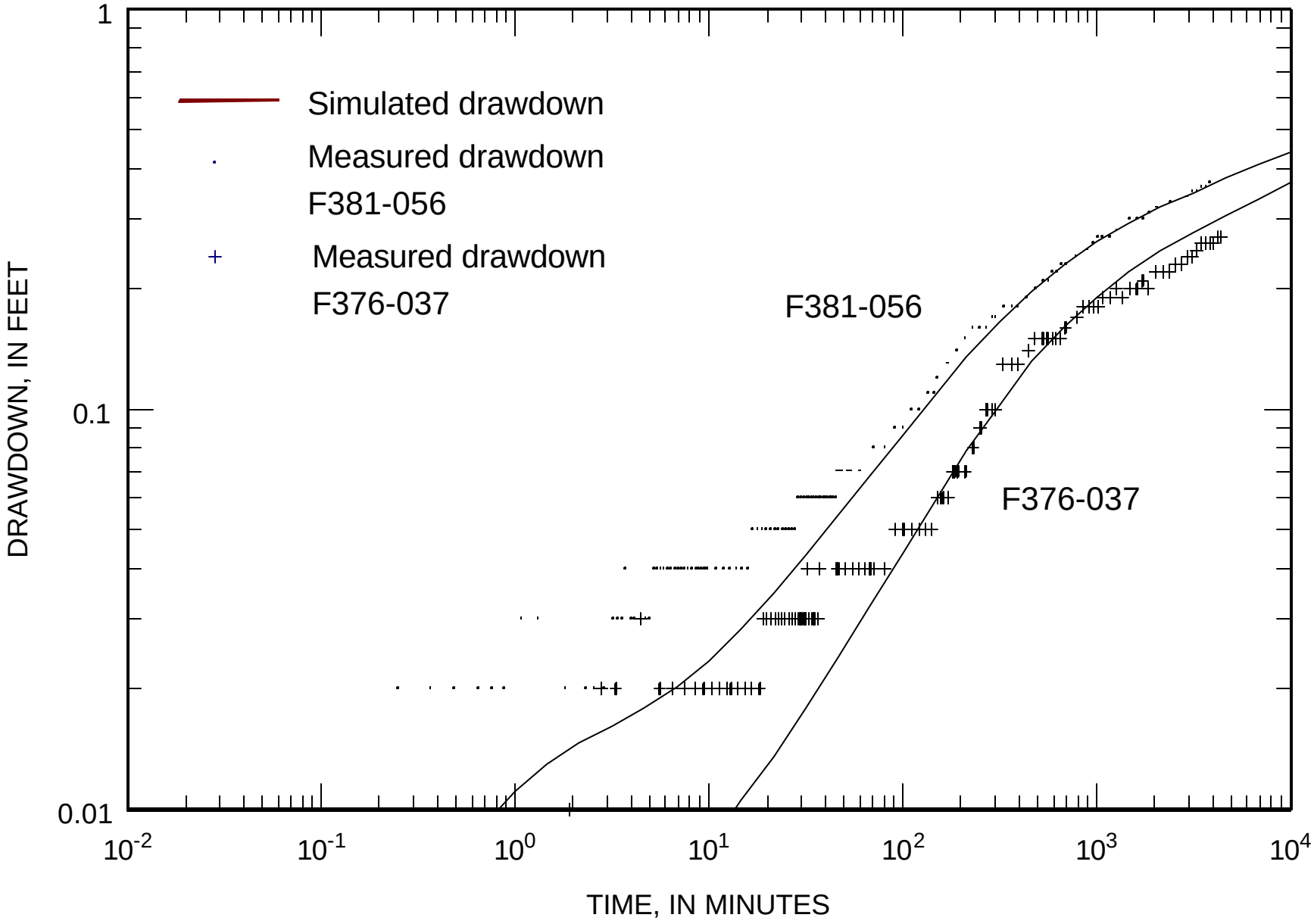
Simulated drawdown
Measured drawdown
F381-056
Measured drawdown
F376-037
F381-056
F376-037
DRAWDOWN, IN FEET
TIME, IN MINUTES
1
0.1
0.01
10-2
10-1
100
101
102
103
104

Fig. 20a

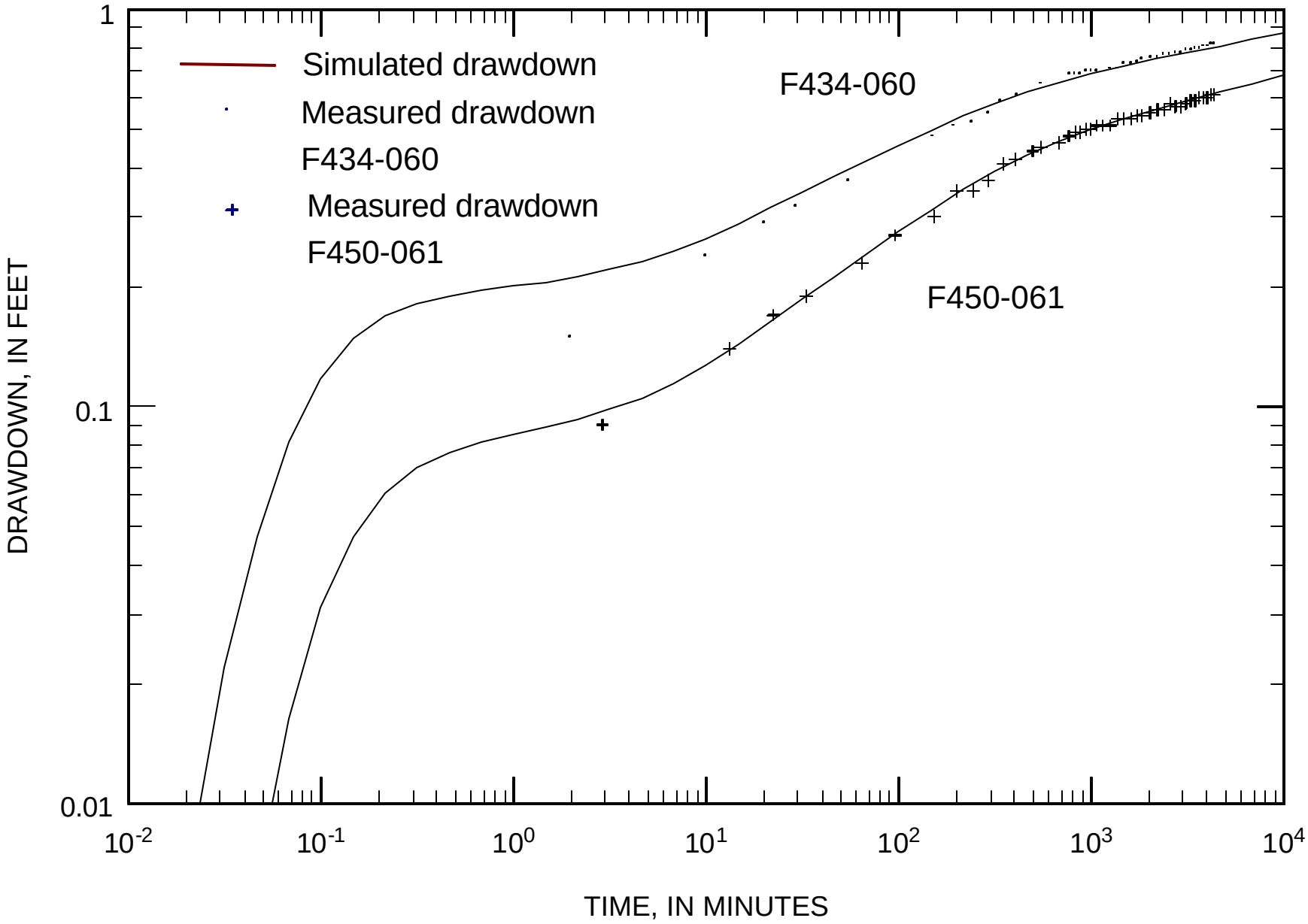
Simulated drawdown
Measured drawdown
F434-060
Measured drawdown
F450-061
F434-060
F450-061
DRAWDOWN, IN FEET
1
0.1
0.01
10^{-2}
10^{-1}
10^{0}
10^{1}
10^{2}
10^{3}
10^{4}
TIME, IN MINUTES

Fig. 20b

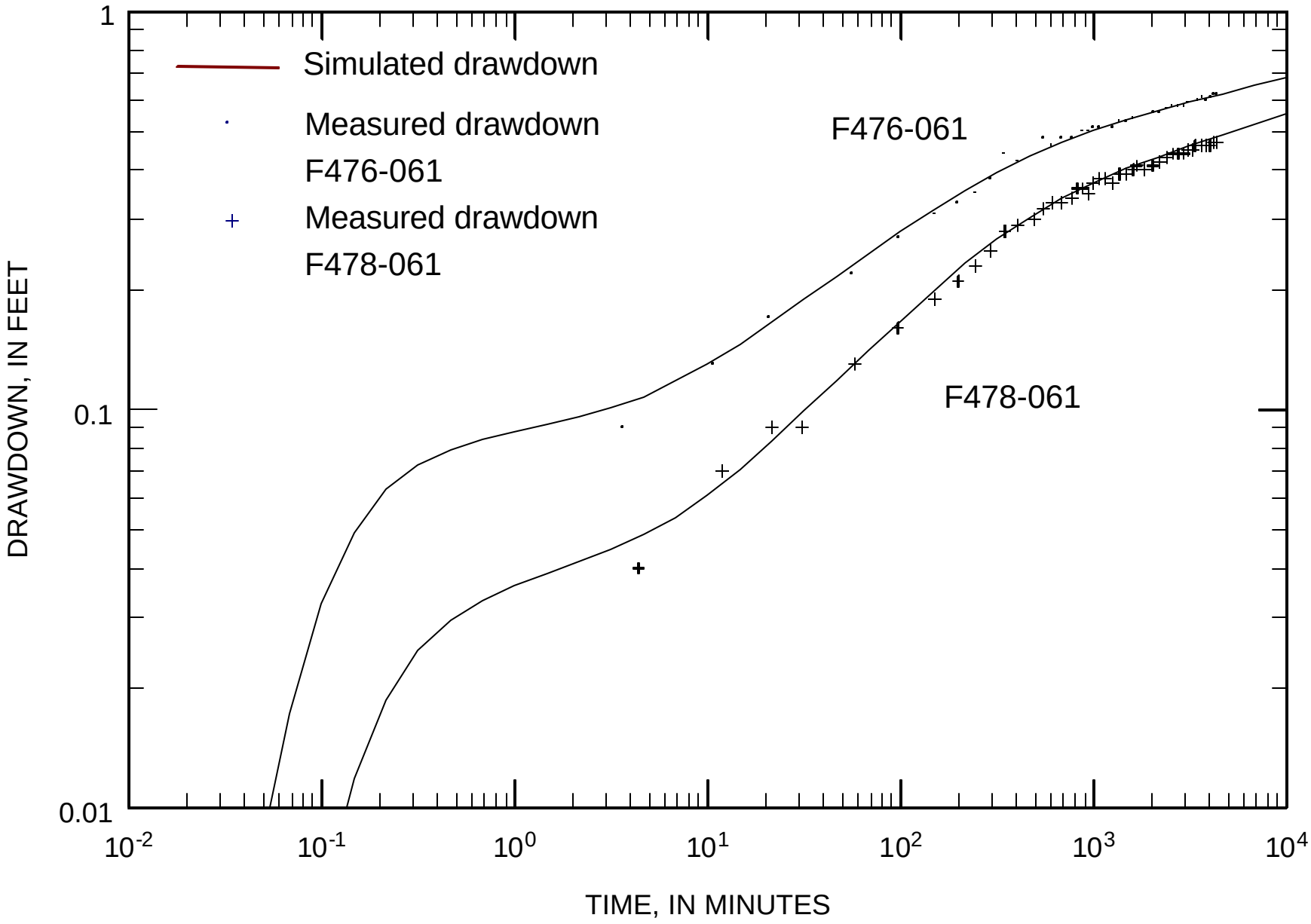
Simulated drawdown
Measured drawdown
F476-061
Measured drawdown
F478-061
F476-061
F478-061
DRAWDOWN, IN FEET
1
0.1
0.01
10^{-2}
10^{-1}
10^{0}
10^{1}
10^{2}
10^{3}
10^{4}
TIME, IN MINUTES

Fig. 21

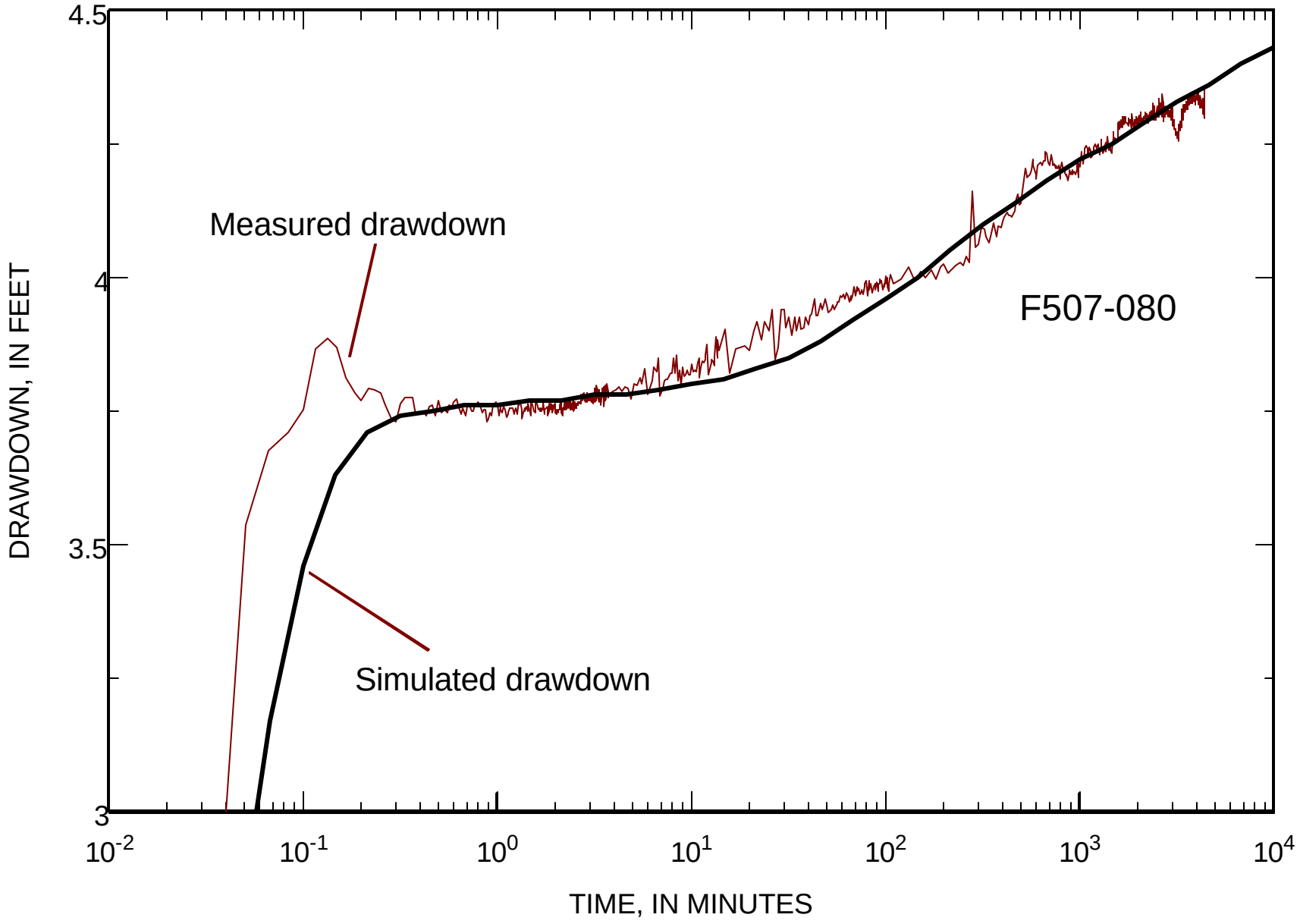
4.5
4
3.5
3
DRAWDOWN, IN FEET
Measured drawdown
Simulated drawdown
F507-080
10^{-2}
10^{-1}
10^{0}
10^{1}
10^{2}
10^{3}
10^{4}
TIME, IN MINUTES

Fig. 22

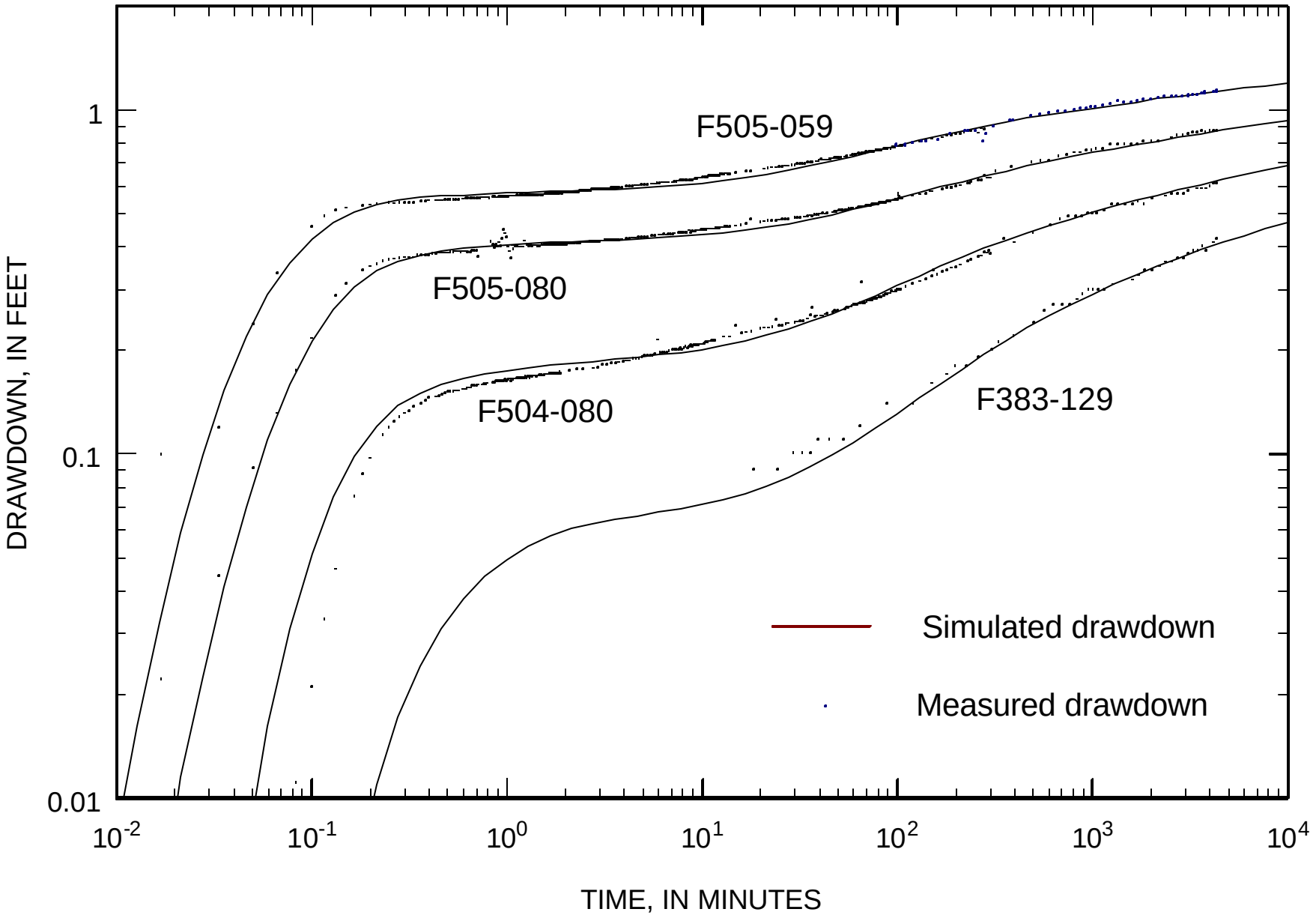
F505-059
F505-080
F504-080
F383-129
Simulated drawdown
Measured drawdown
DRAWDOWN, IN FEET
TIME, IN MINUTES
1
0.1
0.01
10^{-2}
10^{-1}
10^{0}
10^{1}
10^{2}
10^{3}
10^{4}

Fig. 23

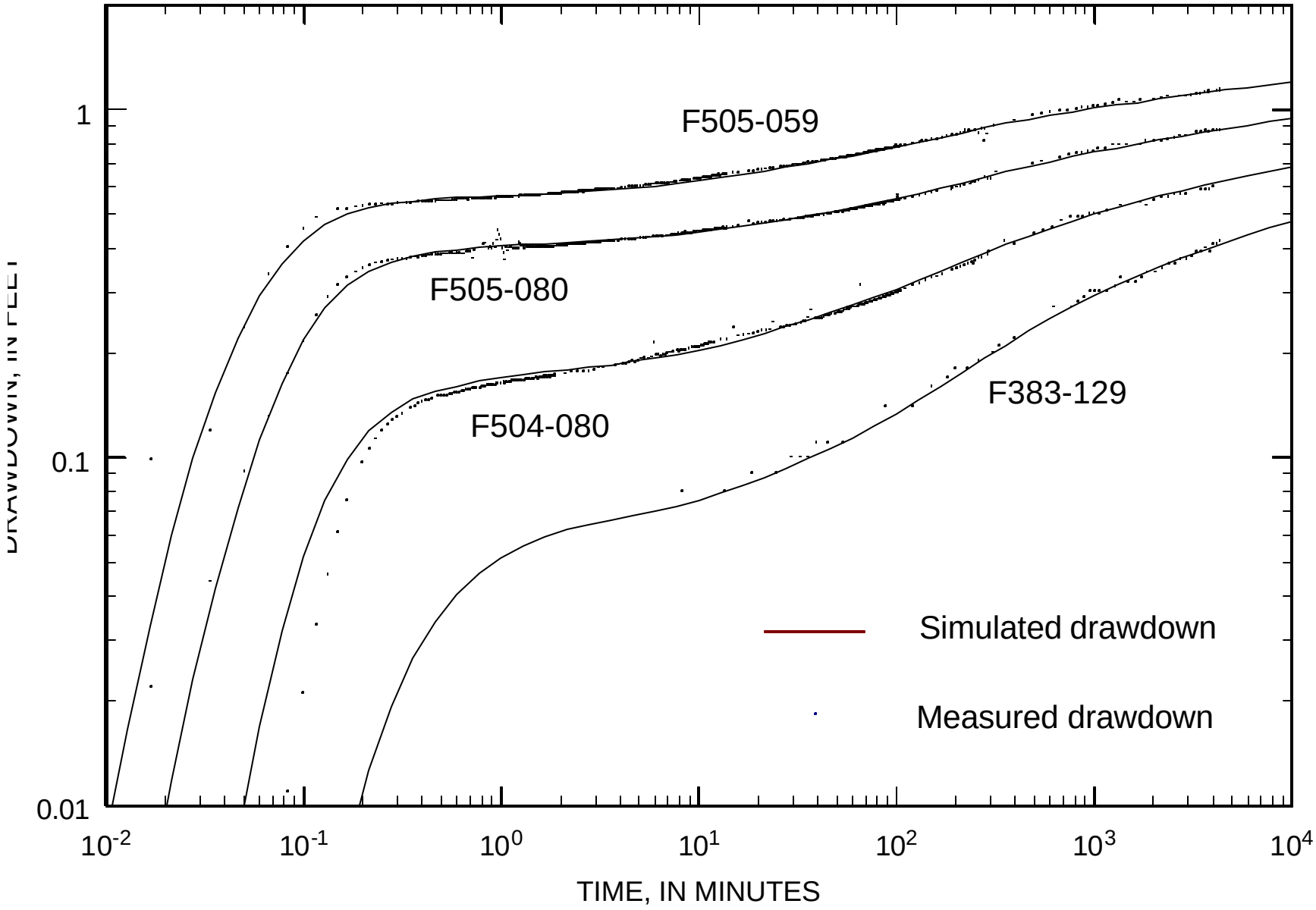
F505-059
F505-080
F504-080
F383-129
Simulated drawdown
Measured drawdown
1
0.1
0.01
10^{-2}
10^{-1}
10^{0}
10^{1}
10^{2}
10^{3}
10^{4}
TIME, IN MINUTES